

Final Report

**PERFORMANCE-RELATED SPECIFICATIONS OF CONCRETE
BRIDGE SUPERSTRUCTURES**

FHWA/IN/JTRP- 2001/8

Vol. 1

Performance Parameters and Related Procedure for Concrete Bridge Superstructures

By

Julio A. Ramirez
Principal Investigator

and

J. Paul Smith – Graduate Research Assistant

Joint Transportation Research Project
Project Number: C-36-56WW
File Number: 7-4-48
SPR - 2325

Conducted in Cooperation with the
Indiana Department of Transportation
and the
Federal Highway Administration

The contents of this report reflect the views of the authors, who are responsible for the facts and the accuracy of the data presented herein. The contents do not necessarily reflect the official views or policies of the Indiana Department of Transportation or the Federal Highway Administration at the time of publication. This report does not constitute a standard, specification, or regulation.

Purdue University
West Lafayette, IN 47907
October 2002



INDOT Research

TECHNICAL *Summary*

Technology Transfer and Project Implementation Information

TRB Subject Code: 25-01 Bridge Design and Performance
Publication No.: FHWA/IN/JTRP-2001/8, SPR-2325

October 2002
Final Report

Performance Related Specifications (PRS) for Concrete Bridge Superstructures- A Four Volume Report

Introduction

The development of Performance Related Specifications (PRS) requires the identification of key performance levels for a given structural system. The first attempt to develop a methodology for PRS can be traced to 1980 when the Federal Highway administration (FHWA) instituted a new research program category. The main two objectives of the program were:

- 1) To provide a more rational basis for payment reduction plans.
- 2) To develop additional specifications related to the performance of flexible and rigid pavement structures.

In the early and mid-1980s, the FHWA, the National Cooperative Highway Research Program (NCHRP), and the American Association of State Highway and Transportation Officials (AASHTO) began a cooperative effort searching for supporting data needed for the development of PRS. The idea was to develop performance models that would allow relating the material and construction testing parameters collected at the time of construction to the future performance of the complete project. However, it was concluded that the existing databases were inadequate to derive the needed performance models. A known example of a PRS is the one developed for Portland Cement Concrete (PCC) pavements by Eres Consultants, Inc. and the FHWA (Darter et. al., 1998) in a cooperative effort. In this study, the overall objectives of a methodology for PRS were not completely fulfilled due to the lack of adequate supporting information in the existent databases to construct accurate

performance predictive models. As a result, the proposed PRS was presented only as a methodology providing a more rational basis for payment plans.

The objective of the research study was to develop the essential components of a PRS for concrete bridge superstructures for application in the state of Indiana. The work conducted in this research project is presented in four volumes. Volume 1 summarizes the work conducted on the identification of performance levels and key parameters, and the development of acceptance criteria are addressed in Volume 1. The main objective of this volume is to present a proposed methodology for a PRS for concrete bridge superstructures. Volume 2 presents the research findings dealing with development of High-Performance Concrete (HPC) for applications in the bridge structures in the state of Indiana. The objective of the study presented in Volume 2 was to identify and develop concrete mixtures with adequate performance characteristics in terms of durability for the purpose of using these characteristics in performance-related specifications. Volume 3 summarizes the work conducted to investigate the behavior of fiber reinforced polymer (FRP) reinforced concrete structures with an emphasis on bond and shear. The main objective of this volume is to provide design guidelines for the use of FRP reinforcement in bridge superstructures. Volume 4 summarizes the results of an evaluation of the bond performance of epoxy-coated bars with a coating thickness up to 18 mils.

Findings

In this study emphasis has been placed on the development of a methodology for a Performance Related Specification, PRS, for concrete bridge superstructures. The implementation of the methodology, presented in the form of a user-friendly computer program in Volume 1 of this report, is project specific. It requires the mean and standard deviation (or definition of a probability distribution) of the input parameters for the performance predictive models. This is done for both the as-designed condition and the as-built condition of the structure. The contractor is expected to achieve certain level of compliance during the construction as dictated by the as-designed condition (which is defined based on the submitted design in compliance with agency specifications).

Based on performance predictive models, cost models, and statistical simulation, the methodology reports a relative as-built/as-designed Life-Cycle Cost (LCC). This relative LCC measures the level of compliance of the as-built structure with the design. The agency (INDOT) implementing the methodology could then consider the relative LCC in the form of a pay factor modifying the contractor's bid price. Statistical simulation is conducted to evaluate the effects of the variations in the input parameters for the performance predictive models. The differences in the LCC for the as-designed and as-built elements come from the differences in the input parameters that are under the control of the contractor (referred to as quality characteristics). The framework of the proposed methodology has been fully developed and illustrated with four numerical examples in an initial case study of a simply supported reinforced bridge deck or slab.

The research effort described in Volume 2 of this report was divided in two phases. Phase I was focused on development of concrete mixtures optimized with respect to selected performance-related parameters. During this phase, ten optimum concrete mixes have been identified from 45 mixes in terms of compressive strength, Young's modulus of elasticity, rapid chloride penetration and chloride conductivity using a statistical design procedure. Through surface response methodology, 27 statistical models were developed for each of four parameters. Based on the models developed, 81 contour maps were generated, which

indicated how performance of concrete varied in response to the change of dosages of binders at constant water-binder ratio. Based on the overlaid contour maps and the threshold values chosen for the properties of concrete, optimum concrete mixtures including Portland cement and the combinations with fly ash, silica fume and slag were identified.

In Phase II of the HPC study, the ten optimum mixtures were further evaluated with respect to mechanical properties and durability characteristics. Several different tests related to the evaluation of the resistance of concrete to chloride permeability were used: rapid chloride permeability test, chloride conductivity test, test for the resistance of concrete under DC electrical field, ponding test for the determination of the resistance of concrete to chloride penetration, and rapid test for the determination of diffusion coefficient from chloride migration. Tests related to the resistance of concrete to freezing & thawing, and scaling were also investigated. Other tests such as, the determination of drying shrinkage, and test for curing effects on the properties of high performance concrete were also evaluated in this research. Special emphasis was placed on determining and quantifying these parameters that control the ingress of the chloride ions.

Based on the results generated during this research, models have been developed that allow for prediction of certain mechanical and durability-related parameters related to the mixture composition. The parameters that can be predicted include strength, rapid chloride permeability (RCP) values, and chloride diffusion coefficient. Limited validation of these models was performed using field data provided by INDOT. The strength and chloride diffusion coefficient values generated by these models can serve as an input for the life-cycle costing (LCC) model described in Vol. 1 of this report

As summarized in Volume 3, experimental investigations were performed to specifically investigate the behavior of FRP reinforced concrete structures in both bond and shear. For the bond investigation, three series of beam splice tests were performed on specimens reinforced with steel, glass FRP, and aramid FRP to determine the effect of the different types of reinforcement on bond, cracking, and deflections. The test results indicate that the use of FRP reinforcement leads to lower bond

strengths and, therefore, require longer development lengths. The specimen crack widths and deflections were substantially larger for FRP specimens than steel specimens due to the significantly lower modulus of elasticity. Analysis of the test results resulted in recommendations for modifying the empirical development length equation of ACI 318-99 design code for use with FRP reinforcement.

For the shear investigation, two series of beam tests were conducted on specimens reinforced with steel, glass FRP, and aramid FRP to determine the effect of the different types of reinforcement on the concrete shear strength. All specimens did not contain transverse reinforcement. The test results show that the use of FRP reinforcement leads to lower concrete shear strengths than steel reinforcement for equal

reinforcement cross-sectional areas (longitudinal reinforcement percentages). In addition, the test results point that the shear strength is a direct function of the longitudinal reinforcement stiffness. The test results further substantiated the findings that larger crack widths and deflections are achieved by FRP specimens relative to steel specimens due to the lower modulus of elasticity. Analysis of the test results resulted in recommendations for the calculation of concrete shear strength.

The experimental work on the bond performance of epoxy-coated bars with thickness up to 18 mils summarized in Volume 4 of the final report indicates that the current AASHTO requirements for development length of epoxy-coated bars could be extended to coating thickness of up to 18 mils.

Implementation

Based on the results from the research conducted on the framework for a PRS, it was concluded that the most practical implementation of the methodology had to consider the corrosion deterioration problem as the only distress determining/affecting the LCC of the structure. It was concluded that other distress indicators applied at “a section level” should be included in the framework of a PRS to give more integrity to the process of quality control. The needed software for the implementation of the proposed PRS has been provided to INDOT as part of this report. It must be noted that corrosion deterioration represents almost 50% of the problems of the current bridge infrastructure in Indiana.

As part of the implementation efforts for the part of the research dealing with HPC, a series of mathematical models were constructed that allow for the prediction of strength, rapid chloride permeability and chloride diffusion coefficient values based on the binder composition of the mixture.

The data generated using these models have been arranged in an Excel sheet, which allows the user to input desired minimum and maximum values of strength (at 28 days) and/or RCP values (at 56 days) and obtain binder combinations which yield/satisfy the desired input values. Binder system 1 refers to mixtures, which contain PC, SF and GGBS. Binder system 2 refers to mixtures, which contain PC, SF and FA. Binder system 3 refers to mixtures, which contain PC, GGBS and FA. The

percentage increments of SF represented in the Excel worksheet are 0, 5 and 7.5 %. The percentage increments of FA and GGBS represented are 0, 20, 25 and 30 %.

The strength and chloride diffusion coefficient values determined for the 10 concrete mixtures tested in Phase II of the study were also used as input values for the LCC model described in Vol. 1 of this report. The LCC model was run for a single, simply supported span. The same type of data was also obtained from three existing Indiana bridges and the LCC model was re-run for these structures. The results indicate that LCC for all laboratory mixtures was lower than the LCC for standard INDOT class C concrete mixture. Furthermore, the LCC of the actual field mixtures was slightly higher than the LCC of standard class C mixture.

Currently, the ability of the models developed as a part of the HPC study to predict the actual properties of a field concrete is being validated on several QC/QA bridge jobs and a supplementary report summarizing the results of these evaluations is expected by June 2003.

Based on the research conducted on the use of FRP reinforcement, design and construction recommendations are provided that can be used in the design and construction of FRP reinforced bridge decks. These recommendations will be implemented in a JTRP study “Implementation of a Non-Metallic Reinforced Bridge Deck.” This study will evaluate the design and construction recommendations in a prototype laboratory deck

specimen as well as through a pilot field study that incorporates nonmetallic reinforcement in a bridge deck.

No change of the bond specifications is required to implement the use of up to #8

diameter deformed bars with epoxy-coating thickness up to 18 mils.

Contact

For more information:

Prof. Julio A. Ramirez

Principal Investigator
School of Civil Engineering
Purdue University
West Lafayette IN 47907
Phone: (765) 494-2716
Fax: (765) 496-1105

Prof. Jan Olek

Co-Principal Investigator
School of Civil Engineering
Purdue University
West Lafayette IN 47907
Phone: (765) 494-5015

Prof. Robert J. Frosch

Co-Principal Investigator
School of Civil Engineering
Purdue University
West Lafayette IN 47907
Phone: (765) 494-5904

Indiana Department of Transportation

Division of Research
1205 Montgomery Street
P.O. Box 2279
West Lafayette, IN 47906
Phone: (765) 463-1521
Fax: (765) 497-1665

Purdue University

Joint Transportation Research Program
School of Civil Engineering
West Lafayette, IN 47907-1284
Phone: (765) 494-9310
Fax: (765) 496-1105

1. Report No. FHWA/IN/JTRP-2001/8		2. Government Accession No.		3. Recipient's Catalog No.	
4. Title and Subtitle Performance Related Specifications for Concrete Bridge Superstructures- Volume 1 – Performance Parameters and Related Procedure for Concrete Bridge Superstructures				5. Report Date October 2002	
				6. Performing Organization Code	
7. Author(s) J. Paul Smith and Julio A. Ramirez				8. Performing Organization Report No. FHWA/IN/JTRP-2001/8	
9. Performing Organization Name and Address Joint Transportation Research Program 1284 Civil Engineering Building Purdue University West Lafayette, Indiana 47907-1284				10. Work Unit No.	
				11. Contract or Grant No. SPR-2325	
12. Sponsoring Agency Name and Address Indiana Department of Transportation State Office Building 100 North Senate Avenue Indianapolis, IN 46204				13. Type of Report and Period Covered Final Report	
				14. Sponsoring Agency Code	
15. Supplementary Notes Prepared in cooperation with the Indiana Department of Transportation and Federal Highway Administration.					
<p>16. Abstract</p> <p>In Volume 1 of the final report, the identification of performance levels and parameters, and the development of acceptance criteria, have been addressed. Emphasis has been placed on the development of a methodology for a Performance Related Specification, PRS, for concrete bridge superstructures. The implementation of the methodology, presented in the form of a user-friendly computer program, is project specific. It requires the mean and standard deviation (or definition of a probability distribution) of the input parameters for the performance predictive models. This is done for both the as-designed condition and the as-built condition of the structure. The contractor is expected to achieve certain level of compliance during the construction as dictated by the as-designed condition (which is defined based on the submitted design in compliance with agency specifications). Based on performance predictive models, cost models, and statistical simulation, the methodology reports a ratio of the as-built/as-designed Life-Cycle Cost (LCC). This LCC ratio measures the level of compliance of the as-built structure with the design. This approach enables the agency (INDOT) implementing the methodology to consider the LCC ratio in the form of a pay factor modifying the contractor's bid price.</p> <p>In proposed methodology, statistical simulation is conducted to evaluate the effects of the variations in the input parameters for the performance predictive models. The differences in the LCC for the as-designed and as-built elements come from the differences in the input parameters that are under the control of the contractor (referred to as quality characteristics).</p> <p>The framework of the methodology has been fully developed with the case study of a simply supported reinforced bridge deck or slab. The proposed methodology is further illustrated with four numerical examples.</p> <p>Based on the work in this phase of the research program, it was concluded that the most practical implementation of the methodology considers the corrosion deterioration problem as the only distress determining/affecting the LCC of the structure. It was also concluded that other distress indicators applied at "a section level" can be included in the framework of a PRS to give more integrity to the process of quality control. It must be noted that corrosion deterioration represents almost 50% of the problems in the current bridge infrastructure in Indiana.</p>					
17. Key Words corrosion, durability, epoxy-coated reinforcement, concrete bridge decks, field evaluation, performance-related-specification.			18. Distribution Statement No restrictions. This document is available to the public through the National Technical Information Service, Springfield, VA 22161		
19. Security Classif. (of this report) Unclassified		20. Security Classif. (of this page) Unclassified		21. No. of Pages	22. Price

TABLE OF CONTENTS

	Page
LIST OF TABLES	iii
LIST OF FIGURES.....	iv
ACKNOWLEDGEMENTS	v
CHAPTER 1 – INTRODUCTION.....	1
1.1 Introduction and Background of a PRS.....	1
1.1.1 Structure of the Methodology for a PRS.....	2
1.1.2 Performance-Related Specifications for PCC Pavements.....	2
1.2 Proposed Approach.....	3
CHAPTER 2 – STRUCTURAL RELIABILITY	5
2.1 Introduction.....	5
2.2 Basic Approach	5
2.3 First Order Second Moment Method.....	5
2.4 Simulation-Based Reliability Methods.....	6
2.4.1 Direct Monte Carlo Simulation.....	6
2.5 Variability of Performance Parameters	7
2.6 Variability of Load Factors and Load Models	9
2.7 Implementation of Reliability Concepts in the Methodology for PRS.....	10
CHAPTER 3 – PRELIMINARY METHODOLOGY FOR PRS- Initial Case Study.....	15
3.1 Introduction.....	15
3.2 Limit Conditions	15
3.2.1 Corrosion Deterioration	15
3.2.2 Excessive Crack Width.....	15
3.2.3 Flexural Failures	16
3.2.4 Excessive Deflections	16
3.3 Constant and Quality Characteristics	16
3.4 Statistical Simulation of Performance Predictive Models.....	16
3.4.1 Time Dependence of the Probabilities of Failure.....	17
3.4.2 Adopted Simulation Procedure	17

3.5 Cost Models	17
3.5.1 Agency Costs	18
3.5.2 User Costs	18
3.6 Numerical Examples	19
3.6.1 Introduction.....	19
3.6.2 Example: Deficient Construction.....	19
3.6.3 Example: High Quality Construction.....	21
3.6.4 Example: Tradeoffs Among Quality Characteristics	21
3.6.5 Example: Use of Epoxy-Coated Reinforcement	21
3.7 Conclusions from the Initial Case Study.....	22
3.8 Other Potential Applications	22
 CHAPTER 4 – IMPLEMENTATION PLAN AND FUTURE WORK	 35
4.1 Introduction.....	35
4.2 Sectional Approach.....	35
4.3 Current Methodology.....	35
4.4 Computer Software Guidelines	36
4.5 Future Work	36
 LIST OF REFERENCES	 37
 APPENDICES.....	 46
APPENDIX A Performance Models for Case Study	47
APPENDIX B Model for Creep and Shrinkage.....	57
APPENDIX C Diffusion Coefficient	60
APPENDIX D Shear Model.....	63
APPENDIX E Software (Guidelines)	64

LIST OF TABLES

Table	Page
2.1 Statistical Parameters for Reinforced Concrete Slab Dimensions.....	12
2.2 Statistical Parameters for Reinforced Concrete Beam Dimensions.....	13
2.3 Statistical Parameters for Dead Load	14
3.1 Summary of the Statistical Values.....	24

LIST OF FIGURES

Figure	Page
3.1 Software Developed for Simulation Process	26
3.2 Application of PRS Methodology- Deficient Construction	27
3.3 Probability of Flexural Failure (Example Section 4.6.2).....	28
3.4 Probability of Excessive Deflection (Example Section 4.6.2)	29
3.5 Probability of Excessive Corrosion Deterioration (Example Section 4.6.2).....	30
3.6 Application of PRS Methodology for a Slab Bridge: High Quality Construction	31
3.7 Application of PRS Methodology for a Slab Bridge: Tradeoffs Among Quality Characteristics	32
3.8 Application of PRS Methodology for a Slab Bridge: Use of Epoxy-Coated Reinforcement.....	33

1 INTRODUCTION

1.1 Introduction and Background of a PRS

The identification of performance levels and key parameters, and the development of acceptance criteria are addressed in Volume 1 of the final report for the project *Performance Related Specifications for Concrete Bridge Superstructures*. The main objective of this volume is to present a proposed methodology for a PRS for concrete bridge elements. The implementation of the methodology developed in this study is project specific. It requires the mean and standard deviation (or definition of a probability distribution) of the input parameters for the performance predictive models. This is done for both the as-designed and the as-built condition of the structure. The contractor is expected to achieve compliance with the as-designed condition, as per agency specifications, during the construction.

Based on performance predictive models, cost models, and statistical simulation, the methodology allows the estimation of the ratio (as-built/as-designed) Life-Cycle Cost (LCC). This ratio represents the level of compliance of the as-built structure with the original design. The agency (INDOT) implementing the methodology is then enabled to consider the LCC ratio as a pay factor used to modify the contractor's bid price. In the methodology, statistical simulation permits the evaluation of the effects of the variations in the predictive models input parameters. The differences in the LCC of the as-designed and the as-built elements are the result of the differences in the input parameters that are under the control of the contractor. In this study the parameters under the control of the contractor are referred to as quality characteristics.

The framework of the methodology is developed with a case study consisting of a simply supported reinforced bridge deck or slab. The proposed methodology is illustrated in this report with four numerical examples. The results of the preliminary case study indicated that the most practical implementation of the methodology should consider the corrosion deterioration problem as the only distress used in the determination of the LCC of the structure. It is also concluded that other distress indicators applied at "a section level" can be included in the framework of PRS to give more integrity to the process of quality control. A modified methodology of a PRS is highlighted in this report. A user-friendly computer program with guidelines is also included.

It is believed that the effort of future research must be concentrated in developing a better model to predict the corrosion deterioration process for the specific conditions in Indiana. This includes describing the corrosion process in presence of commonly used protective treatments such as epoxy-coated reinforcement and defining corrosion parameters in terms of the properties of the materials. It must be noticed that corrosion deterioration represents almost 50% of the problems in the current bridge infrastructure in Indiana.

The first attempt to develop a methodology for PRS can be traced to 1980 when the Federal Highway administration (FHWA) instituted a new research program category (Ohrn and Schexnayder, 1997). The main two objectives of this program were:

- 1) To provide a more rational basis for payment reduction plans.
- 2) To develop additional specifications related to the performance of flexible and rigid pavement structures.

In the early and mid-1980s, the FHWA, the National Cooperative Highway Research Program (NCHRP), and the American Association of State Highway and Transportation Officials (AASHTO) began a cooperative effort searching for supporting data needed for the development of PRS. The idea was to develop performance models that would allow relating the material and construction testing parameters collected at the time of construction to the future performance of the complete project. However, it was concluded that the existing databases were inadequate to derive the needed performance models (Ohrn and Schexnayder, 1997).

A well-known application of a PRS is the one developed for Portland Cement Concrete (PCC) (Darter et al., 1998) in a cooperative. In Darter et al., the overall objectives of a methodology for PRS as presented above were not completely fulfilled due to the lack of adequate supporting information in the existent databases to construct

accurate performance predictive models. As a result, the proposed PRS was presented as a methodology to provide a more rational basis for payment plans.

1.1.1 Structure of the Methodology for a PRS

In the context of a PRS it is assumed that the distress indicators, for which predictive models exist, determine the performance of the given system. Performance is measured in monetary terms as the Life Cycle Cost (LCC) of the system. Parameters expeditiously measurable, under the control of the contractor, and influencing/determining any distress indicator are referred to as *quality characteristics*. If the parameters are not under the control of the contractor, they are referred to as *constant characteristic*. It can be postulated that the ratio of the as-designed to as-built LCC is a function of the quality characteristics on the basis of performance predictive models. An example of a distress indicator is corrosion of the reinforcement, and an example of an associated quality characteristic is the concrete cover.

For quality control purposes, the as-built structure should preserve some level of compliance with the design. The level of compliance can be established by the ratio of the LCC associated with the values of the quality characteristics measured from the actual construction (referred to as $LCC_{as-built}$), and the LCC associated with the values of the quality characteristics of the design (referred to as $LCC_{as-designed}$). This ratio provides a criterion for a management action. This management action could have the form of a pay factor modifying the contractor's bid price. An example of a possible expression for the pay factor is:

$$PF = LCC_{as-designed}/LCC_{as-built} \quad (1-1)$$

1.1.2 Performance-Related Specifications for PCC Pavements

In Darter et al. (1998) methodology for PCC pavements, the first step was to define the key distress indicators determining/affecting performance. First, an exhaustive list of possible distresses was put together (transverse cracking due to repeated loading, transverse cracking due to inadequate or late sawing, and 27 additional items (Darter et al. 1993)). An essential criterion for including a specific distress indicator into the methodology for PRS was the experience of a panel of experts.

Distress indicators such as cracking, joint spalling, and initial smoothness were finally selected for use in the proposed methodology (Darter et al. 1996). The selection of a given distress indicator was determined on the basis of the considerations listed below:

- a) Availability of predictive models.
- b) Model parameters were under the control of the contractor.
- c) Importance as a real problem in current structures.

After selecting the distress indicators, the corresponding quality characteristics were defined. The required conditions for selection were:

- a) Related to the distress indicators selected.
- b) Under the control of the contractor.
- c) Possibility of rapid and reliable evaluation (quantification).

In the methodology of the PRS for PCC pavements (Darter et al. 1998) a pay factor is calculated as follows:

- Target values for the quality characteristic are defined in terms of mean and standard deviation. These values define a quality level the owner is willing to pay 100% of the contractor's bid price.
- For each quality characteristic, a family of curves relating pay factor to mean value is obtained. There is one curve for each possible standard deviation. The range of mean values and the set of standard deviations in these curves are expected to contain the values measured during construction. In obtaining these curves, the first step involves the calculation of a mean target Life Cycle Cost (denoted by $AD-LCC_{mean}$), which is the LCC of the structure assuming that the quality characteristics equal the target values (as-designed structure). Next, a single

point of the pay factor curve is obtained by considering a mean and a fixed standard deviation for that parameter (assuming that the other quality characteristics are equal to the target values). The corresponding mean as-built LCC, denoted by $AB-LCC_{mean}$, is then calculated. The pay factor for such pair (mean and standard deviation) is given by the expression:

$$\text{Pay Factor} = [\text{Bid Price} + (\text{AD-LCC}_{mean} - \text{AB-LCC}_{mean})]/\text{Bid Price} \quad (1-2)$$

The procedure previously described is repeated for several mean values and a fixed standard deviation to get a single pay factor curve. Several standard deviations are further considered in the development of a family of curves (one for each standard deviation) for a given parameter (quality characteristic). Next, the families of curves, one family for each distress indicator, are constructed and utilized in the specific project being evaluated. The evaluation is made on a lot of pavement-basis. A lot is defined as one production day or less. Lots are divided into sublots (minimum length 0.16 km). Two samples of each quality characteristics are then taken from each subplot to determine the corresponding mean and standard deviation for the as-built structure. After the mean and standard deviation are obtained, interpolation is required to get the pay factor for a given parameter in the corresponding family of curves. The product of all pay factors, one for each quality characteristic, gives the overall pay factor of the lot.

Rapid and reliable in-situ testing is mandatory within the application of the methodology for PRS. This is because its result, a pay factor, is directly applied to the contractor's bid price. Therefore, a complete system of sampling/testing is to be defined as part of the structure of the methodology for PRS.

1.2 Proposed Approach

In the methodology of PRS for PCC pavements discussed in Section 1.1.2, only serviceability-related distresses are considered. This can be sufficient to define the performance of a pavement but in the case of a bridge superstructure other distress indicators should be considered. For example, it is possible to envision a situation where in attempting to increase the time for initiation of corrosion in a concrete bridge slab, the use of excessive concrete cover is considered. However, if the overall thickness were kept the same, this action would lead to a reduction in the flexural capacity of the member. The work presented in this volume investigates the application of a methodology of PRS to a concrete bridge superstructure. It considers not only distress related to serviceability but also related to strength.

In subsequent sections, the implementation of reliability theory in accounting for the non-deterministic nature of the input parameters of the models (constant and quality characteristics) is incorporated in the simulation procedure. This approach represents a marked improvement to the methodology discussed in Section 1.1.2. In the PRS for pavements, simulation is carried out by an arbitrary sampling from a certain assumed range of values for the mean values and standard deviations of the quality characteristics neglecting any probability distribution potentially-associated with each variable.

The development of the proposed methodology for concrete bridge superstructures involves several tasks. The details of each task are given in the noted chapters of this report as follows:

- Review the basic principles of statistical simulation and the typical variation of the parameters related to concrete superstructures (material-related properties, geometry, and loads) (Chapter 2).
- Adopt key distress indicators as the basis to evaluate the performance of an initial case study (Appendix A).
- Establish limit conditions for the important distress indicators corresponding to the initial case study (Chapter 3). The event of exceeding the limit condition is referred to as "failure".
- Define constant and quality characteristics for the initial case study (Chapter 3).
- Define reasonable variations (if possible statistical distributions) for the input parameters of the models describing the performance of the initial case study (Chapter 3).
- Set the performance predictive models into a statistical framework. The goal of this task is to be able to report the probability of exceeding the limit condition for the essential distresses of the initial case study (Chapter 3).

Translate the different probabilities of failure into Life Cycle Cost considering costs to the agency and the users (Chapter 3).

- Develop numerical examples to illustrate the use of the suggested methodology for the initial case study (Chapter 3).
- State conclusions from the initial case study and modify the suggested methodology as needed (Chapter 3).
- State a refined methodology of a PRS based on the work conducted with initial case study. Develop a computer application including guidelines. (Chapter 4)

2 STRUCTURAL RELIABILITY

2.1 Introduction

In this chapter, several of the basic concepts from reliability theory to be employed in the proposed methodology for the PRS are introduced. These concepts account for the non-deterministic nature of the key parameters involved in the performance predictive models. They are used to carry out the statistical simulation of the selected distress indicators.

2.2 Basic Approach

There is a source of uncertainty associated with the variables involved in a given predictive model. Therefore, the outcome from the model is also non-deterministic. The implementation of reliability analysis within a given predictive model results in a probability distribution of all possible outcomes of the model. With the definition of a limit condition determining the “failure” or the “loss of serviceability” for the system under study, reliability analysis allows the calculation of a probability of exceeding the chosen limit condition.

The first step in evaluating the reliability of a structure is to define the non-deterministic parameters involved in the predictive model, X_i (alternatively, capacity, R , and demand, S), and the functional relationship among them, $g(X_1, X_2, \dots, X_n)$. This functional relationship is usually referred to as the performance function, Z .

$$Z = g(X_1, X_2, \dots, X_n) = R - S \quad (2-1)$$

The n -dimensional surface $Z = 0$ is the boundary between the safe ($Z > 0$) and unsafe regions ($Z < 0$).

If, f , is the joint probability density function for X_1, X_2, \dots, X_n , then the probability of failure, p_f , which occurs in the region $Z < 0$, is given by the integral:

$$p_f = \iiint_{Z < 0} \dots \int f(x_1, x_2, \dots, x_n) dx_1 dx_2 \dots dx_n \quad (2-2)$$

Equation 2-2 can be considered as the fundamental equation of structural reliability analysis. Since the joint probability density function, f , is very difficult to obtain and, if available, the integral is difficult to evaluate, alternated approaches have been used. These approaches include First Order Second Moment (FOSM) and simulation based reliability methods as discussed in the following.

2.3 First Order Second Moment Method

This method is based on a first-order Taylor's series approximation of the performance function and uses only second moment statistics (i.e., mean and covariance) of the random variables.

If R and S in Equation 2-1 are normally distributed and statistically independent random variables, then Z is also normal with statistical parameters:

$$\mu_Z = \mu_R - \mu_S \quad (2-3)$$

$$\sigma_Z^2 = \sigma_R^2 + \sigma_S^2 \quad (2-4)$$

where, μ and σ are the corresponding mean and standard deviation. The probability of failure is:

$$p_f = P(Z < 0) = \Phi(-\beta) \quad (2-5)$$

where, $\beta = \mu_z/\sigma_z$ is the so-called *reliability index*, and Φ is the standard Normal cumulative distribution.

Equations 2-3 to 2-5 can be generalized to include several random variables X_1, \dots, X_n . In that case, a Taylor's series expansion of Z , around the mean values of the random variables, \bar{X}_i , gives:

$$Z = g(\bar{X}_1, \dots, \bar{X}_n) + \sum_{i=1}^n \frac{\partial g}{\partial X_i} (X_i - \bar{X}_i) + \frac{1}{2} \sum_{i=1}^n \sum_{j=1}^n \frac{\partial^2 g}{\partial X_i \partial X_j} (X_i - \bar{X}_i)(X_j - \bar{X}_j) + \dots \quad (2-6)$$

where, g is the functional relationship among the input parameters of the performance predictive model (X_1, X_2, \dots, X_n). Neglecting second order terms, the first-order approximate mean of Z , μ_z , and variance of Z , σ_z^2 , are obtained:

$$\mu_z = g(\bar{X}_1, \dots, \bar{X}_n) \quad (2-7)$$

$$\sigma_z^2 = \sum_{i=1}^n \sum_{j=1}^n \frac{\partial g}{\partial X_i} \frac{\partial g}{\partial X_j} \text{Cov}(X_i, X_j) \quad (2-8)$$

The second-order mean, which is obtained by considering the square term in the Taylor's expansion of g , can be used to improve the accuracy of the estimation of the mean, especially if the limit function is non-linear. This estimator is given by:

$$\mu_z = g(\bar{X}_1, \dots, \bar{X}_n) + \frac{1}{2} \sum_{i=1}^n \sum_{j=1}^n \frac{\partial^2 g}{\partial X_i \partial X_j} \text{Cov}(X_j, X_i) \quad (2-9)$$

2.4 Simulation-Based Reliability Methods

The basic principle of simulation-based methods, also called Monte Carlo techniques, is the successive evaluation of the model under consideration. Each evaluation, referred to as a simulation run, involves the random selection of a set of values for the input parameters of the predictive model. These values are obtained from the corresponding probability distributions of the parameters. The analytical and computational steps that are needed to perform a Monte Carlo simulation are:

- a) Definition of the system
- b) Generation of input random variables
- c) Evaluation of the model
- d) Statistical analysis of the resulting behavior
- e) Study of efficiency and convergence

The definition of the system should include its boundaries, input parameters, output parameters and models that relate the input with the output parameters. Commonly the system model (physical model) is assumed to be non-random; however, modeling uncertainties can be included in the form of bias factors and additional variability. The definition of the input parameters should include their probabilistic characteristics. The accuracy of the results is expected to increase by increasing the number of simulation cycles.

2.4.1 Direct Monte Carlo Simulation

Monte Carlo simulation consists of drawing random samples of the basic random variables, X_i , according to their probabilistic distributions. A random value for a specific X_i is obtained as:

$$X_i = F^{-1}(u) \quad (2-10)$$

where, F^{-1} is the inverse of the cumulative probability distribution of X_i , and u is a generated random number between zero and one.

Each random sample (X_1, \dots, X_n), which constitutes a single simulation run, is used to evaluate the performance function Z . Therefore, an estimator of the probability of failure (or exceeding a limit condition), \bar{p}_f , can be found as:

$$\bar{p}_f = \frac{N_f}{N} \quad (2-11)$$

where, N_f is the number of simulation runs for which $Z < 0$, and N is the total number of simulation runs.

As N approximates infinity, the ratio approximates the real probability of failure, p_f . The accuracy of the estimation can be evaluated in terms of the variance of \bar{p}_f , $\text{Var}(\bar{p}_f)$. This variance can be computed by assuming each simulation run as a Bernoulli trial (i.e., a trial that results either in one when there is failure, or in zero when there is not failure):

$$\text{Var}(\bar{p}_f) \cong \frac{(1 - \bar{p}_f)\bar{p}_f}{N} \quad (2-12)$$

The statistical accuracy of the estimated probability is customarily measured in terms of the coefficient of variation of the estimator, $\text{COV}(\bar{p}_f)$:

$$\text{COV}(\bar{p}_f) \cong \frac{\sqrt{\frac{(1 - \bar{p}_f)\bar{p}_f}{N}}}{\bar{p}_f} \quad (2-13)$$

Consequently, it may take a large number of simulation runs to achieve a specified accuracy expressed as a small coefficient of variation according to Equation 2-13.

2.5 Variability of Performance Parameters in Concrete Structures

In order to perform probabilistic analysis in reinforced concrete structures, it is necessary to have information on the probability density functions (and/or related statistical distribution) of the parameters (variables) involved. Statistical properties for concrete, reinforcing steel, and geometrical dimensions have been proposed by Mirza, and MacGregor (1976) as follows:

a) Concrete Compressive Strength

In situ concrete compressive strength (f_{cstr}) is described by a Normal distribution with mean (\bar{f}_{cstr}) and coefficient of variation (V_{cstr}). For a loading rate, LR, equal to 0.24 MPa/sec (35 psi/sec):

$$\begin{aligned} \bar{f}_{\text{cstr}} &= (0.675f'_c + 7.59) \leq 1.15f'_c \\ V_{\text{cstr}} &= \sqrt{V_{\text{in-situ}}^2 - V_{\text{in-test}}^2 + V_{\text{ccyl}}^2} \end{aligned} \quad (2-14)$$

For loading rates (LR) other than 0.24 MPa/sec (35psi/sec):

$$\begin{aligned} \bar{f}_{\text{cstrR}} &= 0.89(1 + 0.08 \log_{10} 145\text{LR})(0.675f'_c + 7.59) \leq 1.15f'_c \\ V_{\text{cstrR}} &= \sqrt{V_{\text{in-situ}}^2 - V_{\text{in-test}}^2 + V_{\text{ccyl}}^2 + V_{\text{rate}}^2} \end{aligned} \quad (2-15)$$

where:

f'_c : design compressive strength (MPa),

V_{ccyl} : coefficient of variation (COV) of the compressive strength of concrete obtained from cylinders,

$V_{\text{in-situ}}$: COV of the concrete compressive strength in structure,

$V_{\text{in-test}}$: COV representing in-test variations, and

R: rate of loading (MPa/sec).

Suggested values for $V_{in-situ}$, $V_{in-test}$, and V_{rate} are:

$$V_{in-situ} = 10\%, V_{in-test} = 4\%, V_{rate} = 5\% \quad (2-16)$$

On the basis of test data available, Mirza et al. (1979) suggested that the average coefficient of variation for concrete compressive strength could be taken as roughly constant and equal to 10%, 15%, and 20% of \bar{f}'_c for strength levels below 27.6 MPa (4000 psi) for excellent, average, and poor control respectively. For concrete with average compressive strength above 27.6 MPa (4000 psi), the standard deviation remains approximately constant with values of 2.76 MPa (400 psi), 4.14 MPa (600 psi), and 5.52 MPa (800 psi) for the three levels of control listed previously.

More recently, Stewart and Attard (1999) have suggested a mean value for in-situ concrete compressive strength equal to $\bar{f}'_c + 7.59$ MPa (1100 psi) and a standard deviation equal to 6 MPa (870 psi).

b) Concrete Tensile Strength

Splitting tensile strength of concrete (f_{sp}) is described by a Normal distribution with the following mean (\bar{f}_{sp}) and COV ($V_{f_{sp}}$):

$$\begin{aligned} \bar{f}_{sp} \text{ (MPa)} &= 0.54\sqrt{\bar{f}'_c \text{ (MPa)}} \\ V_{f_{sp}} &= \sqrt{V_c^2 / 4 + 0.12^2} \end{aligned} \quad (2-17)$$

where, \bar{f}'_c and V_c are the mean and COV of the compressive strength of concrete respectively.

c) Modulus of Rupture

The modulus of rupture (f_r) is described by a Normal distribution with the following mean (\bar{f}_r) and COV (V_{f_r}):

$$\begin{aligned} \bar{f}_r \text{ (MPa)} &= 0.66\sqrt{\bar{f}'_c \text{ (MPa)}} \\ V_{f_r} &= \sqrt{\frac{V_c^2}{4} + 0.19^2} \end{aligned} \quad (2-18)$$

d) Modulus of Elasticity of Concrete

The initial tangent modulus, E_{ci} , is described by a Normal distribution with the following mean (\bar{E}_{ci}) and COV ($V_{E_{ci}}$):

$$\begin{aligned} \bar{E}_{ci} &= 5,020\sqrt{\bar{f}_{cstruc} \text{ (MPa)}} \\ V_{E_{ci}} &= \sqrt{\frac{V_{cstruc}^2}{4} + 0.07^2} \end{aligned} \quad (2-19)$$

where, \bar{f}_{cstruc} is the mean compressive strength of concrete in structure, and V_{cstruc} is the COV of compressive strength of concrete in the structure.

e) Secant Modulus

The secant modulus, E_{cs} , is described by a Normal distribution. The mean is computed at any stress level from the initial tangent modulus assuming a parabolic stress-strain curve. The COV ($V_{E_{cs}}$) is given by:

$$V_{E_{cs}} = \sqrt{\frac{V_{cstruc}^2}{4} + 0.12^2} \quad (2-20)$$

f) Yield Strength of Reinforcing Steel

The yield strength of reinforcing steel, f_y , is described by a Beta distribution. The probability density function (PDF) for grade 40 bars is given by:

$$\text{PDF} = 3.7138 \left[\frac{f_y - 248}{221} \right]^{2.2105} \left[\frac{470 - f_y}{221} \right]^{3.8157} \quad (248 < f_y < 470 \text{ MPa}) \quad (2-21)$$

The PDF for grade 60 bar is given by:

$$\text{PDF} = 7.1562 \left[\frac{f_y - 393}{352} \right]^{2.0204} \left[\frac{745 - f_y}{352} \right]^{6.9545} \quad (393 < f_y < 745 \text{ MPa}) \quad (2-22)$$

A reduction of 15% in the mean value should be applied for #14 and #18 bars.

g) Modulus of Elasticity of Steel

The modulus of elasticity of steel, E_s , is described by a Normal distribution with mean (\bar{E}_s) and COV (V_{E_s}) given by:

$$\begin{aligned} \bar{E}_s &= 201,400 \text{ MPa (29,000 ksi)} \\ V_{E_s} &= 0.024 \end{aligned} \quad (2-23)$$

h) Reinforcing Steel Area

The ratio of measured to nominal bar area, A_m/A_n , is described by a Normal distribution truncated at 0.94 and 1.06 with mean (\bar{r}) and COV (V_r):

$$\begin{aligned} \bar{r} &= 0.988 \\ V_r &= 0.024 \end{aligned} \quad (2-24)$$

i) Member Dimensions

Statistical parameters for dimensions of concrete slabs and beams, according to Mirza and MacGregor (1979), are given in Tables 2-1 and 2-2.

j) Corrosion Related Parameters

Based on experimental measurements, Weyers et al. (1994b) suggested typical values for the mean and standard deviations of the diffusion coefficient and the chloride concentration at 2.5 in. deep from the surface of the member. In Indiana, for example, the following mean values and standard deviations were recommended:

- ❖ Diffusion coefficient: 0.1 and 0.04 in²/yr
- ❖ For the surface chloride concentration: 8.9 and 3.7 lbs/yd³

Stewart and Rosowski (1998) have assumed the rate of corrosion after initiation as a Uniform variable ranging from 0.001 to 0.0021 mA/cm².

2.6 Variability of Load Factors and Load Models

Live and dead loads can be part of the input parameters for the performance predictive models for the different distress indicators. Therefore consideration of these parameters as random variables is necessary in carrying out the statistical simulation process. An extensive study to develop probability-based load criteria for structural design of

buildings was reported by Ellingwood et al. (1980), Galambos et al. (1982), and Ellingwood et al. (1982). Common load factors and load combinations were recommended for all construction materials along with guidance for development of resistance factors for various construction materials.

According to Nowak (1993), the dead load of bridge members (load due to self-weight) can be considered as a Normal random variable. After identifying three components of dead load, the corresponding statistical parameters were established as listed in Table 2.3.

Traffic load has two components, namely, static and dynamic. Each component is treated as a random variable. The static component is the self-weight of a truck. The dynamic component is represented by a static-equivalent factor of impact, I . Therefore, if WT is the total truckload, then the live load can be represented by a single random variable w_t :

$$w_t = (1+I)WT \quad (2-25)$$

According to Nowak (1993), the impact factor, I , is statistically independent of the truckload so that the statistical parameters- mean (u_{w_t}) and COV (V_{w_t})- for truckload are given by:

$$u_{w_t} = (1+u_I)u_{WT} \quad (2-26)$$

$$V_{w_t}^2 = V_{(1+I)}^2 + V_{WT}^2 + V_{(1+I)}^2 V_{WT}^2 \quad (2-27)$$

where, u_{WT} , V_{WT} , u_I , and V_I are the mean and COV of the truckload and impact coefficient respectively.

According to data from surveys, truckload has an approximate Normal distribution. Laman and Nowak (1995) suggested the values $u_{WT} = 250$ KN and $V_{WT} = 0.4$. It was found that for multiple-lane bridges the critical load effect occurs when two heavily loaded, fully correlated-weight trucks, are side by side. Laman and Nowak also suggested that the mean value for I does not exceed 0.15 for a single truck, and 0.1 for two trucks side by side. Using the previous information, the statistical parameters for the live load are: $u_{w_t} = 287$ KN and $V_{w_t} = 0.412$ for a single truck, and $u_{w_t} = 275$ KN and $V_{w_t} = 0.408$ for one of two trucks side by side.

The load caused by the heaviest truck is the most important factor in a strength reliability-based assessment. With the number of trucks in the period under consideration denoted by N_T , and Φ as the cumulative Normal standard function, the cumulative statistical distribution of the heaviest truck, F_{N_T} , is given by:

$$F_{N_T} = \left[\Phi \left(\frac{w_t - u_{w_t}}{u_{w_t} V_{w_t}} \right) \right]^{N_T} \quad (2-28)$$

2.7 Implementation of Reliability Concepts in the Methodology for PRS

The required components to conduct a reliability analysis in the framework of a PRS are the predictive models, the corresponding limit conditions for the predicted distresses, and the definition of the statistical characteristics of the input parameters for the predictive models. The performance function, Z , (Eq. 2-1) is equal to the calculated amount of distress (or demand, S) subtracted from the allowable amount of distress (or capacity, R). The main idea of the simulation procedure is to infer the statistical distribution of the performance function. Then the probability of failure, p_f , can be calculated as the probability that the performance function is less than zero ($p_f = P(Z < 0)$).

In the simulation procedure, the predictive models are implemented to calculate the “demand” term, S , and the capacity term, R , into the performance function (Eq. 2-1). Sometimes, the definition of limit states for the different distress indicators determines the capacity term, R . If crack width is a distress indicator, then the allowable crack width is the capacity, and the actual calculated crack width is the demand. If the susceptibility to flexural failure is a distress indicator, then the flexural strength is the capacity, and the maximum external (dead plus live) moment is the demand.

The results of the simulation, a set of probability of failures, define the performance of the element into consideration in the context of a PRS. Subsequently, performance can be expressed in terms of Life Cycle Cost (LCC). If the costs of the “failures” associated with the limit conditions are known, the corresponding probabilities can be monetarily quantified.

Following the approach previously described, the LCC for different systems can be obtained after establishing the corresponding statistical characteristics of the input parameters for the performance predictive models. The goal of the methodology for a PRS is to be able to compare the performance of what is expected from the as-designed structure to what is actually obtained during construction (as-built structure). A first approximation in that effort is to assume that the variations of the quality characteristics for the as-designed structure are the typical variation levels reported in Sections 2.5 and 2.6, and that the mean values are the values submitted in the design. For the as-built structure the mean value and standard deviation for the quality characteristics are obtained from direct measurements in-situ. For some of the constant characteristics of the as-built structure, such as truckload, the statistical parameters could be established according to Sections 2.5 and 2.6.

The performance predictive models corresponding to the selected distress indicators for an initial case study are introduced in Appendix A. Through these models, the definition of the performance function, Z , is possible (Section 2.2) and the simulation procedure is carried out for a simply supported member. The study of this elementary case allows establishing the basis for the proposed generalized methodology.

Table 2.1 Statistical Parameters for Reinforced Concrete Slab Dimensions

	(a) In Situ Slabs			
Description	Nominal Range (in.)	Mean Deviation from Nominal (in.)	Standard Deviation (in.)	<u>Distribution</u>
Thickness	4-9	+1/32	15/32	Normal
Top Reinforcement:				
Effective Depth	4-8	-3/4	5/8	Normal
Concrete Cover	N/A	+25/32	25/32	
Bottom Reinforcement:				
Effective Depth	4-8	-5/16	5/8	Normal
Concrete Cover	N/A	+11/32	13/32	

Table 2.1 (Continued)

	(b) Precast Slabs			
Description	Nominal Range (in.)	Mean Deviation from Nominal (in.)	Standard Deviation (in.)	Distribution
Thickness	6-9	0	3/16	Normal
Top Reinforcement:				
Effective Depth Concrete	4-8	0	3/32	Normal
Cover	N/A	N/A	7/32	
Bottom Reinforcement:				
Effective Depth Concrete	4-8	0	3/32	Normal
Cover	N/A	N/A	7/32	

Table 2.2 Statistical Parameters for Reinforced Concrete Beams Dimensions

	(a) In Situ Slabs			
Dimension Description	Nominal Range (in.)	Mean Deviation from Nominal (in.)	Standard Deviation (in.)	Distribution
Width of Rib	11-12	3/32	3/16	Normal
Overall Depth	18-27	-1/8	1/4	Normal
Top Reinforcement				
Concrete Cover	1½	+1/8	5/8	Normal
Effective Depth	N/A	-1/4	11/16	Normal
Bottom Reinforcement				
Concrete Cover	¾-1	1/16	7/16	Normal
Effective Depth	N/A	-3/16	1/2	Normal
Stirrup Spacing	N/A	0	17/32	Normal
Beam Spacing	N/A	0	11/16	Normal

Table 2.2 (Continued)

	(b) Precast Slabs			
Dimension Description	Nominal Range (in.)	Mean Deviation from Nominal (in.)	Standard Deviation (in.)	Distribution
Width of rib	14	0	3/16	Normal
Width of Flange	19-24	+5/32	1/4	Normal
Overall Depth	21-39	+1/8	5/32	Normal
Top Reinforcement				
Concrete Cover	2-2½	0	5/16	Normal
Effective Depth	N/A	+1/8	11/32	Normal

Bottom Reinforcement				
Concrete Cover	$\frac{3}{4}$	0	5/16	Normal
Effective Depth	N/A	+1/8	11/32	Normal
Stirrup Spacing	N/A	0	11/32	Normal
Beam Spacing	N/A	0	11/32	Normal

N/A: not available

Table 2.3 Statistical Parameters for Dead Load

Component	Bias	COV
<u>Factory-Made Members</u>	1.03	0.08
Cast-in-Place Members	1.05	0.10
Asphalt	99 mm*	0.25

*Mean Thickness

3 PRELIMINARY METHODOLOGY OF PRS -INITIAL CASE STUDY

3.1 Introduction

In this Section, a description of the methodology of a PRS for the initial case study is presented. This initial case study is a simply supported concrete member to be monitored during construction. The performance of a simply supported concrete member has been defined in terms of the following distress indicators:

- 1) Excessive corrosion deterioration
- 2) Excessive transverse cracking
- 3) Excessive deflections
- 4) Susceptibility to flexural failure

The first three distress indicators determine serviceability, and the fourth one addresses the flexural strength of the member into consideration. The aim in this section is to incorporate the performance predictive models presented in Appendix A in a reliability-based framework (Chapter 2). First, the definition of limit conditions for the different distress indicators selected in Appendix A is addressed. Using these limits, and the corresponding predictive models a simulation process is carried out using Monte Carlo simulation for corrosion deterioration. First-Order Second Moment (FOSM) reliability analysis is conducted for the remaining distress indicators. From the simulation, a set of probabilities of failure is calculated for each distress indicator. Next, cost models are presented and implemented to translate the calculated set of probabilities of failure into an estimate of the Life Cycle Cost (LCC) of the structure. The costs calculated for both the as-designed and the as-built structure are used to estimate a pay factor. The pay factor is defined as the ratio of the LCC of the as-designed to the as-built structure. Finally, the proposed methodology for a PRS is illustrated with four numerical examples.

3.2 Limit Conditions

3.2.1 Corrosion Deterioration

Two limit conditions determine the deterioration process associated with corrosion of the steel reinforcement: (a) the critical chloride concentration to initiate corrosion, C_{cr} , and (b) the percentage of deteriorated concrete surface initiating repair/replacement.

Several studies (Cady and Weyers, 1983, Weyers and Cady, 1987, Frangopol et al., 1997, Amey et al., 1998, Stewart and Rosowski, 1998b) have shown that the critical chloride concentration to initiate corrosion, C_{cr} , tends to lie in the range from 0.6 to 1.4 kg/m³ (1 to 2.4 lbs/yd³). As recommended by Stewart and Rosowsky (1999), this parameter is taken as a uniform random variable in the given interval.

The Bridge Rehabilitation Unit of the Indiana Department of Transportation (INDOT) calls for replacement when 25% or more of a given concrete bridge deck needs full depth patching. If more than 40% of a given deck needs partial depth patching, removal of the deck is adopted. Since the model used to estimate the time for a specific percentage of deteriorated concrete surface does not distinguish between deterioration needing full or partial patching, it is assumed that replacement will be required when the percentage of “deteriorated concrete”, p , (see, Section B.1) is between 25% and 40%. The limit condition is therefore considered as a uniform random variable in that interval.

3.2.2 Excessive Crack Width

In the ACI Code (ACI 318-95), crack widths were controlled by restricting the value of a parameter, denoted by z , related to the tensile stress in the reinforcing steel. For interior and exterior exposure, the maximum crack width implicitly evoked is 0.041 and 0.033 cm respectively. The AASHTO standard specifications (1992) restricted, z , to a value such that the allowable crack width for interior and exterior exposure is 0.040 and 0.033 cm respectively. Some investigations (Gergely, 1981, Wilkins and Lawrence, 1983) have shown, however, that corrosion initiation is not significantly affected by crack widths less than about 0.030 to 0.061 cm. After extensive experimental work,

loading concrete elements during a period of 12 years in a simulated marine environment, Francois and Aelguie (1998) concluded that the development of reinforcement corrosion is not influenced by the crack itself, or by crack width, when the former is less than 0.051 cm (0.02 inches).

Based on the previous discussion, it is assumed that the allowable crack width ranges from 0.033 to 0.061 cm (0.013 to 0.024 inches). Adopting a recommendation by Stewart and Rosowsky (1998), the allowable crack width is considered as a random variable uniformly distributed in that interval.

3.2.3 Flexural Failure

Flexural failure occurs whenever the mid-span live load plus dead load moment, assumed as the maximum along the span, exceeds the flexural capacity of the member. The flexural capacity is calculated from the sectional moment-curvature diagram as the moment associated with a maximum strain of 0.003 in the extreme fiber of the concrete flexural compression zone. It is also assumed that the strength of the element diminishes with time according to a deterioration function defined in Section A.5.3

3.2.4 Excessive Deflections

Deflection limits are expressed as a function of the span length, L , in both building and bridge codes. In the ACI 318-99 code, limit values ranging from $L/480$, for roof or floors attached to non-structural elements likely to be damaged (due to sustained plus live load), to $L/180$, for flat roofs not attached to non-structural elements (due to live loads) are given. The AASHTO Standard Specifications (1992) only control deflections due to live load plus impact (in avoiding undesirable vibrations); $L/800$ is the allowable dynamic deflection except in urban areas used in part by pedestrians where $L/1000$ is preferable.

Xanthakos (1994) suggests a limit deflection for bridges of $L/500$ as a compromise between the maximum permitted for several bridge types in various bridge design codes. In Xanthakos (1994), a limiting deflection for the deck plate of $L/300$ is given as entirely justified considering the intent to prevent the deterioration of the wearing surface.

A wide range of values for the maximum allowable deflection can be found in the literature. Therefore, the work for the PRS assumes the allowable sustained plus live load deflection as a uniform random variable in the interval $L/500$ to $L/250$.

3.3 Constant and Quality Characteristics

Sections 2.5 and 2.6 contain the basic information for the typical variations (distributions and/or mean and standard deviations) of some parameters affecting the performance of concrete structures. Table 3.1 summarizes the input values for the models and limits, including their statistical parameters and/or distributions, used in the case study.

It must be pointed out that mean values and standard deviations for the input parameters of the models might be needed in the simulation process. In particular, while carrying out a First Order Second Moment Reliability analysis (FOSM), the mean value and standard deviation are required to define the statistical information of the those input parameters. In some cases, the mean value and standard deviation for input parameters were not directly specified in the literature. For example, yielding stress of steel, maximum truckload, and some limit states having a uniform distribution. In those cases the means and standard deviations were calculated from the original probability distributions. Details of these calculations are not provided in this work. For a discussion about the calculation of the mean and variance of random variables obeying any statistical distributions see Devore, J. L. (1995).

3.4 Statistical Simulation of Performance Predictive Models

The performance predictive models presented in Appendix A are set up on a statistical framework considering both some of the inputs and the output as non-deterministic variables described either by a suitable probability distribution or the corresponding statistical parameters (commonly, mean and standard deviation). The values of the mean and standard deviation for the constant characteristics in both the as-designed and the as-built structure and for

the quality characteristics in the as-designed structure are set in accordance with Table 3.1. The values for the quality characteristics in the as-built structure should be obtained from in-situ measurements.

3.4.1 Time Dependence of the Probabilities of Failure

For all models implemented in the initial case study, except the model predicting crack widths, the probabilities of failure were calculated on a yearly basis. It was assumed that those probabilities were independent from year to year. This assumption implies that, for every specific point in time, a complete statistical simulation is carried out without accounting for the influence of probabilities of failure at earlier ages.

The probability of flexural failure was considered as time-dependent due to both the corrosion deterioration effect (Section A.5.3) and the increasing probability of an extreme truckload as NT (the expected number of heavy trucks) in Equation (2-28) increases with time.

The probability of having excessive deflections was considered time-dependent due to the effects of creep and shrinkage (Appendix B) associated with the dead loads. Live load deflections were computed for the case of a single truck (NT=1).

The probability of excessive corrosion deterioration is clearly time-dependent. For a given time, t, the probability equals the area to the left of, t, under the probability mass function of T_p (the random variable representing the time to repair according to Equation B-1).

The probability of having excessive crack widths was considered as time-independent. Flexural crack widths were calculated only for dead loads because the cracks associated with live load effects tend to close when the loads are removed. The probability of having excessive crack widths was calculated at several sections along the span and averaged for the entire member. Only the average crack width is reported herein.

3.4.2 Adopted Simulation Procedure

For the preliminary PRS methodology, it was decided to use direct Monte Carlo simulation for the corrosion deterioration model (as few as 10,000 cycles were enough to get convergence). FOSM was implemented for the remaining distresses (the probabilities of failure were excessively small and, as a consequence, the computation demand by using direct Monte Carlo was excessive). Software consisting of a spreadsheet having an interface with Microsoft Visual Basic 5.0 was developed to carry out the simulation. Figure 3.1 illustrates the features of the developed spreadsheet. Three main headings are found in the spreadsheet: constant characteristics, quality characteristics, and probabilities of failure. Under the heading of constant characteristics the different input parameters for the models are divided in deterministic and non-deterministic variables. The input parameters under the heading of quality characteristics are considered as non-deterministic variables except water/cement ratio. Deterministic variables require only the definition of mean value whereas non-deterministic variables require the definition of the mean value and standard deviation, or the associated probability distribution. The probabilities of failure for the different distress indicators are plotted on the right corner of the spreadsheet. The Life Cycle Cost for the as-designed and the as-built conditions is presented in the right lower corner of the spreadsheet as well as the estimated Pay Factor. The LCC is calculated as discussed next.

3.5 COST MODELS

The set of probabilities of failure calculated in the simulation procedures, as discussed in Section 3.4, is translated into Life Cycle Cost (LCC) by using the cost models presented in this section. The basic idea is that the LCC of the structure changes as the simply supported member deteriorates and becomes less reliable (more prone to fail in terms of strength and serviceability) with time. The LCC is calculated on a yearly basis. Then the LCC averaged over a horizon life is used to calculate the pay factor. In a given year, t, the present value of the LCC is estimated as:

$$LCC(t) = I + \sum_{i=0}^t \frac{M(i)}{(1+r(t))^i} + \sum_{i=0}^t \frac{U(i)}{(1+r(t))^i} + \sum_{k=1}^n \frac{p_{fk}(t)C_k}{(1+r(t))^t} \quad (3-1)$$

where:

I: investment cost;

M(i): regular maintenance cost at time $i \leq t$;

r(t): discount rate at t;

U(i): user cost due to the additional deterioration of the slab (or beam) condition at time i;

$p_{nk}(t)$: probability of failure at time, t, associated with the k^{th} distress (corrosion deterioration, flexural cracking, corrosion deterioration, or excessive deflections);

n: number of distresses to be controlled (four); and

C_k : repair cost associated with the limit state for the k^{th} distress.

The discount rate, r(t), is equal to the opportunity rate minus the inflation rate. For civil engineering applications, a constant r(t) ranging from 4% to 6% is customarily assumed.

3.5.1 Agency Costs

Agency costs include investment (initial), repair and maintenance costs. In this section the following cost items are implemented:

- a) **removing and patching concrete:** an average value of \$270 per square meter of deteriorated area (Grace Co., 1998)
- b) **concrete overlay:** \$7.5/m² for scarifying deck + \$54/m² for placing and curing 4.4 cm of concrete overlay (INDOT Design Division) + \$22/m² for traffic control (Purbis et al. 1994) = \$83.5 per square meter of slab.
- c) **average replacement cost for concrete bridge slabs:** as reported by Xanthakos (1996) for several departments of transportation in the U.S.A, \$377/m².
- d) **regular maintenance costs:** are assumed as \$0.75/m², which is a reasonable average of the cost reported by several U.S agencies(Xanthakos, 1996).

3.5.2 User Costs

Under certain circumstances, such as large spans, and high average daily traffic, user costs are significantly comparable to the agency costs (investment, maintenance and repair). Thus, it is important to consider the influence of user costs in the LCC of the structure.

User costs are typically divided into: (a) during treatment, and (b) prior to treatment and after treatment costs. The first costs are related to congestion as influenced by the degree of bridge closure and the duration of the construction. The second costs are related to the inconveniences associated with the deterioration of the deck. Purbis et al. (1994) suggested expressions for these types of user costs. It was found that the model estimating during treatment costs produced negligible results when compared to prior and after treatment costs. As a result, only prior and after treatment costs were considered in this work. The user cost, U, (\$/year) associated with the worsening of the deck in a specific time, t, when its condition is dictated by the condition index, S(t), is given by:

$$U(t) = 365 aT_f K_1 [S(t)/S_m]^4 q_0 \quad (3-2)$$

where:

S_m : maximum allowable condition index for the deck (limit condition to adopt repair),

q_0 : average two-way daily traffic volume across the bridge (vehicles/day),

a: incremental travel time when $S = S_m$ (expressed as a fraction of T_f),

T_f : free-flow travel time across the bridge (minutes) calculated as the span over the speed limit, and

K_1 : value of bridge user's time while crossing (\$/vehicle/minute).

To make use of Equation (3-2) the ratio S/S_m is taken as the probability of failure, $P_f(t)$. Hence, the equation is written as:

$$U(t) = 365 aT_f K_1 [P_f(t)/S_m]^4 q_0 \quad (3-3)$$

3.6 NUMERICAL EXAMPLES

3.6.1 Introduction

For the element under consideration (slab bridge), probabilities of flexural failure and lack of serviceability due to excessive corrosion deterioration, crack widths, and deflections were calculated for both the as-designed and the as-built structures. These probabilities were then translated into LCC using Equation 3-1. The average LCC across a horizon life is used for calculating the pay factor. This horizon life is arbitrarily assumed as 50 years.

The following cost items were assumed:

- (a) replacement cost of $\$377/\text{m}^2$ due to either flexural failure, excessive deflections, or excessive corrosion deterioration;
- (b) repair cost for concrete overlay of $\$83/\text{m}^2$ due to excessive transverse cracking;
- (c) user cost while crossing the bridge (Purbis et al, 1994) of $K_1 = \$0.166/\text{vehicle}/\text{minute}$; and
- (d) new construction cost of $\$323/\text{m}^2$.

Regular maintenance costs, $\$0.75/\text{m}^2$, are included as a separate category. Accidents and/or mortality costs are not considered in the analysis.

Additional assumptions are:

- constant interest rate, r , of 4%;
- two-way daily traffic of 10,000 vehicles (corresponds to interstate rural highways in Indiana according to Saito and Sinha, 1989);
- speed limit of 50 mph;
- incremental time while crossing the bridge due to excessive corrosion deterioration of 50% of the free travel time (i.e., $a = 0.5$ in Eq. 3-2).

For the conditions described above, four similar examples are presented to illustrate the working structure of the proposed methodology for a PRS. The first example is carried out in full detail. Only a summary of the results is presented for the other three examples.

In the first example the contractor is penalized because of the inferior quality of the construction with respect to the design. In the second example, comparative high standards in the execution of the construction lead the contractor towards receiving an incentive. In the third one, tradeoffs among quality characteristics result in a unity pay factor. The last example is intended to illustrate the beneficial effect of corrosion treatments in the achievement of a pay factor greater than 1.0.

3.6.2 Example: Deficient Construction

Figure 3.2 gives a summary of the input parameters for the models under the heading “constant characteristics” and “quality characteristics”. Using the simulation procedures described in Chapter 2, with the performance predictive models presented in Appendix A, the corresponding probabilities of failure for the as-designed and the as-built structure are calculated. The mean values and standard deviations for the non-deterministic constant characteristics and for the as-designed quality characteristics are obtained from Table 3.1 either directly, or by calculation from the corresponding statistical distribution as discussed in Section 3.3.

In Figure 3.2, under the heading “quality characteristics” it is noted that:

- For the category water over cement ratio, w/c , the as-built structure exhibits a higher mean value than the as-designed structure.
- The mean value for the concrete cover and the effective depth are smaller in the as-built structure.
- The standard deviation for several input parameters is higher in the as-built structure as indicated by the shaded areas.

For excessive crack widths, a time-independent probability of failure is reported (average of single probabilities calculated in ten sections along the span) in Figure 3.2. This probability equals 2.1×10^{-7} for the as-designed and 4.5×10^{-7} for the as-built structure. Figures 3.3, 3.4 and 3.5 (all extracted from Figure 3.2) show the variation with time of the probabilities of flexural failure, excessive deflection, and excessive corrosion deterioration for both the as-designed and the as-built structure. Notice that the inferior standards of the construction (as listed above) compared to the design, result in higher probabilities of failure for the as-built structure. As expected, since the design is satisfactory, small probabilities of flexural failure (Fig. 3.3), ranging from 2×10^{-9} to 5.7×10^{-7} , are found due to small differences between the as-designed and the as-built structure. For excessive deflections (Fig. 3.4) the probabilities of failure range from 1.3×10^{-3} to 6.4×10^{-2} . For corrosion deterioration (Fig. 3.5) the probabilities of failure are relatively much higher, reaching 0.95 at 50 years.

In order to illustrate the use of Equation 3.1, the calculation of the present value of the Life Cycle Cost, LCC, for the as-designed structure at year 30 is discussed next. From Figures 3.3 to 3.5, the probability of flexural failure, excessive deflection, and excessive corrosion deterioration at year 30 is obtained, respectively, as: 5.43×10^{-8} , 0.049, and 0.804. In addition, the probability of excessive crack widths is 2.1×10^{-7} (the same at any year).

All the individual terms of Equation 3-1 are calculated according to the cost items discussed in Section 3.6.1. The area of the slab is estimated as $10.7 \text{ m} \times 14 \text{ m} = 149.8 \text{ m}^2$

- I = investment cost = $\$323/\text{m}^2 \times 149.8 \text{ m}^2 = \$48,385$ (first term of Equation 3-1)
- M = regular maintenance costs (accumulated up to year 30 in present value) =
$$\$0.75/\text{m}^2 \times 149.8 \text{ m}^2 \times \sum_{i=0}^{30} \frac{1}{(1+0.4)^i} = \$2,055$$
 (second term of Equation 3-1)
- Repair costs:

Based on the small probabilities of flexural failure, excessive crack widths, and excessive deflections obtained in Figure 3.2 the impact of the repair costs associated with such distresses on the LCC can be neglected.

The repair cost for excessive corrosion deterioration associated with corrosion deterioration is $\$377/\text{m}^2 \times 149.8 \text{ m}^2 \times 0.804/1.04^{30} = \$14,000$

- User cost:

Only the costs associated with corrosion deterioration are considered for user costs, since this model is the only implemented as a distress indicator for the calculation of the LCC.

For a speed limit of 50 mph the free travel time is:

$$T_f = 10.7 \text{ m} \times 3.28 \text{ ft/m} \times 1/(50 \text{ mi/h} \times 1 \text{ h}/60 \text{ min} \times 5280 \text{ ft/mi}) = 0.008 \text{ min}$$

Using Equation 3-3 and letting $p_f(i)$ denote the probability of excessive corrosion deterioration at year i , the third term of Equation 3-1 (representing the user cost) is:

$$365 \text{ day/year} \times 0.5 \times 0.008 \text{ min} \times \$0.167/\text{vehicle/min} \times 10,000 \text{ vehicles/day} \times [p_f(0) + p_f(1)/1.04 + \dots + 0.804/1.04^{30}] = \$1,133$$

Note that since user costs are cumulative, they become significant towards the end of the horizon life of the structure.

The present value of the LCC of the as-designed structure at year 25, adding up all the terms of Equation 3.1 is $\$65,573$.

Following the same procedure, the present cost at other years (50 in total) is calculated. The average LCC for the as-designed structure turns out to be $\$59,121$. Similarly, the corresponding LCC for the as-built structure is calculated as $\$60,791$.

As a result of the lack of compliance during the construction with the as-design condition the contractor's bid price could be modified by a Pay Factor = $LCC_{\text{as-designed}}/LCC_{\text{as-built}} = 0.973$.

3.6.3 Example: High Quality Construction

In this example the input parameters for the models are the same than in the previous example (Section 3.6.2) except for some of the quality characteristics of the as-built structure. Figure 3.6 summarizes the information regarding the input parameters of the models as well as the corresponding probabilities of failure for each distress indicator. The higher quality during construction as compared to the as-designed structure is noted under the heading “quality characteristics” for the following categories:

- The water over cement ratio, w/c, for the as-built structure is lower than for the as-designed structure.
- The concrete cover for the as-built structure is greater than for the as-designed structure.
- Furthermore, the standard deviations for the as-built structure are less than for the as-designed structure as indicated in the shaded cells of the spreadsheet.

Only repair and user costs due to corrosion deterioration were considered in the calculation of the LCC. It is found that the estimated LCC for the as-designed structure is \$60,764 and the corresponding LCC for the as-built structure is \$59,211. As a result the contractor’s bid price could be modified by a favorable Pay Factor = 1.026.

3.6.4 Example: Tradeoffs Among Quality Characteristics

The example presented in Section 3.6.2 is slightly modified by changing some of the values (means and standard deviations) of the quality characteristics. The information regarding the input parameters for the models is summarized in Figure 3.7 as well as the corresponding probabilities of failure. As can be noted under the heading “quality characteristics” some of the standards during the construction are higher and some are lower than the as-designed standards. It is important to observe that:

- A lower concrete cover was measured for the as-built condition as compared to the as-designed condition (deficient quality during construction)
- A lower water to cement ratio, w/c, was obtained during construction as compared to the as-designed condition (improved quality during construction).

Again, repair costs associated with distresses other than corrosion deterioration were neglected. Only user cost due to corrosion deterioration were considered. The resulting LCC for the as-designed and the as-built structure are respectively: $LCC_{\text{as-designed}} = \$59,245$, and $LCC_{\text{as-built}} = \$59,337$. A Pay Factor = 0.998 is obtained as a consequence.

3.6.5 Example: Use of Epoxy-Coated Reinforcement

The same example discussed in Section 3.6.2 is presented in this section with the only difference being that for the as-built structure, epoxy-coated reinforcement was implemented instead of black steel (as specified in the as-designed condition). The intent of using epoxy-coated reinforcement during construction was to improve the performance of the structure in terms of corrosion deterioration. As assumed in Section A.2.5, the effect of such treatment on the corrosion deterioration process is represented by an increase in the critical chloride concentration required to initiate corrosion from 1.4 to 4 kg/m³ (for Indiana) (2.4 to 6.7 lbs/yd³). Figure 3.8 contains the input parameters and the corresponding probability of failure curves for the different distress indicators.

It is observed that the LCC for the as designed structure is \$59,121 and for the as-built structure is \$53,678. The associated pay factor is 1.101. This represents an increase of $1.1/0.97 = 1.13$ in the pay factor due the use of epoxy-coated bars.

3.7 Conclusions from the Initial Case Study

The initial case study serves as the foundation for a more general methodology of a PRS. The main conclusions that drawn from such study are:

- 1) The level of compliance between the as-built and the as-designed conditions of a concrete bridge element can be measured through the implementation of performance predictive models, statistical simulation, and cost models. Reliability theory provides a rational tool to account for the non-deterministic nature of the input parameters in the predictive models and to allow evaluating a relative LCC ($LCC_{as-designed} / LCC_{as-built}$) as a criterion for management actions. The methodology has been successfully implemented for a simply supported member. After that experience, the incorporation of other structural configurations must follow.
- 2) The methodology is capable of capturing small differences in quality standards implemented during the case study. This is reflected by the calculation of favorable and unfavorable pay factors for the different cases.
- 3) Tradeoffs among quality characteristics are possible in the suggested methodology as illustrated in the third example (Section 3.6.4). This allows the contractor to make up for possible deficiencies during construction.
- 4) The fourth example (Section 3.6.5), showed the case where a high pay factor (1.10) was obtained. This indicates that the agency implementing the methodology for PRS should define boundaries for such pay factor, i.e., a minimum value below which the construction is rejected (unacceptable quality), and a maximum value to ensure realistic monetary adjustments. In the methodology for PRS for PCC pavements a maximum pay factor from 1.05 to 1.10 was preliminary established from two field trials of the methodology but it was claimed that each agency should determine its own limit.
- 5) Transverse cracking, susceptibility to flexural failure, and excessive deflections are not significant in the calculation of the average LCC for the examples presented because the associated probabilities of failure were so small. For structural configurations other than simply supported members (initial case study) such probabilities of failure will tend to decrease due to the ability of the structure to provide alternate load paths. Consequently, transverse cracking, susceptibility to flexural failure, and excessive deflections need not significantly contribute to the LCC in more complex structural configurations. This conclusion is further supported with the results of surveys carried out by Departments of Transportation in the U.S where corrosion deterioration was declared as the most common distress indicator encountered in current concrete structures. This finding suggests a simplified approach that would include only the repair and user costs associated with corrosion deterioration in the computation of the LCC. Regardless, the difficulties involved in the monetary quantification of distresses other than corrosion deterioration makes it impractical to include them at this time in the estimation of the LCC. However, the simulation of such distresses could be kept in the framework of PRS as flags to prevent the improper use of the methodology. Notice, for example, that if corrosion deterioration were the only distress to be included in the framework of PRS, the contractor might be misled to excessively increase the concrete cover while at the same time maintaining the same overall thickness in an attempt to obtain a favorable pay factor. This is a detrimental action to the safety of the member, and can be detected if a model simulating the probability of flexural failure is available.

3.8 Other Potential Applications

Maintenance strategies can also be developed through the implementation of performance models, reliability theory, and cost models. As a first approximation, consider corrosion deterioration as the unique distress indicator. Using the predictive model presented in Section A.2 and statistical simulation, it is possible to estimate the time-dependent probability of exceeding a certain limit condition. Such limit condition can be defined, for example, as the percentage of deteriorated slab to adopt replacement (which is somewhere between 25% and 40% according to INDOT's policies). If it is further assumed, for simplicity, that after corrective actions are taken the probability of failure is reduced to zero, then several alternative treatments can be studied to minimize the associated repair costs.

Consider the situation in which the agency has the alternative of taking corrective actions at two different times, t_1 , and, t_2 , such that $t_1 < t_2$. Assume that the present cost of the corrective actions is C . At times t_1 and t_2 , the probabilities

of exceeding the performance limits are calculated (from the simulated model) as, p_{f1} , and, p_{f2} , respectively. Obviously $p_{f1} < p_{f2}$. For a constant interest rate, r , the expected present cost of repair at, t_1 , is:

$$\frac{C \times p_{f1}}{(1+r)^{t_1}} \quad (3-4)$$

The corresponding cost of repair at t_2 is:

$$\frac{C \times p_{f2}}{(1+r)^{t_2}} \quad (3-5)$$

From the comparison of these two costs, the agency can decide when to repair in order to get minimum costs. The methodology can be refined and applied to aim towards optimum repair and/or maintenance strategies.

Table 3.1 Summary of the Statistical Values

(a) Constant Characteristics

<u>Deterministic Variables</u>		<u>Units</u>			
Life Service (Years)		years			
Age at Loading		days			
Age When Drying Begins		days			
Aggregate/Cement		none			
Cement Content of Concrete		lb/ft ³			
Span (L)		ft			
Diameter of Top Bar		in.			
Number Heavy Trucks/Year		none			

<u>Non-Deterministic Variables</u>	<u>Units</u>	<u>Distribution</u>	<u>Reference</u>	<u>Suggested Values</u>	
				<i>Mean</i>	<i>Std. Dev.</i>
Relative Humidity	(decimal)	Uniform	None	None	None
Corrosion Rate	mA/ft ²	Uniform	Stewart and Rosowsky (1998)	Max = 1.96	Min = 0.93
Critical Chloride Concentration	kg/m ³	Uniform	Multiple	Max = 1.4	Min = 0.6
Allowable Deflection	in.	Uniform	None	Max = L/250	Min = L/500
Allowable Crack Width	in.	Uniform	Stewart and Rosowsky (1998)	Max = 0.024	Min = 0.013
Area of Tensile Steel	in ²	Normal	Mirza and MacGregor (1976)	0.988×Nominal	0.024×Nominal
Area of Compressive Steel	in ²	Normal	Mirza and MacGregor (1976)	0.988×Nominal	0.024×Nominal
Superimposed Dead Load	kip/ft	Lognormal	Ellingwood et al. (1980)	1.05×Nominal	0.105×Nominal
Steel Yielding Stress, G40	-	Beta ¹	Mirza and MacGregor (1976)	A = 36, B = 68 ksi	$\alpha = 3.2105, \beta = 3.8157$
Steel Yielding Stress, G60	-	Beta ¹	Mirza and MacGregor (1976)	A = 57, B = 108 ksi	$\alpha = 3.0204, \beta = 7.9545$
Modulus of Elasticity of Steel	ksi	Normal	Mirza and MacGregor (1976)	29,200	700
Surface Chloride Concentration*	lb/ft ³	Lognormal	Weyers et al. (1994)	0.33	0.14
Diffusion Coefficient*	in ² /yr	Normal	Weyers et al. (1994)	0.09	0.036
Single Truck Load	kip	Normal	Nowak and Hong (1991)	65	27

Table 3.1 Summary of the Statistical Values

(b) Quality Characteristics²

<u>Parameter</u>	<u>Unit</u>	<u>Distribution</u>	<u>Reference</u>	<u>Suggested Values</u>	
				<i>Mean</i>	<i>Std. Dev</i>
w/c	None	None	Indot Specifications (1999)	0.5	None
Width	ft	None	None	None	None
Unit Weight of Concrete	pcf	Normal	None	150	10
Concrete Compressive Strength	ksi	Lognormal	Attard and Stewart (1999)	$f'_c + 1.1 \text{ ksi}$	0.87
Concrete Cover Top	in.	Normal	Mirza and MacGregor (1979a)	Nominal + 0.78 in. (Nominal) ₃	0.65 (0.22) ₃
Effective Depth	in.	Normal	Mirza and MacGregor (1976)	Nominal - 0.3 (Nominal) ₃	0.63 (0.09) ₃
Depth of Compression Steel	in.	Normal	Mirza and MacGregor (1979a)	Nominal + 0.78 in.	0.65
Spacing of Tensile Steel	in.	Normal	None	Nominal	0.63 ⁴
Lateral Cover	in.	Normal	None	Nominal	0.63 ⁴
Thickness	in.	Normal	Mirza and MacGregor (1976)	Nominal + 0.03 in. (Nominal) ₃	0.47 (0.19) ₃

*Values Recommended by Weyers et al. (1994) for Indiana, the associated w/c is assumed as 0.4

(1) A(ksi),B(ksi), α (non-dimensional) and β (non-dimensional) are the parameters of the corresponding Beta distribution

(2) In principle, the statistical parameters apply for the as-designed structure. For the as-built structure, the statistical parameters of the quality characteristics are expected to be obtained from in-situ measurements

(3) Values in parenthesis are for pre-cast members as suggested in the literature (Section 2.5)

(4) Values are not available in the literature, further study is required to define their variations

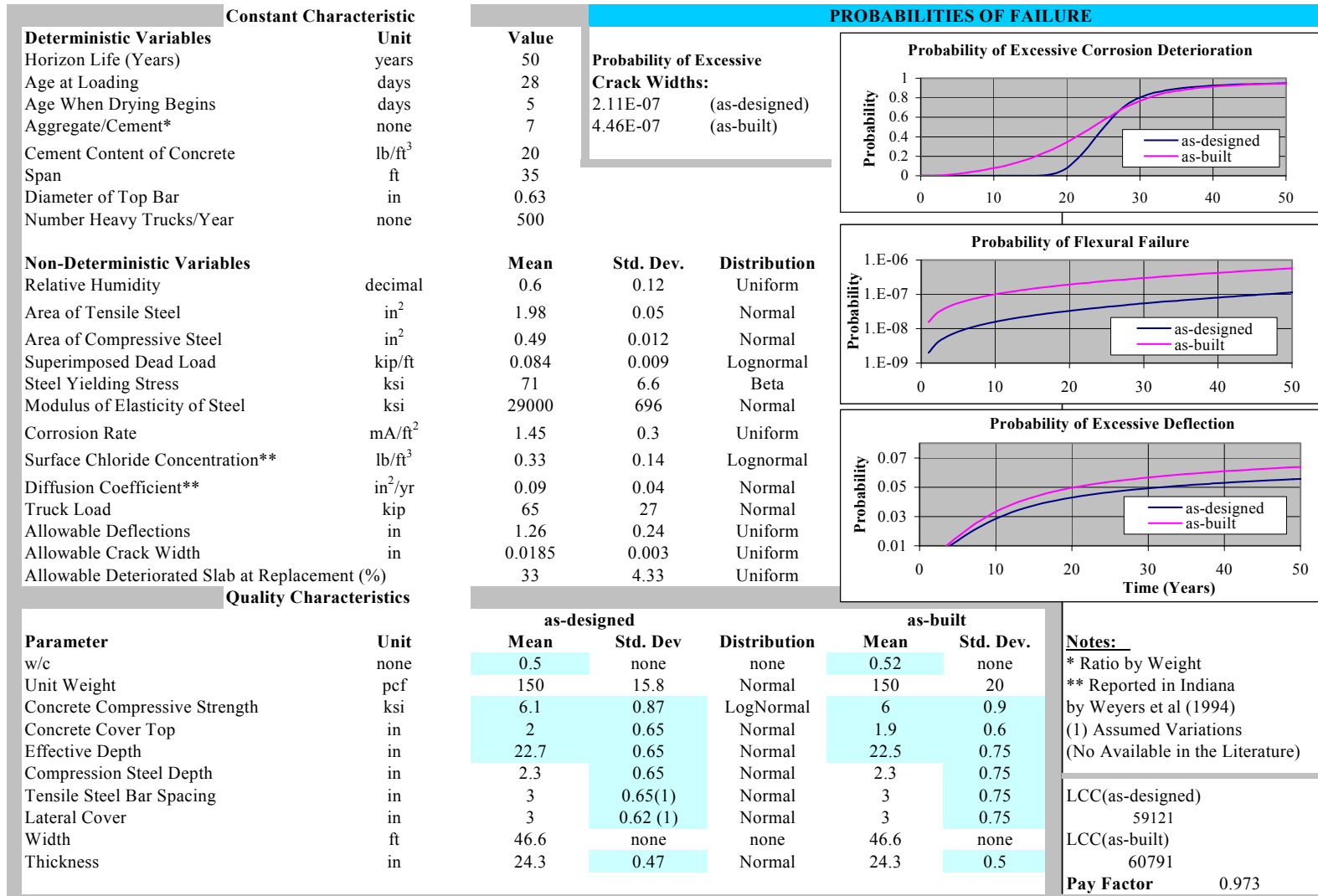


Figure 3.2 Application of PRS Methodology- Deficient Construction

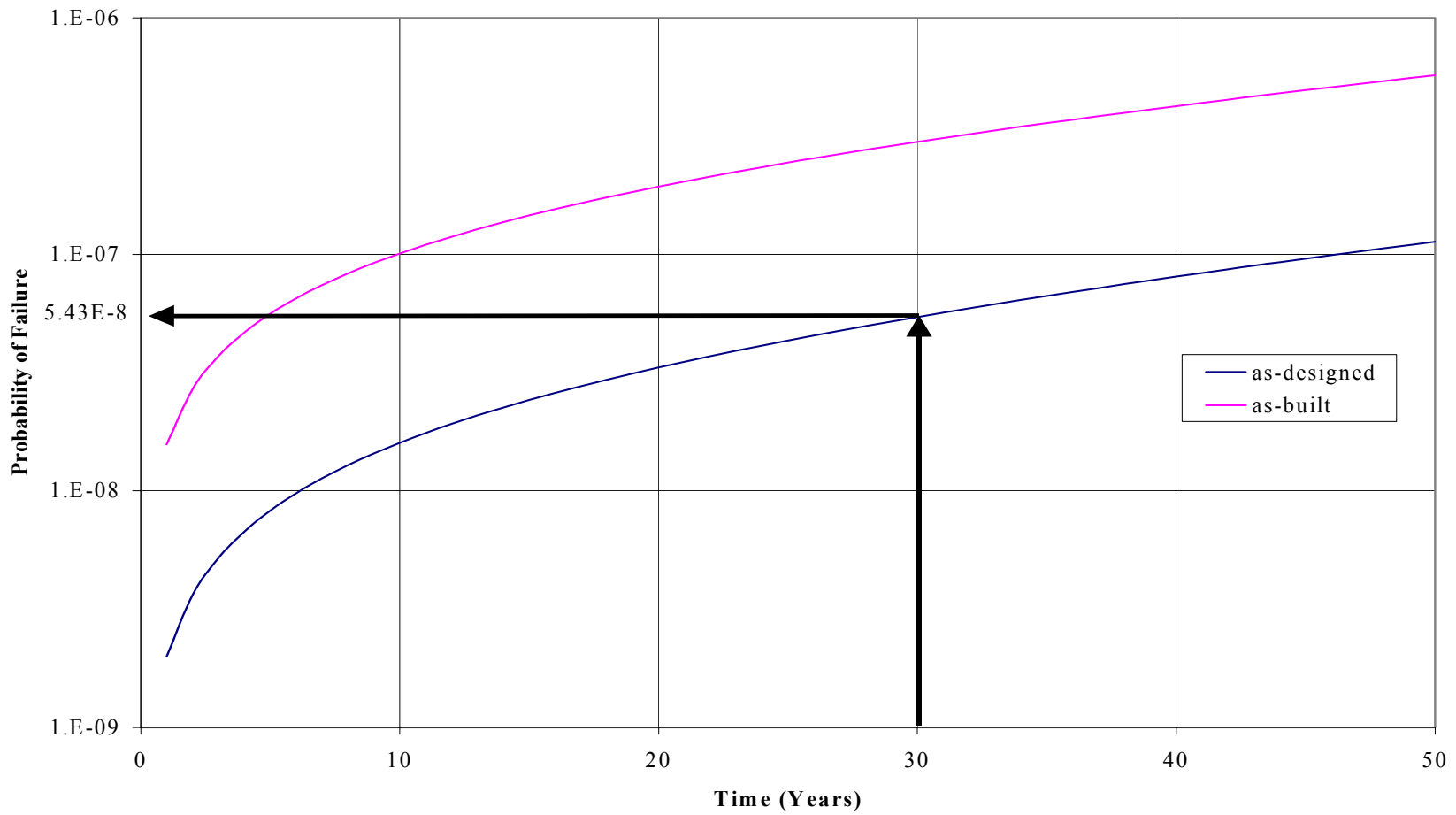


Figure 3.3 Probability of Flexural Failure (Example Section 4.6.2)

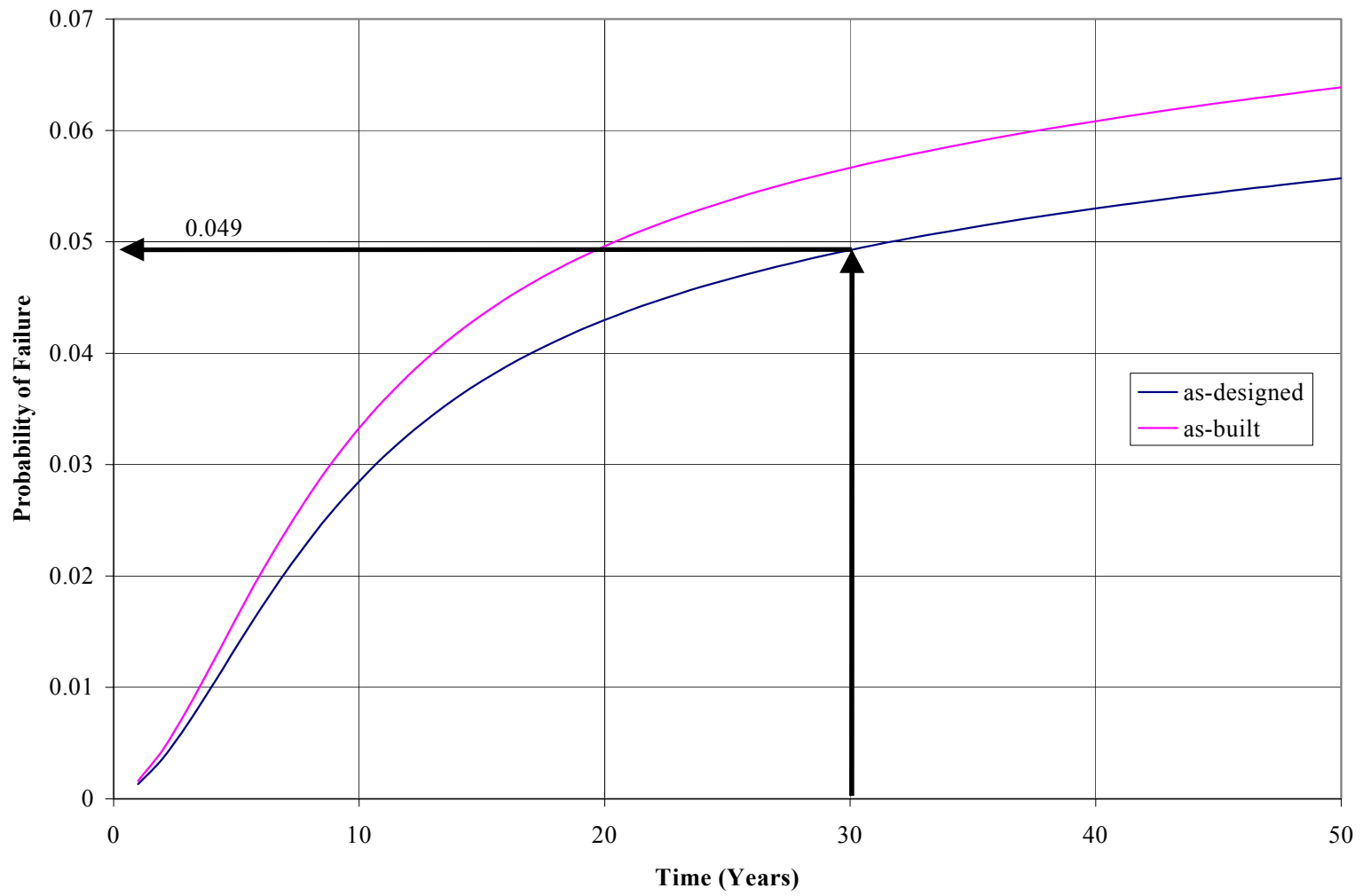


Figure 3.4 Probability of Excessive Deflection (Example Section 4.6.2)

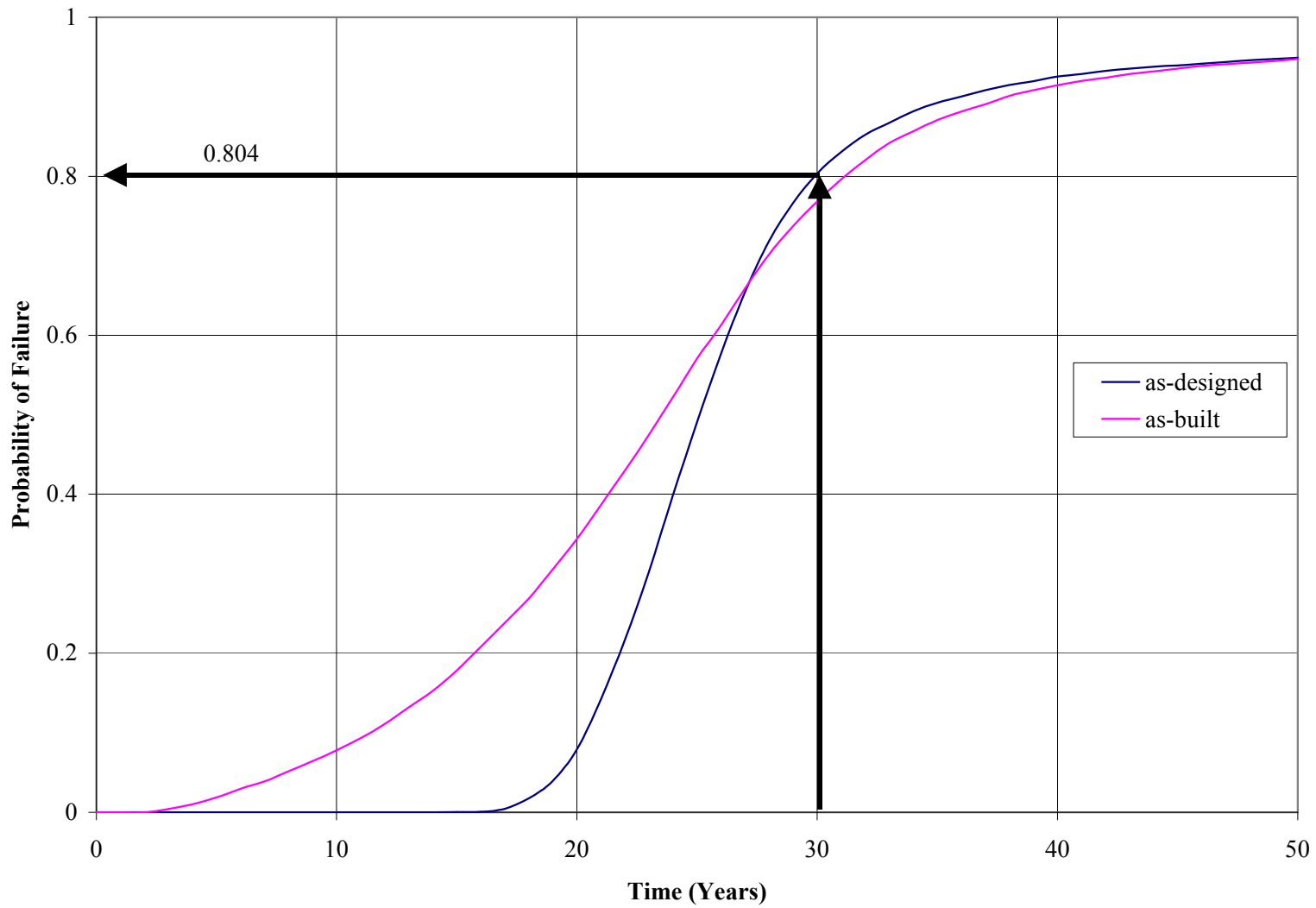


Figure 3.5 Probability of Excessive Corrosion Deterioration (Example Section 4.6.2)

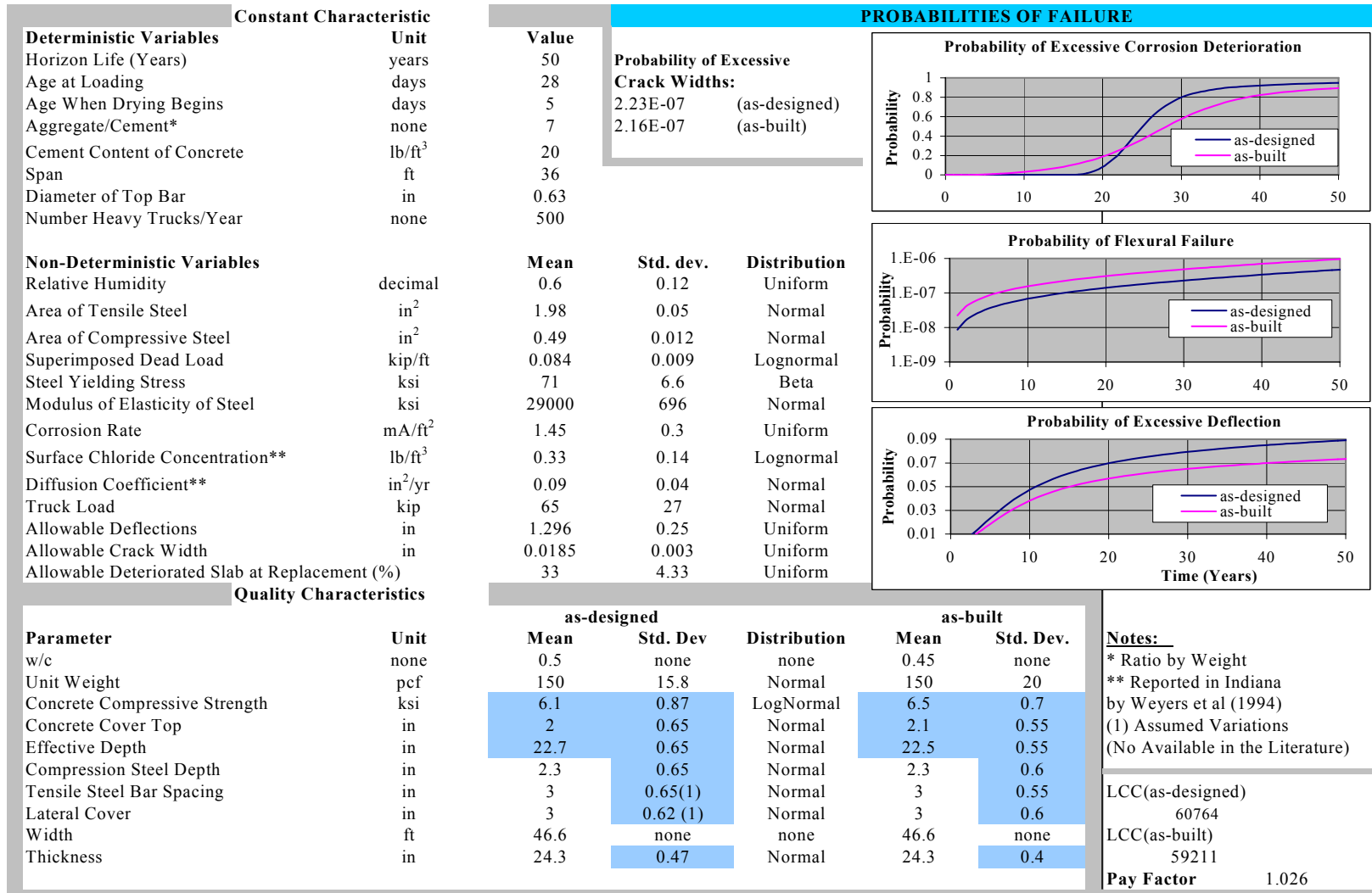


Figure 3.6 Application of PRS Methodology for a Slab Bridge: High Quality Construction

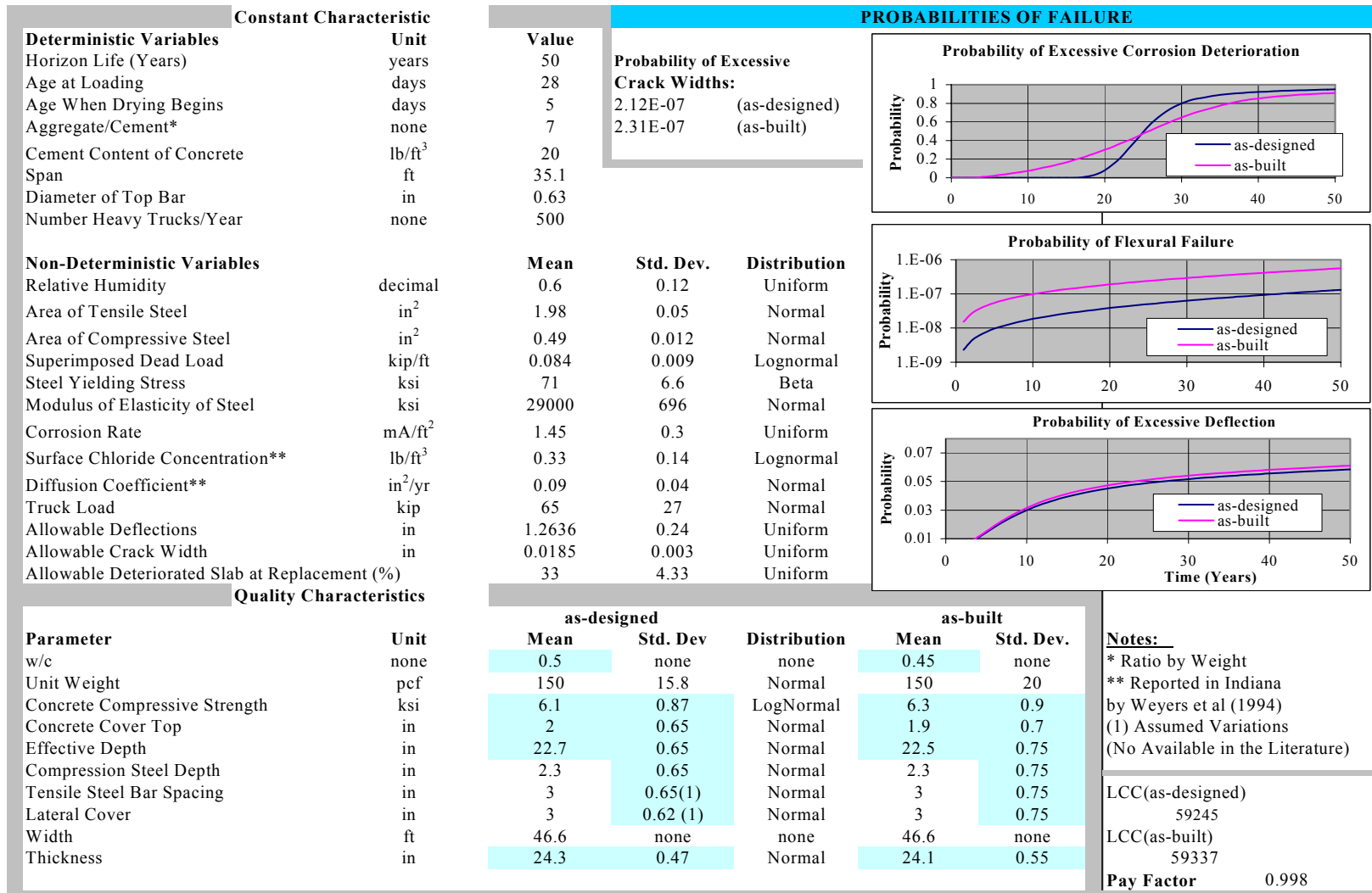


Figure 3.7 Application of PRS Methodology for a Slab Bridge: Tradeoffs Among Quality Characteristics

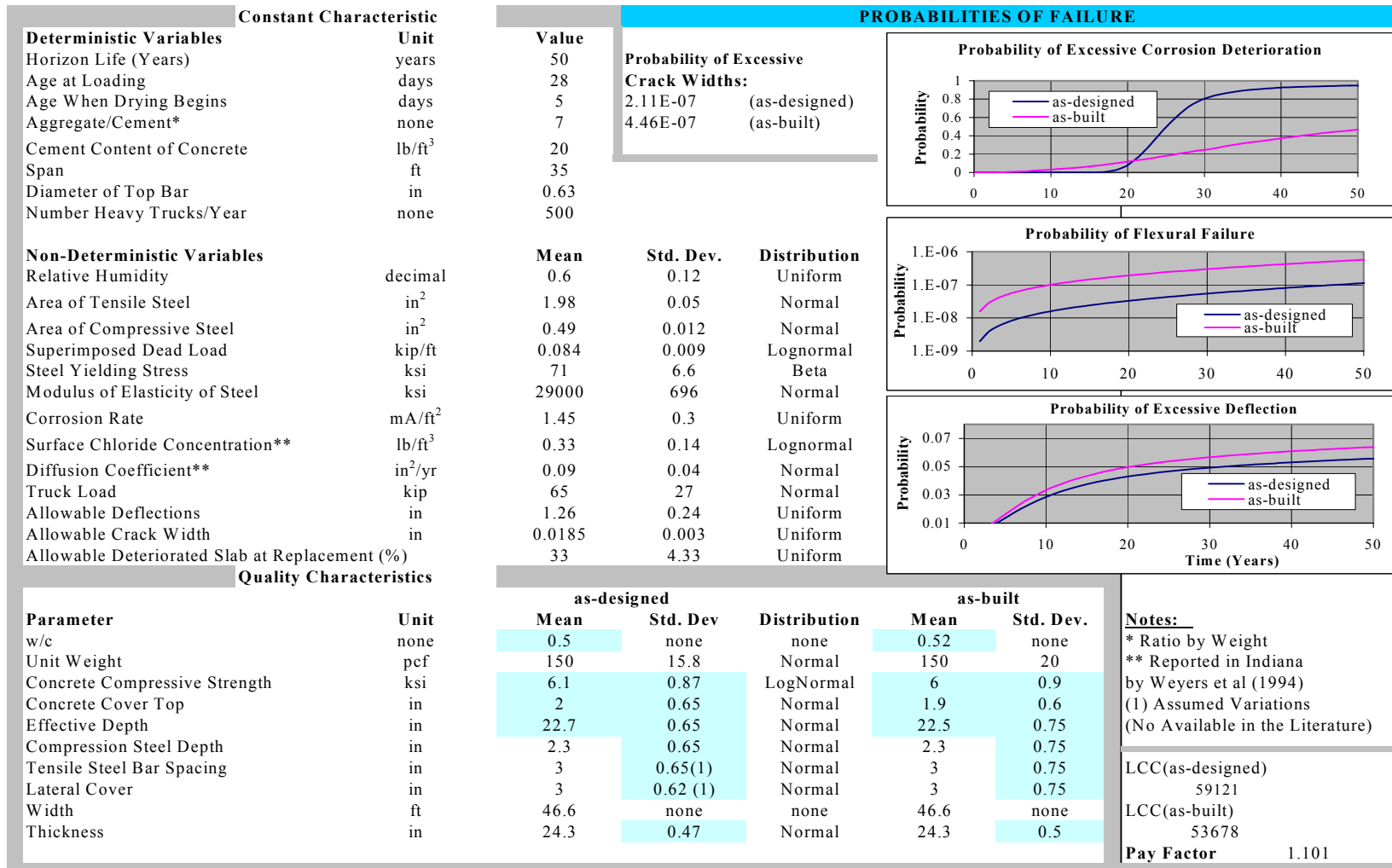


Figure 3.8 Application of PRS Methodology for a Slab Bridge: Use of Epoxy-Coated Reinforcement

4 IMPLEMENTATION PLAN AND FUTURE WORK

4.1 Introduction

Clearly, the main limitation in the implementation of PRS for concrete bridge superstructures as compared to PCC pavements is the immense range of structural configurations possible. Admittedly, the methodology for PRS presented in the initial case study fully applies to simple supported members only. Since the corrosion deterioration model implemented (Section A.2) is entirely material-dependent i.e., it does not depend of the configuration of the structure, the methodology could also be used to monitor any kind of concrete structure if additional distress indicators are not included. It was shown, however, that the inclusion of additional distress indicators gives more integrity to the procedure of quality control and guards against possible mistakes detrimental to the safety of the structure. The range of applicability of the methodology to a wide range of structural configurations and including distresses in addition to corrosion deterioration is possible through the sectional approach proposed in this chapter.

4.2 Sectional Approach

The methodology of a PRS was originally conceived as a mechanism for quality control during construction according to the quality level defined in the design and/or in specifications. This implies that the design is deemed satisfactory in the context of a PRS. As a consequence, all the information that comes from the design, such as the critical external actions obtained from structural analysis, can be implemented as additional input parameters.

Distresses reduced to a section level can be included in the framework of PRS without adding complexity. Section level distresses are those that can be evaluated at a critical section representative of a complete region of the element/structure. The maximum positive moment would be a section level distress that could be evaluated. This maximum design bending moment can be used to calculate the probability of flexural failure for both the as-designed and the as-built structure by knowing the properties of the selected section. The approach avoids the need to carry out the analysis of each evaluated structure. Notice that the analysis of each structure would unduly complicate the process. Excessive flexural crack widths, susceptibility to flexural failure, and other distresses, such as susceptibility to shear failure can be included in the framework because they can be reduced to a section level. The inclusion of excessive deflections presents added complications since it requires the estimation of an effective stiffness to permit sectional level calculations.

4.3 Current Methodology

The current methodology of PRS contains corrosion deterioration as the main distress indicator. The scarce information in the literature regarding costs of repair and the comparatively small probabilities of failure for other distress indicators lead to calculate the LCC based on the corrosion deterioration only. Additional distress indicators are being included to compute the associated the probabilities of failure (or exceeding a certain limit condition). These probabilities of failure are reported to prevent the misuse of the methodology and give integrity to the process of quality control. The methodology has been set up to handle rectangular, T and I-shape sections.

Susceptibility to flexural and shear failures are considered in the framework of PRS as the additional distress indicators. Excessive crack width has not been included because: a) it is not related with safety, b) its determination is extremely uncertain, and c) it was not found to influence the LCC of the structure. The predictive model for susceptibility to shear failure is presented in Appendix D. A user-friendly computer program has been prepared for practical purposes. The main features of the software are presented in Section 4.4. The methodology is open to include other distress indicators for which predictive models are available provided that: a) they are reducible to a section level (Section 4.2), or b) they are strictly materials-dependent. Material-dependent distress indicators are those whose model formulation remains the same no matter the structural configuration. The model predicting corrosion deterioration implemented in this work is an example a material-dependent distress indicator.

4.4 Computer software and Guidelines

A user-friendly computer program has been prepared for the implementation of the methodology of PRS. The current version includes corrosion deterioration, susceptibility to flexural failure, and susceptibility to shear failure as the key distress indicators. The predictive models for corrosion deterioration, and susceptibility to flexural failure are presented in Appendix A. The model for susceptibility to shear failure is presented in Appendix D. Corrosion deterioration is the only distress considered in the computation of the LCC, and to estimate pay factors. The simulation of the corrosion distress allows monitoring serviceability, whereas the flexural and shear distress indicators are used for safety purposes. In addition to the on-line help, guidelines are provided in Appendix E (Figures E.1 to E.12) for the use of the software.

In the procedure of quality control using a PRS, the successive application of the software is envisioned, at least once for the key structural components within the concrete bridge superstructure. The user would end up with a set of probabilities of failure and/or a pay factor for each structural component (corresponding to the typical section considered). Not all distress indicators have to be considered for each component monitored. For example, that susceptibility to shear failure is not usually a concern when the member under consideration is the deck, whereas corrosion deterioration and susceptibility to flexural failure are important matters. The software gives the option of selecting the distress indicators to be monitored allowing the user of the methodology to decide about the important ones.

4.5 Future Work

To accomplish the general objective of the methodology of PRS, the following tasks, in order of importance, are recommended:

- The complete framework for PRS for concrete bridge superstructures should be extensively tested in real structures as an integral part of the implementation process.
- There cost models and the cost items associated with the process of corrosion deterioration (as the main component of the LCC) need update. It is also desirable to determine and update as needed the repair and user cost associated with distresses indicators other than corrosion deterioration. This knowledge would permit a more comprehensive estimate of the LCC of the structure. Surveys among different U.S Departments of Transportation could be used to determine such cost items.
- The main source of information regarding typical variations of some constant and quality characteristics of concrete structures (Table 3.1) goes as far back as the late 70's and early 80's. The current construction practices may not reflect the same level of variations than in past dates. It is recommended to consider updating the information from these studies with new surveys.
- The principal distress in terms of LCC was determined to be corrosion deterioration, therefore, it is recommended to improve the corresponding predictive model. This recommendation is further supported by the fact that currently corrosion deterioration is the most common distress in concrete bridge decks. A better model for prediction of corrosion deterioration reflecting realistic local conditions is primarily required. It is also desirable to establish the magnitude of corrosion-related parameters, such as diffusion coefficient, based on known variables such as material properties. In the work presented, the diffusion coefficient and surface chloride concentration are only rough average values available for Indiana, as discussed in Section 2.5. The effects of certain protective treatments on the process of corrosion deterioration need to be studied and incorporated in the corresponding predictive model. Epoxy-coated reinforcement is one of the protective treatments for corrosion deterioration most widely used in the US. Other distress indicators either materials-dependent or applied at a section level could be included as desired in order to make the methodology more complete for quality control purposes.
- The proposed methodology can also be used to provide optimum service life repair strategy for planning purposes. In applying the methodology for repair activities, the time-dependent probabilities could be updated in accordance with the new information collected during inspection.

REFERENCES

1. ACI 318 (1995), Building Code Requirements for Structural Concrete (ACI 318-95) and Commentary (ACI 318R-95), American Concrete Institute, Detroit.
2. ACI COMMITTEE 117, Standard Specifications for Tolerances for Concrete Construction and Materials (ACI 117-90) and Commentary (ACI 117R-90) and latter editions.
3. AHMAD, S. A., BHATTACHARJEE, B., AND WASON, R. (1997), Experimental Service Life Prediction of Rebar-Corroded Reinforced Concrete Structure, *ACI Materials Journal*, 94(1), pp. 311-316.
4. AL-BAHAR, S., ATTIOGBE, AND KAMAL, H. (1998), Investigation of Corrosion Damage in a Reinforced Concrete Structure in Kuwait, *ACI Materials Journal*, 95(3), pp. 226-231.
5. ALMUSALLAM, A. A., AL-GAHTANI, A. S., AZIZ, A. R., DAKHIL F. H., AND RASHEEDUZZAFAR. (1996), Effect of Reinforcement Corrosion on Flexural Behavior of Concrete Slabs, *Journal of Materials in Civil Engineering*, ASCE, 8(3), pp. 123-127
6. AMEY, S. L., JOHNSON, D. A., MILTENBERGER, M. A., AND FARZAN, H. (1998), Predicting the Service Life of Concrete Marine Structures: An Environmental Methodology, *ACI Structural Journal*, March-April, pp. 205-214.
7. ATTARD, M. M., AND STEWART, M. G. (1998), A Two Parameter Stress Block for High Strength Concrete, *ACI Structural Journal*, (in press).
8. BAKOSS, S. L., GILBERT, R. I., FAULKES, K. A., AND PULMANO, V. A. (1982), Long-Term Deflections of Reinforced Concrete Beams, *Magazine of Concrete Research*, 34(121), pp. 203-211.
9. BAWEJA, D., ROPER, H., AND SIRIVIVATNANON, V. (1998), Chloride Induced Steel Corrosion in Concrete: Part 1-Corrosion Rates, Corrosion Activity, and Attack Areas, *ACI Materials Journal*, 95(3), pp. 207-217.
10. BAZANT Z. P (1999), Criteria for Rational Prediction of Creep and Shrinkage of Concrete, *ACI Special Publication Creep and Shrinkage of Concrete*, Editor, 1999 (in press).
11. BAZANT, Z. P.(1979), Physical Model for Steel Corrosion in Concrete Sea Structures-Application, *ASCE Journal Structural Division*, 105, pp. 1155-1166.
12. BAZANT, Z. P., AND BAWEJA, S. (1999), Creep and Shrinkage Prediction Model for Analysis and Design of Concrete Structures, *ACI Special Publication Creep and Shrinkage of Concrete*, A. Al-Manaseer, Editor, in press.
13. BRANSON, D. E. (1968), Design Procedures for Computing Deflections, *ACI Journal*, September, pp. 730-742.
14. BRANSON, D. E. (1977), *Deformation of Concrete Structures*, McGraw-Hill Book Company, New York, 546 p.
15. CADY, P. D., AND WEYERS, R. E. (1983), Chloride Penetration and Deterioration of Concrete Bridge Decks, *Cement, Concrete, and Aggregates*, Vol. 5, No. 2.
16. CADY, P. D., AND WEYERS, R. E. (1984), Deterioration Rates of Concrete Bridge Decks, *Journal of Transportation Engineering*, ASCE, 110 (2), pp. 34-44.

17. CADY, P. D., AND WEYERS, R. E. (1983), Chloride Penetration and Deterioration of Concrete Bridge Decks, *Cement Concrete and Aggregates*, 5(2), pp. 81-87.
18. CARRERA, J. G. (1996), Deterioration of Concrete Due to Reinforcement Steel Corrosion, *Cement & Composites*, Vol. 18, pp. 47-59.
19. CEB-FIP MODEL CODE 1990, Comite Euro-International du Beton, Bulletin D'Information No. 213/314, 437p.
20. CHRISTENSEN, P. T., BAKER, M. J. (1982), *Structural Reliability Theory and Its Applications*, Springer-Verlag, 267p.
21. CHU. K.H, AND CARREIRA, D. J. (1985), Stress-Strain Relationship for Plain Concrete in Compression, *ACI Journal*, November-December, pp. 797-804.
22. CHU. K.H, AND CARREIRA, D. J. (1986a), Time-Dependent Cycle Deflections in R/C Beams, *Journal of Structural Engineering*, ASCE, 112(5), pp. 943-959.
23. CHU. K.H, AND CARREIRA, D. J. (1986b), The Moment-Curvature Relationship of Reinforced Concrete, *ACI Journal*, March-April, pp. 191-198.
24. CHU. K.H, AND CARREIRA, D. J. (1986c), Stress-Strain Relationship for Reinforced Concrete in Tension, *ACI Journal*, March-April, pp. 21-28.
25. CORNELL, C. A. (1967), Bounds on the Reliability of Structural Systems. *Journal of Structural Division*, ASCE 93(1): 171-200.
26. DAGHER, H. J., AND KULENDRAN, S. (1993), Finite Element Modeling of Corrosion Damage in Concrete Structures, *ACI Structural Journal*, 89(6), pp. 699-707.
27. DARTER, M. I., ABDELRAHMAN M., OKAMOTO, P. A., KOPAC. P. A. (1998), Papers Summarizing the Development of a Prototype Performance-Related Specifications for Concrete Pavements (1990-1998). FHWA, March 1998.
28. DARTER, M. I., ABDELRAHMAN M., OKAMOTO, P. A., SMITH K. D. (1993), Performance-Related Specifications for Concrete Pavements. Volume I: Development of a Prototype Performance-Related Specification. FHWA, Report No. RD-93-042, November 1993.
29. DARTER, M.I., HOERNER, T.E., SMITH, K.D., OKAMOTO, P.A. AND KOPAC, P.A. (1996), Development of prototype performance-related specifications for concrete pavements. Transportation Research Record 1544, Transportation Research Board, Washington, DC.
30. DEVORE, J. L. (1995), *Probability and Statistics for Engineering and the Sciences*, Duxbury, 743 p.
31. DITLEVSEN, O. (1979), Narrow Reliability Bounds for Structural Systems. *Journal of Structural Mechanics* 7:435-451.
32. DUNKER K. F., AND RABBAT G. B. (1990), Highway Bridge Type and Performance Patterns, *Journal of Performance of Constructed Facilities*, Vol. 4, No. 3, Pp. 161-173.
33. DUNKER, K. F., AND RABBAT B. G. (1990), Performance of Highway Bridges, *Concrete International*.

34. ELLINGWOOD, B., GALAMBOS, T. V., MACGREGOR, J. G., AND CORNELL, C. A. (1980), Development of a Probability Based Load Criterion for American National Standard A58. NSB Special Publication No. 577. Washington, D C: National Bureau of Standards.
35. ELLINGWOOD, B., MACGREGOR, J. G., GALAMBOS, T. V., AND CORNELL, C. A. (1982), Probability Based Load Criteria: Load Factors and Load Combinations, Journal of Structural Division, ASCE 108(5): 978-997.
36. ENRIGHT, M. P., AND FRANGOPOL D. M. (1998), Service life prediction of deteriorating concrete bridges, ASCE Journal of Structural Engineering, Vol. 124, No. 3, Pp. 309-316.
37. ESTES, A. C. (1997), A System Reliability Approach to the Lifetime Optimization of Inspection and Repair of Highway Bridges, PhD Thesis, Department of Civil, Environmental and Architectural Engineering, University of Colorado, Boulder, Colorado.
38. ESTES, A. C., AND FRANGOPOL D. M. (1999), Repair Optimization of Highway Bridges Using System Reliability Approach, Journal of Structural Engineering, 125(7), pp. 766-774.
39. ESTES, A. C., AND FRANGOPOL, D. M. (1998), RELSYS: A Computer Program for Structural System Reliability Analysis, Structural Engineering and Mechanics, 6(8), pp. 901-919.
40. FRANCOIS, R., AND AELIGUIE, G. (1998), Influence of Service Cracking on Reinforcement Steel Corrosion, Journal of Materials in Civil Engineering, ASCE, 10(1), pp. 14-20.
41. FRANGOPOL, D. M., LIN, K., AND ESTES, A. C. (1997), Reliability of Reinforced Concrete Girders under Corrosion Attack, Journal of Structural Engineering, 123(3), pp. 286-297.
42. FROSCHE, R. J. (1999), Another Look at Cracking and Crack Control in Reinforced Concrete, ACI Structural Journal, 95 (2), pp. 437-442.
43. GALAMBOS, T. V., ELLINGWOOD, B., MACGREGOR, J. G., AND CORNELL, C. A. (1982), Probability Based Load Criteria: Assessment of Current Design Practice. Journal of Structural Division, ASCE 108(7): 959-977.
44. GERGELY, P. (1981), Role of Cover and Bar Spacing in Reinforced Concrete, Significant Developments in Engineering Practice and Research: a Tribute to Chester P. Siess, ACI SP-72, American Concrete Institute, Detroit, Michigan., pp. 133-147.
45. GHALI, A. (1993), Deflection of Reinforced Concrete Members: A Critical Review, ACI Structural Journal, 90(4), pp. 364-373.
46. GRACE CONSTRUCTION PRODUCTS (1998), Durability Report: Corrosion Protection Analysis, Grace Construction Company, 1124 Fairbanks Dr. Carmel, OH 46033 U.S.A.
47. HASAN, H. O. (1994), Structural Performance of Concrete Bridge Decks Reinforced with Epoxy-Coated Steel under Fatigue Loading, Ph.D. Dissertation Thesis, Department of Civil Engineering, Purdue University, West Lafayette, Indiana.
48. HOFFMAN, P.C. AND WEYERS, R.E (1994), Predicting Critical Chloride Levels in Concrete Bridge Decks, Structural Safety and Reliability: Proceedings of ICOSSAR'93, G.I Schueller, M. Shinozuka and J.T.P Yao (Eds), A.A. Balkema, Rotterdam, pp. 957-959.

49. HOGNESTAD, E. (1961), High Strength Bars as Concrete Reinforcement, Part 1, Introduction to a Series of Experimental Reports, Journal of PCA Research and Development Laboratories, V. 3, No. 3, Sept., PCA Development Department Bulletin D52.
50. HOGNESTAD, E. (1962), High Strength Bars as Concrete Reinforcement, Part 2, Control of Flexural Cracking, Journal of PCA Research and Development Laboratories, V. 4, No. 1, January, PCA Development Department Bulletin, pp. 46-62.
51. HONG, Y., AND NOWAK, A. S. (1992), Bridge Live-Load Models, Journal of Structural Engineering, ASCE, 117(9): 2757-2767.
52. HWANG, E., AND NOWAK, A. S. (1991), Simulation of Dynamic Load for Bridges, Journal of Structural Engineering, ASCE, 117(5): 1413-1434.
53. KAAR, P. H., AND MATTOCK, A. H. (1963), High Strength Bars as Concrete Reinforcement, Part 4, Control of Cracking, Journal of PCA Research and Development Laboratories, V. 5, No. 1, January, pp. 15-38.
54. KILARESKI, W. P. (1980), Corrosion Induced Deterioration of Reinforced Concrete-as Overview, Mat. Perf. Assn. Corrosion Engrs., Houston, Tex., 19(3), 48-50.
55. LAMAN, J. A., AND NOWAK, A. S. (1995), Site-Specific and Component-Specific Bridge Load Model, Reliability and Optimization of Structural Systems, Proceedings of Sixth IFIP Working Conference on Reliability and Optimization of Structural Systems, 1994.
56. LEWIS, E.E (1994), Introduction to Reliability Engineering, John Wiley & Sons, Inc., 435p.
57. LI, Z., LI F., ZDUNKEN A., LANDIS E., SHAH S. (1998), Application of acoustic Emission Technique to Detection of Reinforcing Steel Corrosion in Concrete, ACI Materials Journal, Vol. 95, No.1, Pp. 68-76.
58. LI, Z., LI, F., ZDUNEK, A., LANDIS, E., SHAH, S. (1998), Application of Acoustic Emission Technique to Detection of Reinforcement Steel Corrosion in Concrete, ACI Materials Journal, 95(1), pp. 68-76.
59. LIU Y. (1996), Modeling the Time-to-Corrosion Cracking of the Concrete Cover in Chloride Contaminated Reinforced Concrete Structures, PhD Thesis, Department of Civil Engineering, Virginia Polytechnic Institute and State University, Blacksburg, Virginia.
60. LIU, Y., AND WEYERS, R. E. (1996), Time to Cracking of Chloride-Induced Corrosion in Reinforced Concrete, Corrosion of Reinforcement in Concrete Construction, C. L., Page, P. B. Bamforth, J. W. Figg (Ed.), Royal Society of Chemistry, Cambridge, England, pp. 88-104.
61. LIU, Y., AND WEYERS, R. E. (1998), Modeling the Time to Corrosion Cracking in Chloride Contaminated Reinforced Structures, ACI Materials Journal, 95(6), pp. 675-681.
62. MAAGE. M., HELLAND. S., POULSEN. E., VENNESLAND. O., CARLSEN J. (1996), Service life prediction of existing concrete structures exposed to marine environment, ACI Materials Journal, Vol. 93, No. 6, Pp. 602-608.
63. MATSUSHIMA, M., SEKI H., AND MATSUI K. (1998), Reliability Approach to Landing Pier Optimum Repair Level, ACI Materials Journal, Vol. 95, No. 3, Pp. 218-225.

64. MCCARTER, W. J. (1993), Influence of Surface Finish on Sorptivity on Concrete, *Journal of Materials in Civil Engineering*, ASCE, 5(1), pp. 130-135.
65. MEHTA P. K. (1991), *Concrete in Marine Environment*, Elsevier Applied Science, Barking, U.K.
66. Melchers, R. E. (1987), *Structural Reliability*, Ellis Horwood, 400p.
67. MIRZA, S. A., AND MACGREGOR, J. G. (1976), A Statistical Study of the Variables Affecting the Strength of Reinforced Concrete Normal Weight Members, *Structural Engineering Report No.58*, Edmond, Alberta, Canada: University of Alberta.
68. MIRZA, S. A., HATZINIKOLAS, M., MACGREGOR, J. G. (1979), Statistical Descriptions of Strength of Concrete, *Journal of the Structural Division*, ASCE, 105 (ST. 6): 1021-1036.
69. MIRZA, S. A., MACGREGOR, J. G. (1979a), Variability of Mechanical Properties of Reinforcing Bars, *Journal of the Structural Division*, ASCE, 105 (ST. 5): 921-937.
70. MIRZA, S. A., MACGREGOR, J. G. (1979b), Variations in Dimensions of Reinforced Concrete Members, *Journal of the Structural Division*, ASCE, 105(ST. 4): 921-937.
71. MORI, Y., AND ELLINGWOOD, B. R. (1994), Maintaining Reliability of Concrete Structures II: Optimum Inspection/Repair, *Journal of Structural Engineering*, ASCE, 846-862.
72. MOSES, F., N. KHEDEKAR, AND GHOSN (1993), System Reliability of Redundant Structures Using Response Functions, *Proceedings of the Offshore Mechanics and Arctic Engineering Symposium*. New York: American Society of Civil Engineering.
73. NOWAK, A. S., Live Load Model for Highway Bridges, *Structural Safety*, 13: 53-66.
74. OHRN, L. G., AND SCHEXNAYDER, C. (1997), Effect of Performance-Related Specifications on Highway Construction, *Practice Periodical on Structural Design and Construction*, Vol. 2, No. 4, November.
75. PONTIS: Release 3.0 User's Manual (1995). Cambridge Systematic, Inc., Cambridge, Massachusetts.
76. PURVIS R., BABAEI K., MARKOW M. J. (1994), Life-Cycle Cost Analysis for Protection and Rehabilitation of Concrete Bridges Relative to Reinforcement Corrosion, *Strategic Highway Research Program (SHRP, S-377)* Washington, DC., pp. 1-289.
77. RAMIREZ, J.A., FROSCH, R. J. AND OLEK, J. (1998), Proposal for research study of Performance-related design specifications for concrete bridge superstructures. Joint Transportation Research Program. Project no. C-36-56WW, School of Civil Engineering, Purdue University, July.
78. RAMSAY, R. J., MIRZA, S. A., AND MACGREGOR, J. G. (1979), Monte Carlo Study of Short Time Deflections of Reinforced Concrete Beams, *ACI Journal*, August, pp. 81-102.
79. RICHART, F. E. (1927), An Investigation of Web Stresses in Reinforced Concrete Beams, *Bulletin #166*, Engineering Experiment Station, University of Illinois, Urbana, IL, pp. 1-105
80. ROUX, N., ANDRADE, C., AND SANJUAN, M. A. (1996), Experimental Study of Durability of Reactive Powder Concrete, *Journal of Materials in Civil Engineering*, ASCE, 8(1), pp. 1-6.

81. SAITO, M., AND SINHA, K. C. (1989), The Development of Optimal Strategies for Maintenance, Rehabilitation and Replacement of Highway Bridges, Final Report Vol. 4: Cost Analysis, Joint Highway Research Project, FHWA/IN/JHRP-89/11.
82. SAMPLES L. M., AND RAMIREZ, J. A. (1999), Methods of Corrosion Protection and Durability of Concrete Bridge Decks Reinforced with Epoxy-Coated Bars-Phase I, Joint Transportation Research Program, FHWA/IN/JTPR-98-15, Indiana Department of Transportation, Purdue University.
83. SAMRA, R. M. (1997), Time-Dependent Deflections of Reinforced Concrete Beams Revisited, *Journal of Structural Engineering*, ASCE, 123(6), pp. 823-829.
84. SMITH, G.R. (1998), Synthesis of Highway Practice 263, State DOT management techniques for materials and construction acceptance, National Cooperative Highway Research Program. National Academy Press, Washington D.C.
85. STEWART, M. G. (1997), Time-Dependent Reliability of Existing RC Structures, *Journal of Structural Engineering*, Vol. 23, No. 7, July. 896-902.
86. STEWART, M. G. (1998), Risk-based approaches to the assessment of existing bridges, Research Report No. 168.10.1998, Department of Civil, Surveying and Environmental Engineering, The University of Newcastle, Australia.
87. STEWART, M. G. AND VAL, D. M. (1999), Role of Load History in Reliability-Based Decision Analysis of Aging Bridges, *Journal of Structural Engineering*, ASCE, 125(7), pp. 776-783.
88. STEWART, M. G., AND ROSOWSKY D. V. (1998a), Time Dependent Reliability Analysis of Deteriorating Reinforced Concrete Bridge Decks, *Structural Safety*, Vol. 20.
89. STEWART, M. G., AND ROSOWSKY D. V. (1998b), Structural Safety and Serviceability of Concrete Bridges Subject to Corrosion, *Journal of Infrastructure Systems*, ASCE, 4(4), pp. 146-154.
90. STEWART, M. G., ROSOWSKY D. V. (1998c), Structural Reliability for Chloride Diffusion, Cracking, Spalling and Corrosion of Concrete Bridges, Research Report No. 162.02.1998, Department of Civil, Surveying and Environmental Engineering, The University of Newcastle, Australia.
91. STEWART, M. G., AND ATTARD, M. M. (1999), Reliability and Model Accuracy for High-Strength Concrete Column Design, *ASCE Journal of Structural Engineering*, Vol. 125, No. 3.
92. STRUTT, J. E., NICHOLLS, J. R., AND BARBIER, B. (1985), The Prediction of Corrosion by Statistical Analysis of Corrosion Profiles, *Corrosion Science*, 25(5), pp. 305-315.
93. SUBCOMMITTEE 4, ACI COMMITTEE 435 (1967), Recommendation for ACI Building Code Provision on Deflections, Report Approved by Committee 435 and Submitted to ACI Committee 318, October.
94. SUGIYAMA, T., BREMNER, T.W. (1996), and Tsuji, Y., Determination of Chloride Diffusion Coefficient and Gas Permeability of Concrete and Their Relationship, *Cement and Concrete Research*, 126(5), pp. 781-790.
95. SUNDARARAJAN, C. (RAJ) (1995), *Probabilistic Structural Mechanics Handbook*, Chapman & Hall, 745 pp.
96. THOFT-CHRISTENSEN, P. AND BAKER, M. J. (1982), *Structural Reliability Theory and Its Applications*, Springer, Berlin.

97. THOFT-CHRISTENSEN, P. AND MUROTSU, Y. (1986), Application of Structural Systems Reliability Theory, Springer, Berlin.
98. TING, S. C. (1989), The Effects of Corrosion on the Reliability of Concrete Bridge Girders, Ph.D. Thesis, Department of Civil Engineering, University of Michigan, Ann Arbor, Michigan.
99. TUMIDAJSKI, P. J., AND CHAN, G. W. (1996), Boltzmann-Matano Analysis of Chloride Diffusion into Blended Cement Concrete, Journal of Materials in Civil Engineering, ASCE, 8(4), pp. 195-196.
100. URUGAL, A. C. (1987), Advanced Strength and Applied Elasticity, Elsevier, New York, 471p.
101. VAL, D., AND MELCHERS, R. E. (1997), Reliability of Deteriorating RC Slab Bridges, Journal of Structural Engineering, ASCE, 123(12): 1638-1644.
102. VESHOSKY D., BEIDLEMAN C. R, BUETOW G. W., AND DEMIR. M. (1994), Comparative analysis of bridge superstructure deterioration, Journal of Structural Engineering, ASCE, V. 120.
103. WASHA, G. W. (1947), Plastic Flow of Thin Reinforced Concrete Slabs, Journal of the American Concrete Institute, 19(3), pp. 237-260.
104. WATSTEIN, D., AND PARSONS, D. E. (1947), Width and Spacing of Tensile Cracks in Axially Reinforced Concrete Cylinders, Research Paper RP1545, U. S Department of Commerce, National Bureau of Standards, July, 24 pp.
105. WEE, T. H., WONG, S. F., SWADDIWUDHIPONG, S., AND LEE, S. L. (1997), A Prediction Method for Long Term Chloride Concentration Profiles in Hardened Cement Matrix Materials, 94(6), pp. 565-576.
106. WEYERS, R. E. (1998), Life Service Model for Concrete Structures in Chloride Laden Environments, ACI Materials Journal, July-August, pp. 445-453.
107. WEYERS, R. E., AND CADY, P. D. (1987), Deterioration of Concrete Bridge Decks from Corrosion of Reinforcing Steel, Concrete International, January, pp. 15-20.
108. WEYERS, R. E., AND HOFFMAN, P. C. (1994a), Predicting Critical Chloride Levels in Concrete Bridge Decks, Structural Safety and Reliability, pp. 957-959.
109. WEYERS, R. E., FITCH, P. L., AL-QADI, I. L., CHAMBERLIN, W. P., AND HOFFMAN, P. C (1994b), Concrete Bridge Protection and Rehabilitation: Chemical and Physical Techniques, SHRP-S-668, SHRP, Washington, DC. 248 pp.
110. WEYERS, R. E., PYC, W., AND SPRINKEL, M. M. (1998), Estimating the Service Life of Epoxy-Coated Reinforcing Steel, ACI Materials Journal, 95(5), pp. 546-557.
111. WILKINS, N.J.M AND LAWRENCE, P.F (1983), The corrosion of Steel Reinforcements in Concrete Immersed in Seawater, Corrosion of Reinforcement in Concrete Construction, A.P. Crane (Ed), Ellis Horwood, Chichester, pp. 119-141.
112. XHANTAKOS, P. P. (1994), Theory and Design of Bridges, John Wiley & Sons, N.Y (U.S.A), 1443 p.
113. XHANTAKOS, P. P. (1996), Bridge Strengthening and Rehabilitation, Prentice Hall PTR, N. J. (U.S.A), 966p.

114. XI, Y., AND BAZANT, Z. P. (1999), Modeling Chloride Penetration in Saturated Concrete, *Journal of Materials in Civil Engineering*, 11(1), pp. 58-65.
115. YU, W., AND WINTER, G. (1960), Instantaneous and Long-Time Deflections of Reinforced Concrete Beams under Working Loads, *Journal of the American Concrete Institute*, July, pp. 29-49.

APPENDIX A

PERFORMANCE MODELS FOR CASE STUDY

A.1 INTRODUCTION

The overall performance of a beam or slab such as the one shown in Figure A.1 is described in terms of limit states (distress indicators) related to serviceability and flexural strength:

- 1) Excessive corrosion deterioration
- 2) Excessive transverse cracking
- 3) Excessive deflections
- 4) Flexural failure

The first three distress indicators determine serviceability, and the last one refers to strength. An additional distress indicator was added at a later stage in the research, one-way shear failure. This distress indicator is discussed in detail in Appendix D of this report. The effects of creep and shrinkage in the estimation of crack width and long term deflections are included. The model used to quantify long term effects due to creep and shrinkage is discussed in Appendix B.

In this appendix, the performance models used to evaluate the distress indicators listed above are reviewed. These models are implemented in the methodology for PRS as described in Section 1.2.

A.2 EXCESSIVE CORROSION DETERIORATION

A.2.1 Introduction

Problems related to corrosion deterioration are an essential concern in concrete bridge structures. Weyers (1998) reported that, 40% of the budget to cover problems related to bridge rehabilitation needs in the United States, was attributable to corrosion of reinforcing steel in concrete. Moisture and the presence of significant amount of free chlorides fuel the trigger mechanism for corrosion of the reinforcement. In the United States, the primary source of chloride is in the deicing salts applied to roadways and bridges to help with snow removal during the winter months. Cady and Weyers (1983) reported that more than 10^7 tons of road salts were applied to highways and bridges each winter. A typical bridge in the Snow Belt is estimated to receive up to 1.2 kg/m^2 (0.25 lb/ft^2) of salts during each winter.

A.2.2 Corrosion Mechanism

Electromechanical forces drive corrosion of reinforcing steel. The necessary conditions for electromechanical corrosion are the contact of a metal with an electrolyte and the presence of a potential difference between two or more regions at the surface of the metal (Reis et al. 1964). The simple combination of iron, oxygen, and air yields an oxide rust product. Other factors leading to corrosion are differential aeration, moisture content and salt concentrations.

Exposed reinforcing steel will corrode at a rate depending on the severity of the environmental conditions. Concrete, however, provides a remarkable protection because of its high pH, which is about 12.5 (high alkalinity). Usually a thin film of iron is present on the surface of the rebar, this protective film is kept stable due to high pH associated with the hydration of the Portland cement (Kilaeski, 1980). In the absence of chlorides, reinforcing steel bars embedded in concrete should not corrode. If moisture penetrating to the reinforcement level contains soluble salts, such as chlorides, the protective value resulting from the high pH is considerably reduced. Low quality of the concrete has a negative effect regarding the corrosion process:

a) the high porosity of low quality concrete facilitates the ingress of chlorides, and b) its low electrical resistance allows the electromechanical forces driving corrosion to occur.

Two types of corrosion mechanisms are recognized: general and localized corrosion. General corrosion can be easily identified because its product, common rust, causes cracking and ultimately spalling of concrete. Localized corrosion occurs in small areas of the reinforcement. It is claimed (Val and Melchers, 1997) that for localized corrosion the maximum penetration of pitting is about four times the average penetration on the surface of the rebar.

The corrosion process is better described by defining the time in years, T_p , to have a specific percentage of the slab (or deck) surface deteriorated, p . After examining 169 bridge decks of similar ages, Cady and Weyers (1984) suggested the expression:

$$T_p = T_c + \frac{(p - 0.5X)}{R} \quad (A-1)$$

where, T_c , is the time to cracking due reinforcement corrosion in years, R , is the average deterioration rate, and X , is the percentage of top reinforcing steel subject to subsidence cracking. For average conditions, R , was reported as 2% per year. In addition, X , can be found approximately in terms of the concrete cover, C_t , (Bazant, 1979) as:

$$\begin{aligned} X &= 4.43C_t^2 - 53C_t + 158.72 \text{ for } C_t = \text{Cover} < 6.4 \text{ cm} \\ X &= 0.5\% \text{ for } C_t \geq 6.4 \text{ cm} \end{aligned} \quad (A-2)$$

The time to cracking, T_c , has two components: the time to initiation of corrosion, T_i , and the time for cracking after initiation, T_d .

$$T_c = T_i + T_d \quad (A-3)$$

The time to initiation, T_i , is customarily associated with a diffusion process only. The time to damage, T_d , represents the time required for accumulation of a volume of the rust products enough to produce tensile stresses in excess of the concrete tensile strength.

A.2.3 Time for Initiation of Corrosion

If the chloride concentration at the level of the reinforcement attains a threshold value, C_{cr} , then the passive film of iron around the rebar is destroyed and corrosion initiates.

The chloride ions in the concrete are classified as chlorides bounded to the internal surface of cement, and chlorides diffused freely through the concrete (Wee et al., 1997, Xi and Bazant, 1999). Research has shown (Xi and Bazant, 1999) that steel corrosion is related only to the content of free chlorides.

The chloride diffusion process is described either by Fick's second law of diffusion, or by the Nernst-Planck law of electrochemistry and Nernst-Einsten equation. The first approach describes the process on a macroscopic level (i.e., parameters averaged over a representative volume). The second approach describes the process on a microscopic level and an increase of six orders of magnitude is required to compare with test results at a millimeter scale.

The time to initiation of corrosion can be obtained from Fick's second law of diffusion as:

$$\frac{\partial C}{\partial t} = \frac{\partial}{\partial x} \left(D_e \frac{\partial C}{\partial x} \right) = \frac{\partial D_e}{\partial x} \frac{\partial C}{\partial x} + D_e \frac{\partial^2 C}{\partial x^2} \quad (A-4)$$

where, C , is the chloride concentration (in kg/m^3 or equivalent units) at a depth, x , and time, t , and, D_e , is the diffusion coefficient of concrete.

Assuming a constant diffusion coefficient over time and depth, a constant chloride concentration at the surface level, C_0 , and considering a semi-infinite medium, a closed-form solution for Equation A-4 is given by:

$$C(x, t) = C_0 \left[1 - \operatorname{erf}\left(\frac{x}{\sqrt{4Dt}}\right) \right] \quad (\text{A-5})$$

where, erf is the mathematical error function given by:

$$\operatorname{erf}(z) = \frac{2}{\sqrt{\pi}} \int_0^z e^{-t^2} dt \quad (\text{A-6})$$

Although the assumptions involved in the derivation of Equations A-4 and A-5, are not satisfied in concrete structures, Equation A-5 has been exhaustively calibrated against test results. It is considered to be the best descriptor of the diffusion process. In particular, the presence of cracking is considered through an average diffusion coefficient being commonly reported in the literature.

Setting $x = C_t =$ concrete cover, and $C(x, t) = C_{cr}$ into Equation A-5, and solving for the time, t , the time for initiation of corrosion, T_i , is obtained:

$$T_i = \frac{C_t^2}{4D_e \left[\operatorname{erf}^{-1}(1 - C_{cr}/C_0) \right]^2} \quad (\text{A-7})$$

It is widely recognized that the water over cement ratio, w/c , is the main parameter affecting D_e . As a compromise for the experimental results and suggestions reported in several references (Appendix C), the next relationship can be used:

$$D_e(w/c)/D_e(0.4) = 15 \times (w/c)^{3.0174} \quad (\text{A-8})$$

where, $D_e(0.4)$, is the diffusion coefficient for $w/c = 0.4$. Equation A-8 was derived by using a least square adjustment of the data reported in those references. Requiring the diffusion coefficient for a w/c of 0.4 is a convenient way of accounting for the effect of, w/c , on, D_e . It should be mentioned that since in the literature the chloride concentration, C_0 , is reported not at the surface but a 1.3 cm from it, the calculation of the time for initiation involves the concrete cover, C_t , diminished by that magnitude (i.e., $C_t - 1.3$ cm instead of C_t). The option exists to also input specific values for this parameter.

A.2.4 Time to Cracking

Since the volume of the corrosion products is greater than the corresponding volume of rust, tensile stresses in the concrete are induced as corrosion progresses with time. Transverse cracking occurs when the tensile strength of the concrete is exceeded.

According to Metha (1991), the rust products of the corrosion process could have a volume equal to 300% of the corresponding corroded steel. Liu and Weyers (1998) presented the relative volume of the rust products as a function of the nature of the chemical reaction associated with the corrosion process. If the resulting rust product of the iron, Fe, oxidation is FeO, or Fe_3O_4 , or Fe_2O_3 , the volume increases by a factor of two. If the rust product is $\text{Fe}(\text{OH})_2$ or $\text{Fe}(\text{OH})_3$, the volume increases by a factor of four. If the rust product is $\text{Fe}(\text{OH})_3 \cdot 3\text{H}_2\text{O}$, the volumes increases by a factor of six.

In modeling the time to longitudinal cracking after the initiation of corrosion, a calibrated model, developed by Liu and Weyers (1998), is presented. In this approach, three basic phases are distinguished:

- Free expansion

When corrosion starts, there is a porous zone around the rebar. The volume of that porous zone is directly related to the water/cement ratio, degree of hydration, degree of consolidation, and surface area of reinforcement. During this phase, as the passive film around the rebar is broken, the porous zone is gradually filled with the corrosion products. No stresses are induced because the amount of corrosion products, W_t , is less than the amount required to fill the pores, W_p .

- Stress initiation

An expansive pressure of the surrounding concrete occurs as W_t increases and $W_t > W_p$

- Cracking

When, W_t , equals a critical volume, $W_{critical}$, the internal tensile stresses exceed the tensile strength of the concrete and cracking occurs, eventually leading to spalling of concrete.

Considering the steel/concrete interface is somewhat like the transition zone between cement paste and aggregate, W_p , may be expressed as:

$$W_p = \rho_{rust} V_p \quad (A-9)$$

where, ρ_{rust} , is the density of the corrosion products, and, V_p , is the total volume of interconnected pores around the steel/concrete interface.

If, d_0 , is the thickness of the porous zone around the steel/concrete interface, and, D , is the bar diameter, then for a unit length of steel bar the assumption $d_0 \ll D$ implies:

$$W_p \approx \pi \rho_{rust} d_0 D \quad (A-10)$$

There are not studies determining d_0 . A calibrated value, $d_0 = 12.5 \mu m$, has been suggested by Liu and Weyers (1998).

The critical amount of rust products, $W_{critical}$, consists of two parts: the amount of corrosion products required to fill the pores, W_p , and the amount of corrosion that generates the critical tensile stress, W_s :

$$W_{critical} = W_p + W_s \quad (A-11)$$

Denoting, d_s , as the thickness of the corrosion products needed to generate critical tensile stresses, and assuming that $d_s \ll D$, the value of, W_s , can be estimated as:

$$W_s \approx \rho_{rust} \left[\pi D d_s + \frac{W_{st}}{\rho_{st}} \right] \quad (A-12)$$

where, ρ_{st} , is the density of steel and, W_{st} , is the amount of corroded steel. Substituting Equations A-10 and A-12 into Equation A-11:

$$W_{critical} \approx \rho_{rust} \left[\pi (d_s + d_0) D + \frac{W_{st}}{\rho_{st}} \right] \quad (A-13)$$

The amount of the corroded steel depends on the rust products so that, W_{st} , can be expressed as:

$$W_{st} = \alpha W_{critical} \quad (A-14)$$

where, α , is the ratio of molecular weight of steel and corrosion product. This ratio equals 0.523 or 0.622, if the corrosion products are $\text{Fe}(\text{OH})_3$ or $\text{Fe}(\text{OH})_2$ respectively.

An approximate closed-form solution for, d_s , is obtained by considering concrete as a homogeneous elastic material and a thick-wall concrete cylinder around the rebar with inner radius $a = (D+2d_0)/2$ and outer radius $b = a + C_t$. Assuming that cracking occurs above and parallel to the reinforcement, the following expression is obtained from elastic theory (Ugural, 1987):

$$d_s = \frac{C_t f'_t}{E_{ef}} \left(\frac{a^2 + b^2}{b^2 - a^2} + \nu_c \right) \quad (\text{A-15})$$

where:

f'_t : tensile strength of concrete,

E_{ef} : effective elastic modulus of concrete given by the expression $E_c/(1+\phi)$,

E_c : elastic modulus of the concrete,

ν_c : Poisson's ratio for concrete,

ϕ : concrete creep coefficient.

Substituting Equations A-14 and A-15 into Equation A-13 an explicit equation for, W_{critical} , is obtained.

The rate of production of rust, $\frac{dW_t}{dt}$, is considered inversely proportional to the oxide layer thickness:

$$\frac{dW_t}{dt} = \frac{k_p}{W_{\text{rust}}} \quad (\text{A-16})$$

where, W_t , is the amount of rust products in mg/mm, t , is the elapsed time after the initiation of corrosion (years) and k_p , is a parameter related with the rate of metal loss. k_p has been expressed in terms of the corrosion rate (Liu, 1996), i_{cor} (mA/cm^2), as follows:

$$k_p = 91(1/\alpha)\pi D i_{\text{cor}} \quad (\text{A-17})$$

where, D , is the rebar diameter in mm.

The interval of time to obtain the critical amount of rust products, W_{critical} , is precisely the time to damage, T_d . For a constant corrosion rate, integrating Equation A-16 and setting $t = T_d$ for $W_t = W_{\text{critical}}$, it is obtained:

$$T_d = \frac{W_{\text{critical}}^2}{2k_p} \quad (\text{A-18})$$

A.2.5 Mitigation of Corrosion

Several studies have aimed to evaluate of the beneficial effects of different treatments and mixes mitigating the process of corrosion deterioration on the Life-Cycle-Cost of concrete structures. Weyers et al. (1998), pointed out the possible alternatives to extend the corrosion-related service life of concrete decks as follows:

- Delay the onset for initiation of corrosion by: increasing the cover depth, and/or reducing the construction tolerances on the placement of reinforcing steel, and/or reducing the rate of corrosion diffusion by using low permeable concrete, and/or increase the chloride threshold limit by using a corrosion inhibitor admixture.
- Delay the onset for deterioration after initiation of corrosion by: decrease the rate of corrosion of steel in areas critically contaminated with chlorides by using coated reinforcing steel, and/or using non-corroding reinforcing, such as fiber-reinforced plastic (FRP), and galvanized steel.

It has also been found (Amey et al., 1998) that silica fume increases significantly the estimated service life of the structures by decreasing chloride transport in the concrete and by decreasing the buildup of chloride in the near surface region of the structure. In a report by Grace Company (1998), it is claimed that adding 5% of silica fume to the concrete mix reduces the diffusion coefficient by 40%.

Calcium nitrite has also a favorable effect on the corrosion initiation process by increasing the critical chloride concentration to initiate corrosion. Extensive laboratory testing (Grace Company, 1998) has shown that by adding 10, 15, 20 or 25 liters/m³ of calcium nitrite, the threshold value, C_{cr} , can be increased from 0.9 kg/m³ to 3.6, 5.9, 7.7 or 8.9 kg/m³ respectively.

Weyers and Cady (1987) evaluated the positive effect of using epoxy-coated bars on the corrosion deterioration process by examining 22 bridge decks and comparing the relative extent of corrosion for uncoated and coated bars. Weyers and Cady found that 40% of the decks containing bare reinforcing steel were in the stage of initiation of corrosion whereas none of the decks with epoxy-coated bars were deteriorated because of corrosion. However, Weyers et al. (1998) studied the life service of epoxy-coated reinforcing steel concrete elements and experimentally demonstrated that a different corrosion protection failure mode could exist in the field than in short term laboratory tests. In the laboratory studies, the degree of corrosion protection is a function of the quality of the coating. In field structures, the epoxy coating debonds from steel in wet concrete.

In Indiana, the corrosion protection procedure most commonly used is through the use of epoxy-coated reinforcement. Surveys have shown average chloride concentrations at the level of the top mat of reinforcement as high as 4 kg/m³ without signs of deterioration (Hasan, 1994).

A.3 EXCESSIVE CRACK WIDTH

A.3.1 Introduction

Deflections and crack width had not been an issue for reinforced concrete structures before high strength steel bars were available. The adoption of strength design in the sixties made the distress even more critical because the stresses at the level of the reinforcement at service loads were increased by about 50% (Mac Gregor, 1997). Reis et al. (1964) gives an excellent description of the causes of cracking, and related-control provisions.

Customarily, cracking by itself is not considered as a serviceability problem. However, excessive cracking can influence the functionality of the structure in terms of durability and aesthetics. The major durability problem associated with cracking is corrosion of reinforcement. Excessive crack width can influence the time for initiation by facilitating the arrival of chlorides to the rebar. Several investigations (Cabrera, 1996, Liu and Weyers, 1996, Francois and Aeliguie, 1998) have suggested, however, that crack width does not significantly influence the deterioration process occurring after initiation of corrosion.

A.3.2 Implemented Crack Width Model

For the initial case study crack widths are calculated as recommended by Frosch (1999) but including the effect of shrinkage as introduced in the CEB-FIP (1992) code, that is, the shrinkage strain is subtracted from the strain at the level of the reinforcement when calculating the crack width, w :

$$w = (\varepsilon_s - \varepsilon_{sh}) \delta^* \Psi_s \quad (A-19)$$

where:

ε_{sh} : average sectional shrinkage strain;

Ψ_s : crack spacing factor. This factor equals 1.0, 1.5 or 2.0 for minimum, average or maximum crack spacing; and

δ^* : controlling cover distance given by:

$$\delta^* = \text{Max} \{ \sqrt{\delta_c^2 + (S/2)^2}, \sqrt{\delta_s^2 + \delta_c^2} \} \quad (\text{A-20})$$

where, δ_c , is the bottom cover, δ_s , is the lateral cover and, S, is the spacing of the reinforcement bars under tension.

If the crack width at the beam surface is to be computed, the last equation should be multiplied by the strain gradient factor, γ , given by:

$$\gamma = (h - c) / (d - c) \quad (\text{A-21})$$

where, h, is the overall thickness of the member, d, is the effective depth and, c, is the depth of neutral axis measured from the uppermost fiber of the concrete section.

A.4 EXCESSIVE DEFLECTIONS

A.4.1 Introduction

Two different schools of thought for calculating deflections are identified in the literature. The first approach attempts to define the flexural stiffness term, EI, according to the structural condition of the member; cracked, partially cracked or uncracked section. This average flexural stiffness along the span of the member, referred to as effective moment of inertia, is then implemented in carrying out an elastic analysis to obtain the required deflection.

In the second approach, the curvature at each abscise along the span of the member into consideration is obtained from the external moment and the sectional moment curvature diagram (which defines the structural condition of the section: cracked, partially cracked, or uncracked). A double integration of the curvature along the span is carried out to get the deflection. The limits of the integral determine the location at which the deflection is evaluated. The procedure allows obtaining the flexural stiffness at each point and time; therefore, it is considered physically more realistic than using an average flexural stiffness along the span. The former approach was implemented in this work for the computation of deflections.

A.4.2 Computation Procedure for Deflections

The moment-curvature diagram is implemented for the computation of deflections herein. For a simply supported beam (Figure A.1), the deflection Δ_a at any abscise, a, measured from the left support is given by:

$$\Delta_a = \int_0^a \psi(x) \left[1 - \frac{a}{L} \right] x dx + \int_a^L \psi(x) \left[1 - \frac{x}{L} \right] a dx \quad (\text{A-22})$$

where, L, is the span length and, $\psi(x)$, is the curvature at any abscise, x.

The curvature, $\psi(x)$, can be written as:

$$\psi(x) = \psi_o(x) + \psi_t(x) \quad (\text{A-23})$$

where:

$\psi_o(x)$: time-independent curvature obtained from the corresponding moment-curvature diagram as a function of the truckload moment at, x, and

$\psi_t(x)$: time-dependent curvature obtained from the corresponding moment-curvature diagram as a function of the dead load moment at, x. $\psi_t(x)$, includes both the effects of creep and shrinkage.

For the statistical simulation of the model, the maximum elastic deflection along the member is of particular interest. The maximum deflection is assumed to occur at midspan. This is a reasonable

approximation provided that the dead load is considerably larger than the design truckload (commonly the case for slab bridges).

A.4.3 Maximum Midspan Elastic Deflection due to Truckload

It is assumed that the maximum deflection due to the truckload occurs at midspan. To calculate such deflection it is necessary to know the position of the truck producing the maximum effect. A regression analysis of the influence lines for deflections provides the following expression for the abscise, X_{max} , measured from the left support in Figure A.1, at which the front axle of the AASHTO HS20-44 truck must be placed in order to get the maximum deflection at midspan:

$$X_{max}/L = [1 - (1.17 \times 10^{-6}L^4 - 1.24 \times 10^{-4}L^3 + 4.66 \times 10^{-3}L^2 - 6.66 \times 10^{-2}L + 0.645)] \quad (A-24)$$

Equation A-24 has associated a coefficient of correlation, $r^2 = 0.9995$. The span, L , in the right side of the expression must be given in (m).

Having the location of the HS20-44 truck to get the maximum midspan deflection, the distribution of the bending moment for live load is obtained from equilibrium, and the corresponding curvature ($\psi_o(x)$ in Equation A-23) is obtained from the time-independent moment curvature diagram. Equation A-24 was derived for span lengths ranging from 12 to 40 m.

For the case of slabs, the bending moment associated with truckload is calculated as a moment per unit width. The truckload is assumed uniformly distributed in the transversal direction of the slab along certain design strip. The width of this strip is a function of the span, L , and the width, W , of the slab. An expression for the distribution width for truckload, E_{strip} , is given by:

$$E_{strip} = 3 \text{ m} + 5\sqrt{LW} \quad (A-25)$$

Equation A-25 has been recommended in the AASHTO (1994) design specifications.

A.5 SUSCEPTIBILITY TO FLEXURAL FAILURE

A.5.1 Calculation Procedure

To estimate the flexural capacity of the element corresponding to the initial case study (Fig. A.1), the condition at failure in flexure is set in terms of a maximum compressive strain in the concrete, $\epsilon_c = 0.003$. The corresponding nominal moment is obtained from the time-independent moment-curvature diagram.

Failure occurs if the maximum external moment along the span due to both live (truck) and dead load exceeds the nominal moment.

The maximum external moment is assumed to occur at midspan. This is true for the component due to the dead load and a good approximation for the component due to the truckload. In the case of a concrete slab bridges the dead load is significantly larger than the live load. Therefore, the approximation of the total maximum external moment (dead plus live load) occurring at midspan is reasonable.

A.5.2 Maximum Moment Due to Truck Load

A study of the influence lines for truckload was carried out. It was found that by dividing the whole span into N sections evenly spaced, the maximum moment, M_{max} (KN-m), at a section located at a distance, $x_i = i(L/N)$, from the left support (Figure A.1) is given by:

$$M_{max_i} = \frac{4WT}{9}(A_iL - B_i) \quad (A-26)$$

where:

N: total number of sections along the span,

i: subscript denoting the particular abscise at which the maximum moment is evaluated (i varies from 1 to N/2, and the remaining sections are evaluated by symmetry),

WT: total truckload (for an HS20-44 truck),

A_i, B_i: coefficients depending on the abscise at which the maximum truckload bending moment is being evaluated, and

L: span length (in m).

The coefficients, A_i, and, B_i, were obtained from a regression analysis as:

$$\begin{aligned} A_i &= -2.2[i/N]^2 + 2.2[i/N] + 0.0006 & : r^2 &= 1 \\ B_i &= 5.6[i/N]^2 - 8.5[i/N] + 0.17 \quad (m) & : r^2 &= 0.9995 \end{aligned} \quad (A-27)$$

where, r² is the corresponding correlation coefficient of the fitted equation.

Equations A-26 and A-27 can be used to find the maximum truckload moment at any section along the beam/slab shown in Figure A.1 by an appropriate selection of, i, and, N. The expressions have been derived for span lengths, L, ranging from 12 to 40 m.

For the case of slabs, the maximum moment due to truckload is calculated as a moment per unit width uniformly distributed along the design strip, E_{strip}, given by Equation A-25.

For the statistical simulation of this model towards calculating the probability of flexural failure, the maximum moment at midspan (assumed as absolute maximum) is implemented. This maximum moment is obtained by setting, i = N/2, in Equations A-26 and A-27.

A.5.3 Strength Degradation

In a study of reinforced concrete bridge beams by Enright and Frangopol (1998) it was proposed several resistance degradation functions for different deterioration levels related to corrosion. Low, medium, and high deterioration were defined as a function of the time for initiation of corrosion, T_i. The semi-empirical expression below was suggested:

$$R(t) = R_0 \cdot d(t) \quad (A-28)$$

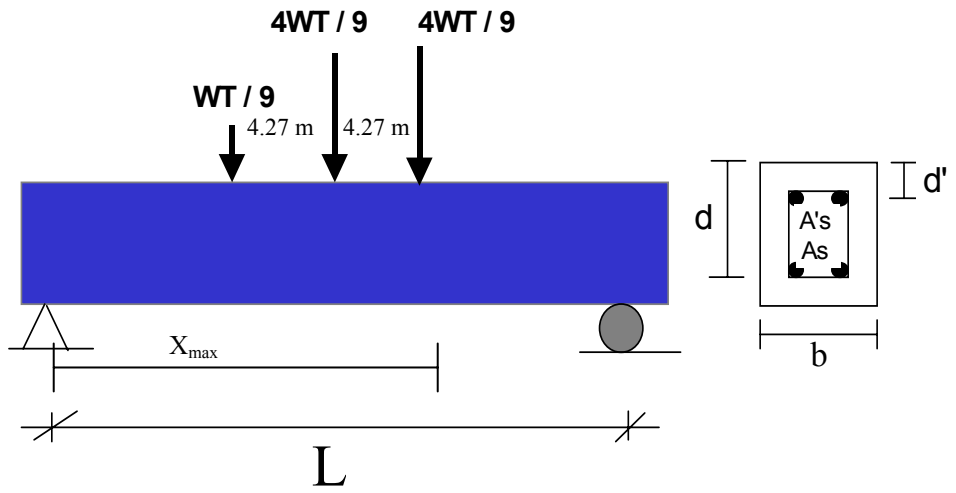
where, R(t) is the strength at time in years, t, R₀, is the initial (time-independent) strength, and, d(t), is a degradation function given by:

$$d(t) = 1 - k_1 t + k_2 t^2 \quad (A-29)$$

where, k₁ and k₂ are degradation coefficients given by:

k₁ = 0.0005 and k₂ = 0 for T_i = 10 years (low deterioration)

k₁ = 0.005 and k₂ = 0 for T_i = 5 years (medium deterioration) k₁ = 0.01 and k₂ = 0.00005 for T_i = 2.5 years (high deterioration)



WT = Total Truckload, AASHTO HS20-44 Configuration.

Figure A.1: Initial Case Study for the Reliability-Based Analysis of a Concrete Member.

APPENDIX B MODEL FOR CREEP AND SHRINKAGE

B.1 INTRODUCTION

A rigorous analysis of the structure should be accompanied by a reasonable determination of the creep and shrinkage properties as inputs for the structural analysis. In this work, creep and shrinkage affect the model for the calculation of deflections, the model predicting corrosion deterioration, and the model calculating crack widths.

The next discussion is entirely based on a work by Bazant and Baweja (1999).

B.2 RANGE OF APPLICABILITY

The range of applicability of the model in terms of the involved parameters is the following:

$$\begin{aligned} 0.35 &\leq w/c \leq 0.85 \\ 2.5 &\leq a/c \leq 13.5 \\ 160 &\leq c \leq 720 \text{ kg/m}^3 \\ 17 &\leq f'_c \leq 70 \text{ MPa} \end{aligned} \tag{B-1}$$

where:

w/c: water over cement ratio,

a/c: aggregate over cement ratio by weight,

c: cement content, and

f'_c : 28-day standard cylinder compression strength of concrete.

The range of applicability and accuracy can be extended by an adequate calibration of the model. Some indications are provided in Bazant and Baweja (1999).

B.3 BASIC CREEP AND SHRINKAGE EQUATIONS

In concrete members at the service stress range (up to about $0.45 f'_c$) creep may be assumed to be linear.

For a constant stress, σ , applied at a age t' (days), the strain $\epsilon(t)$ at a particular time t (days) can be written as:

$$\epsilon(t) = J(t, t')\sigma + \epsilon_{sh}(t) + \alpha\Delta T(t) \tag{B-2}$$

where:

$J(t, t')$: compliance function (1/MPa) = creep plus elastic strain at time t caused by a unit uniaxial constant stress applied at age t' (days),

$\epsilon_{sh}(t)$: average shrinkage strain of cross section,

$\Delta T(t)$: temperature change from a reference temperature at time t , and

α : thermal expansion coefficient.

The compliance function is further divided as:

$$J(t, t') = q_1 + C_0(t, t') + C_d(t, t', t_0) \tag{B-3}$$

where:

q_1 : empirical parameter associated with the instantaneous strain due to unit stress,

$C_0(t, t')$: compliance function for basic creep, i.e., creep at constant moisture content and no moisture movement through the material,
 $C_d(t, t', t_0)$: additional compliance function due to simultaneous drying, and
 t_0 : age when drying begins (days).

Commonly, the most convenient way to introduce creep into structural analysis is through the creep coefficient $\phi(t, t')$,

$$\phi(t, t') = E(t')J(t, t') - 1 \quad (\text{B-4})$$

where, $E(t)$ is the Young's modulus of elasticity of concrete at age t (days).

B.4 CREEP AND SHRINKAGE PARAMETERS

- Creep

The coefficients of Equations B-2 to B-4 were statistically derived from calibration of theoretical models with the data bank as follows:

The basic creep compliance function is given by:

$$C_0 = q_2 Q(t, t') + q_3 \ln[1 + (t - t')^{0.1}] + q_4 \ln\left(\frac{t}{t'}\right) \quad (\text{B-5})$$

where, q_2, q_3, q_4 are empirical parameters, and $Q(t, t')$ is a binomial integral that cannot be expressed analytically. The empirical parameters are given by:

$$q_1 = 0.6/E(28) \quad (\text{B-6})$$

$$q_2 = 185.4 \sqrt{c} (f'_c)^{-0.9} \quad (f'_c \text{ is given in MPa and } q_2 \text{ in } 10^{-6}/\text{MPa}) \quad (\text{B-7})$$

$$q_3 = 0.29(w/c)^4 q_2 \quad (\text{B-8})$$

$$q_4 = 20.3(a/c)^{-0.7} \quad (q_4 \text{ is given in } 10^{-6}/\text{MPa}) \quad (\text{B-9})$$

where, $E(28) = 4,734 \sqrt{f'_c}$ (both f'_c and E in MPa).

The function $Q(t, t')$ can be obtained approximately as (According to Bazant and Baweja, 1999, with errors of the order of 1% with respect to the exact function):

$$Q(t, t') = Q_f(t') \left\{ 1 + \left[\frac{Q_f(t')}{Z(t, t')} \right]^{r(t')} \right\}^{-1/r(t')} \quad (\text{B-10})$$

where, $Q_f(t')$, $Z(t, t')$, and $r(t')$ are functions given, respectively, by:

$$Q_f(t') = [0.086(t')^{2/9} + 1.21(t')^{4/9}]^{-1} \quad (\text{B-11})$$

$$Z(t, t') = (t')^{-0.5} \ln[1 + (t - t')^{0.1}] \quad (\text{B-12})$$

$$r(t') = 1.7(t')^{0.12} + 8 \quad (\text{B-13})$$

- Shrinkage

The mean shrinkage strain in the cross section is given by:

$$\varepsilon_{sh}(t, t_0) = -\varepsilon_{sh\infty} k_h S(t) \quad (\text{B-14})$$

where, $\varepsilon_{sh\infty}$ is the ultimate shrinkage strain, $S(t)$ is the time dependence function, and k_h is the humidity dependence function. $S(t)$ and k_h are given by:

$$S(t) = \tanh \sqrt{\frac{t - t_0}{\tau_{sh}}} \quad (B-15)$$

$$k_h = \begin{cases} 1 - h_u^3 & \text{for } h_u \leq 0.98, \\ 12.74 - 12.94h_u & \text{for } 0.98 \leq h_u \leq 1 \end{cases} \quad (B-16)$$

where, h_u is the relative humidity (decimal), and τ_{sh} is the size dependence function given by:

$$\tau_{sh} = k_t(k_s D')^2 \quad (B-17)$$

where:

$D' = 2(v/s)$: v/s = volume to surface ratio of the concrete member;

k_s : cross sectional shape factor = 1.00, 1.15, 1.25, 1.30, or 1.55 for an infinite slab, an infinite cylinder, an infinite square prism, a sphere, or a cube, respectively;

k_t : function given by:

$$k_t = 8.5t_0^{-0.8} (f'_c)^{-1/4} \quad (f'_c \text{ in MPa and } k_t \text{ in days/cm}^2) \quad (B-18)$$

The ultimate shrinkage strain is expressed as:

$$\varepsilon_{sh\infty} = \varepsilon_{s\infty} \frac{E(607)}{E(t_0 + \tau_{sh})} \quad (B-19)$$

where, $E(t)$ is the modulus of elasticity of concrete at time t , and $\varepsilon_{s\infty}$ is a constant (in 10^{-6} cm/cm). $E(t)$ and

$\varepsilon_{s\infty}$ are given, respectively, by:

$$E(t) = E(28) \left[\frac{t}{4 + 0.85t} \right]^{1/2} \quad (B-20)$$

$$\varepsilon_{s\infty} = -\alpha_1 \alpha_2 \left[1.9 \times 10^{-2} w^{2.1} (f'_c)^{-0.28} + 270 \right] \quad (f'_c \text{ in MPa}) \quad (B-21)$$

where:

w : water content of concrete mix = $(w/c)c$ (in kg/m^3),

α_1 and α_2 : parameters related to cement type and curing procedure. α_1 equals 1.00, 0.85, or 1.10 for cement types I, II, or III. α_2 equals 0.75, 1.20, or 1.00 for stem-curing procedure, sealed or normal curing in air with initial protection against drying, or curing in water or at 100% relative humidity.

The compliance function for additional creep due to drying is given by:

$$C_d(t, t', t_0) = q_5 \left\{ \exp[-8H(t)] - \exp[-8H(t_0')] \right\}^{1/2} \quad (B-22)$$

where, $H(t)$ is the spatial average of pore relative humidity within the cross section and t_0' is a model parameter given by:

$$t_0' = \max(t', t_0) \quad (B-23)$$

$$H(t) = 1 - (1 - h_u)S(t) \quad (B-24)$$

For the case $t \leq t_0'$, $C_d(t, t', t_0)$ must be taken equal to zero.

The parameter q_5 is given by:

$$q_5 = 7.57 \times 10^5 (f'_c)^{-1} \left| 10^6 \varepsilon_{sh\infty} \right|^{-0.6} \quad (f'_c \text{ in MPa}) \quad (B-25)$$

APPENDIX C DIFFUSION COEFFICIENT

The time for initiation of corrosion increase as the value of D_e decreases. A smaller coefficient of diffusion is associated with a better quality of the concrete in terms of durability. Magnitudes for the diffusion coefficient have been reported in several references:

In a study by Weyers et al. (1994) 2764 samples corresponding to 321 bridges in 16 sates were collected in order to determine typical average diffusion coefficients. In Indiana (where 43 samples were taken), for instance, the mean diffusion coefficient and the corresponding coefficient of variation (COV) were respectively $0.09 \text{ in}^2/\text{yr}$ and 0.40.

It is widely recognized that the water over cement ratio, w/c, is the main parameter affecting D_e . As can be intuitively expected, a greater w/c (more porosity) leads to a greater diffusion coefficient and therefore a greater chloride concentration for a given depth and time interval. Stewart and Rowosky (1998) presented the equation:

$$D_e (\text{cm}^2 / \text{s}) = 10^{-10+4.66w/c} \quad (\text{C-1})$$

Sugiyama et al. (1996) determined experimentally the chloride diffusion coefficient of concrete by using an accelerated electrical testing method. The chloride diffusion coefficient was found to be controlled by the water over cement ratio, w/c, being approximately 2.2 times higher for concrete with w/c = 0.6 than for concrete with w/c = 0.4.

For plausible values of w/c (ranging from 0.3 to 0.7), Frangopol et al. (1997) presented the expression:

$$D_e (\text{cm}^2 / \text{s}) = 10^{-6.274-0.076w/c+0.00113(w/c)^2} \quad (\text{C-2})$$

As can be observed, the previous equation is atypical in relation to what is intuitively expected and to what many researchers have reported; it says that the diffusion coefficient is inversely proportional to the water over cement ratio for practical values of w/c.

The dependence of the diffusion coefficient on the temperature has been presented in Amey et al. (1998) by introducing the concept of the temperature-corrected diffusion coefficient. This diffusion coefficient was determined by applying the Nernst-Einstain relation, as:

$$D_2 = D_1 \left(\frac{T_2}{T_1} \right) \text{Exp} \left[q \left(\frac{1}{T_1} + \frac{1}{T_2} \right) \right] \quad (\text{C-3})$$

where, D_1 and D_2 are the diffusion coefficients at temperatures T_1 and T_2 , and q is a constant that has been experimentally measured for different concretes over the range of temperatures from 5 to 25 °C.

Tumidajski and Chan (1996) has calculated the non-steady state chloride diffusion coefficient for blended cement concrete, which incorporated fly ash and ground granulated blast furnace slag. The experimental results showed that D_e decreases with time and increases with the depth at which the chloride is measured.

Furthermore, it was shown that there was a marked reduction in D_e when the slag content and curing time were increased.

Maage et al. (1996) pointed out the inverse dependence with time of the chloride diffusion coefficient, specifically with the maturity age of concrete:

$$D_e(t) = D_0 \left(\frac{t_0}{t} \right)^k \quad (C-4)$$

where, D_0 and k are parameters experimentally determined, t is the maturity age of concrete, and t_0 is a typical maturity age of concrete (normally the time for first exposure of concrete to deicing salts).

Figure C-1 shows the variation of the diffusion coefficient with w/c according to several references. Significant differences are observed. A curve fitting in the best possible way all findings/suggestions presented above (coefficient of correlation equals 0.8) was suggested for the proposed methodology for PRS. The corresponding fitted equation is given by:

$$D_e(w/c) / D_e(0.4) = 15 \times (w/c)^{3.0174} \quad (C-5)$$

where, $D_e(0.4)$ is the diffusion coefficient for w/c a water over cement ratio of 0.4.

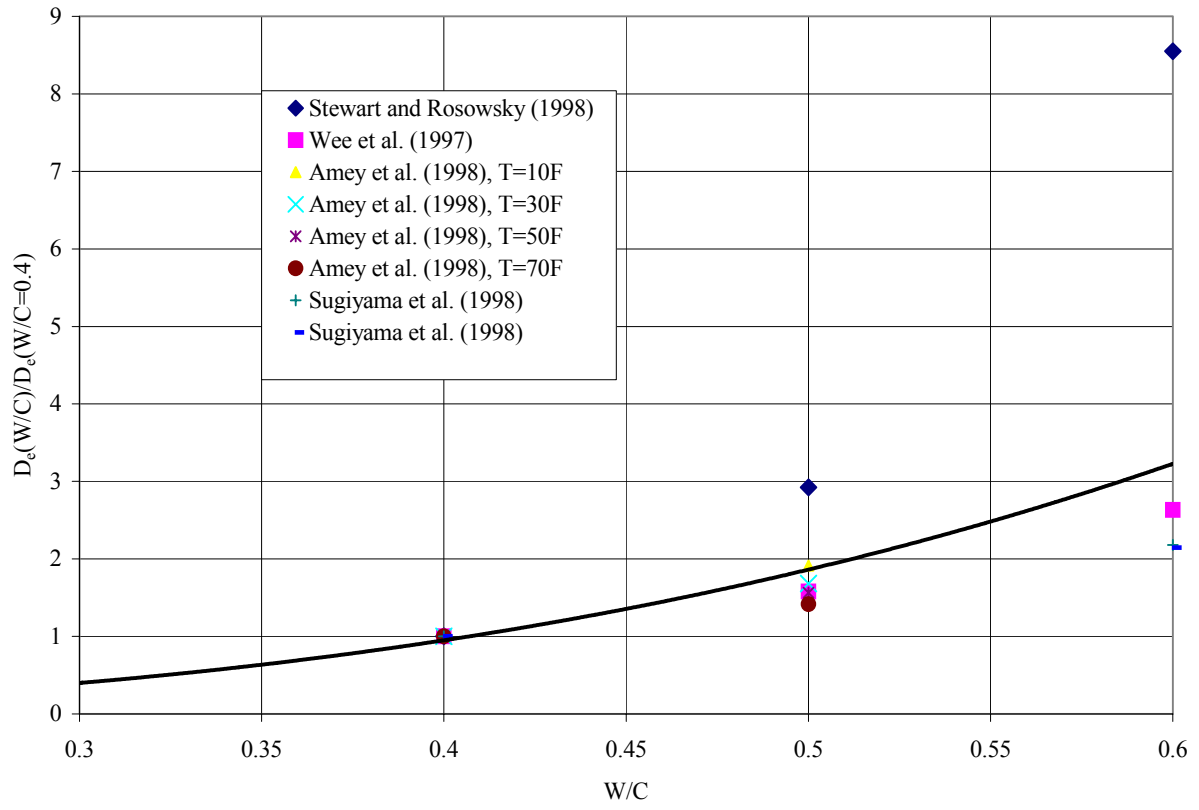


Figure C.1: Variation of D_e with w/c According to Several References

APPENDIX D SHEAR MODEL

D.1 REMARKS

Susceptibility to shear failure has been included in the generalized methodology of PRS. The distress is considered at the section level so that the user of the methodology must provide the information corresponding to the maximum external shear force in a concrete member or a portion of it. Recall that in the updated methodology the computation of the external actions is not carried out because they are part of the input parameters defined by the user. Only the parameters defining a typical section (representing the whole member or part of it) are required to compute the strength of the section.

D.2 COMPUTATION PROCEDURE

In the simulation procedure failure occurs if the maximum external shear (input parameter) exceeds the nominal shear capacity. Since the probability of exceeding the limit condition at failure is customarily very small FOSM analysis is implemented for the reliability analysis.

The nominal shear capacity, V_n , of a I-section having a effective depth, d , web width, b_w , and transverse reinforcement with area, A_v , is estimated as:

$$V_n = v_c b_w d + A_v f_y d / s_v \quad (D-1)$$

where: s_v is the spacing of the transverse reinforcement, f_y is the yielding stress of the transverse reinforcement, and v_c is the unit shear strength for concrete computed as:

$$v_c (\text{MPa}) = 0.17 \sqrt{f'_c (\text{MPa})} \quad (D-2)$$

Equation D-1 is a simplified version of the “truss analogy” as originally proposed by Richart (1927). It corresponds to vertical stirrups and imaginary compressive struts acting at 45°. It also assumes yielding of the transverse reinforcement at ultimate.

APPENDIX E: SOFTWARE (Guidelines)

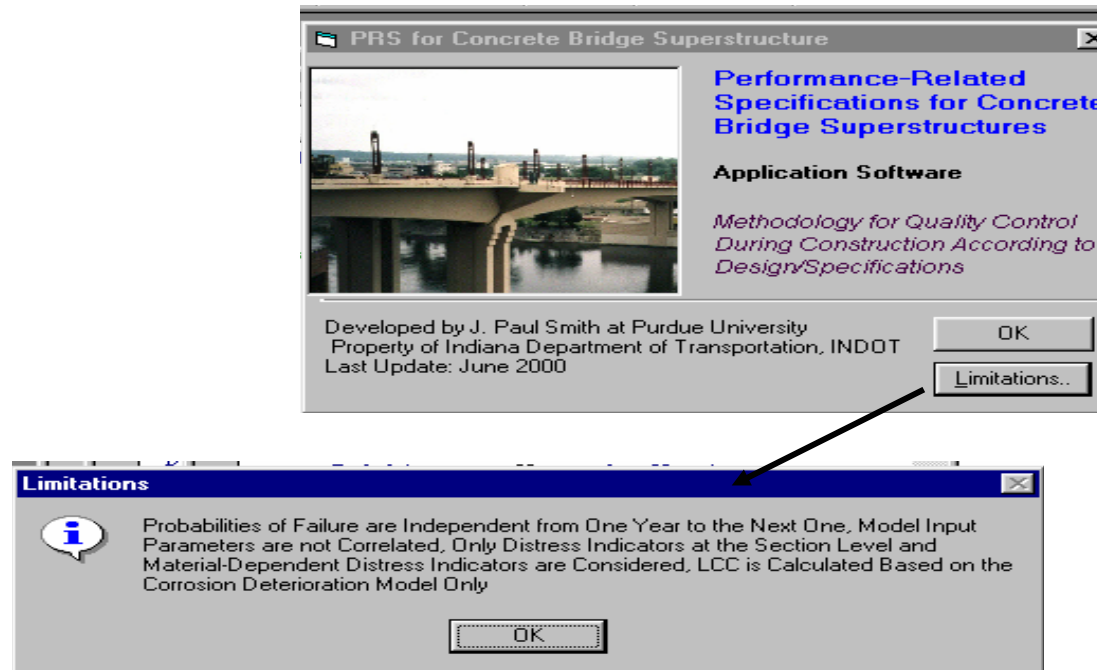


Figure E.1: Heading of Computer Program

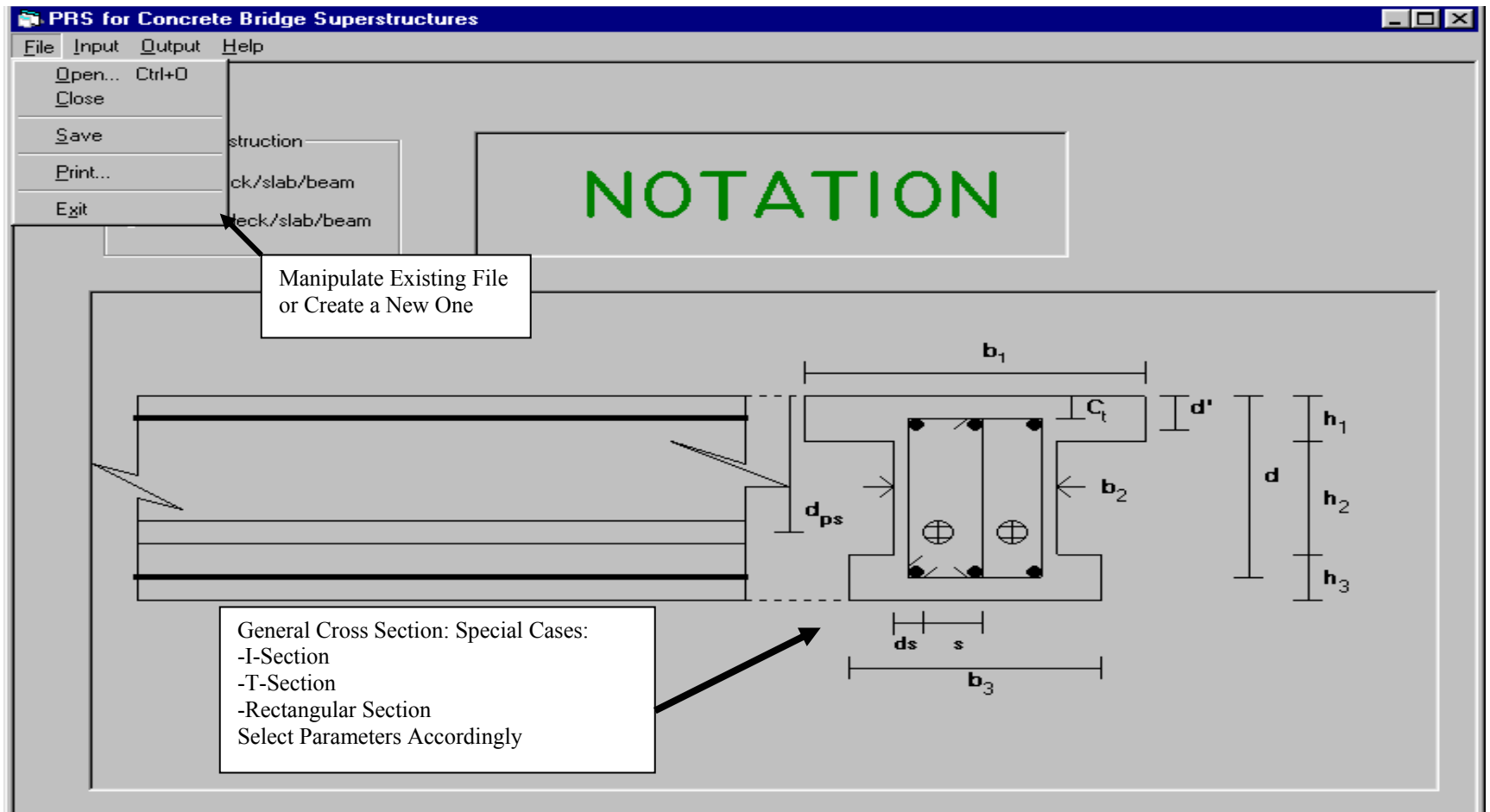


Figure E.2: Main Page of Computer Program

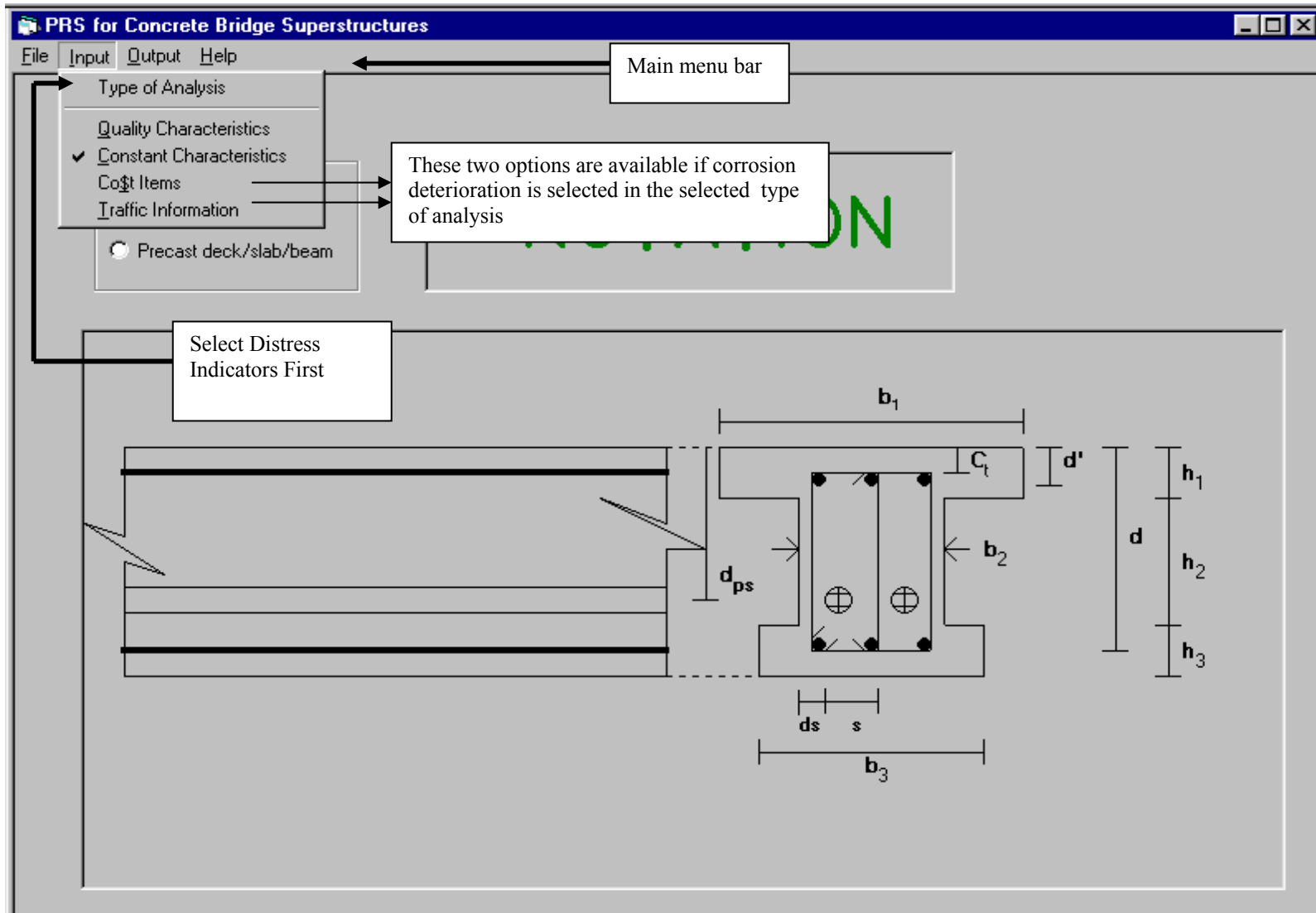


Figure E.3: Input Parameters of Computer Program

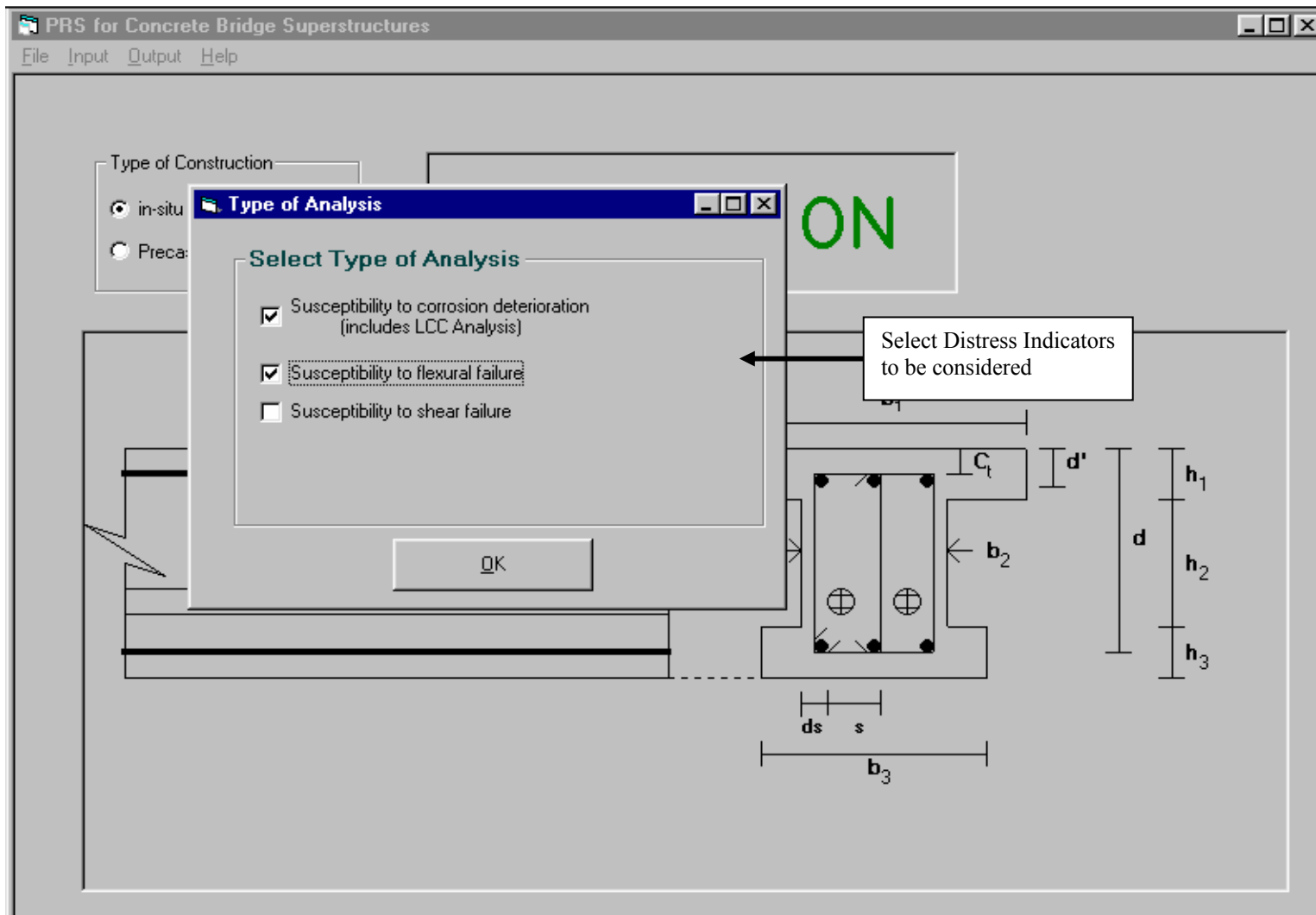


Figure E.4: Alternative Distress Indicators (Input Menu of Computer Program)

Quality Characteristics

Variable	Units	As-Designed		As-Built	
		Mean	Std. dev	Mean	Std. dev
Water/cement ratio	none	<input type="text"/>	<input type="text"/>	<input type="text"/>	<input type="text"/>
Presstress Force	kips	<input type="text"/>	<input type="text"/>	<input type="text"/>	<input type="text"/>
Concrete compressive strength	ksi	<input type="text"/>	0.87	<input type="text"/>	<input type="text"/>
Cover top, Ct	in.	<input type="text"/>	<input type="text"/>	<input type="text"/>	<input type="text"/>
Effective depth, d	in.	<input type="text"/>	<input type="text"/>	<input type="text"/>	<input type="text"/>
Compression reinforcement depth, d'	in.	<input type="text"/>	<input type="text"/>	<input type="text"/>	<input type="text"/>
Presstress Depth	in.	<input type="text"/>	<input type="text"/>	<input type="text"/>	<input type="text"/>
Stirrups Spacing	in.	<input type="text"/>	<input type="text"/>	<input type="text"/>	<input type="text"/>
I-Shape Section?	yes no				
Width, b	in.	<input type="text"/>	0.19	<input type="text"/>	<input type="text"/>
Thickness, h	in.	<input type="text"/>	0.47	<input type="text"/>	<input type="text"/>

Shaded cells are not activated (according to the selected type of analysis)

If "yes" define additional quality characteristics (no need of defining b and h below)

Values already appearing are by default (recommended in the literature)

Figure E.5: Quality Characteristics (Input Menu of Computer Program)

...Quality Characteristics

Applicable for T, or I-Section Type

<u>Variable</u>	<u>Units</u>	<u>As-Designed</u>		<u>As-Built</u>	
		<u>Mean</u>	<u>Std. dev</u>	<u>Mean</u>	<u>Std. dev</u>
Top flange width, b1	in.	<input type="text"/>	<input type="text"/>	<input type="text"/>	<input type="text"/>
Web width, b2	in.	<input type="text"/>	<input type="text"/>	<input type="text"/>	<input type="text"/>
Bottom flange width, b3	in.	<input type="text"/>	<input type="text"/>	<input type="text"/>	<input type="text"/>
Top flange thickness, h1	in.	<input type="text"/>	<input type="text"/>	<input type="text"/>	<input type="text"/>
Web thickness, h2	in.	<input type="text"/>	<input type="text"/>	<input type="text"/>	<input type="text"/>
Bottom flange thickness, h3	in.	<input type="text"/>	<input type="text"/>	<input type="text"/>	<input type="text"/>

OK Cancel

Figure E.6: Additional Quality Characteristics (Input Menu of Computer Program)

Constant Characteristics

Deterministic Variables

Variable	Units	Magnitude
Horizon life.....	years	<input type="text"/>
Age at loading.....	days	<input type="text"/>
Age when drying begins.....	days	<input type="text"/>
.....	none	<input type="text"/>
.....	lb/ft3	<input type="text"/>
.....	in.	<input type="text"/>
Yielding stress of steel (G40 or G60)	ksi	<input type="text"/>

Cement Type: I II III

Curing Procedure: Steam cured Cured in water Sealed

Define maximum solicitations for the member or part of the member being monitored

Non-Deterministic Variables

Variable	Unit	Statistical Parameters	
Relative humidity		Max <input type="text"/>	Min <input type="text"/>
Area of Reinforcement		Mean <input type="text"/>	Std. dev <input type="text"/>
Area of Reinforcement		Mean <input type="text"/>	Std. dev <input type="text"/>
Area of Transverse Reinforcement	in2	Mean <input type="text" value="N/A"/>	Std. dev <input type="text" value="N/A"/>

Values already appearing are by default (recommended)

Maximum External Actions

Flexure Moment	[Kip-in.]	mean <input type="text"/>	st.d <input type="text"/>
Shear	[Kip]	mean <input type="text" value="N/A"/>	st.d <input type="text" value="N/A"/>

N/A correspond to parameters not applicable for the selected distress indicators

Predetermined Variables

Variable	Units	Mean	Std. dev
Modulus of elasticity of steel	ksi	<input type="text" value="29000"/>	<input type="text" value="700"/>
Diffusion coefficient	in2/year	<input type="text" value="0.09"/>	<input type="text" value="0.036"/>
Surface chloride concentration	lb/ft3	<input type="text" value="0.33"/>	<input type="text" value="0.14"/>
		Max.	Min.
Chloride threshold value	lb/ft3	<input type="text" value="0.087"/>	<input type="text" value="0.037"/>
Corrosion rate	mA/ft2	<input type="text" value="1.96"/>	<input type="text" value="0.93"/>
Deteriorated area at replacement	%	<input type="text" value="40"/>	<input type="text" value="25"/>
Allowable crack widths	in.	<input type="text" value="0.024"/>	<input type="text" value="0.013"/>

Figure E.7: Constant Characteristics (Input Menu of Computer Program)

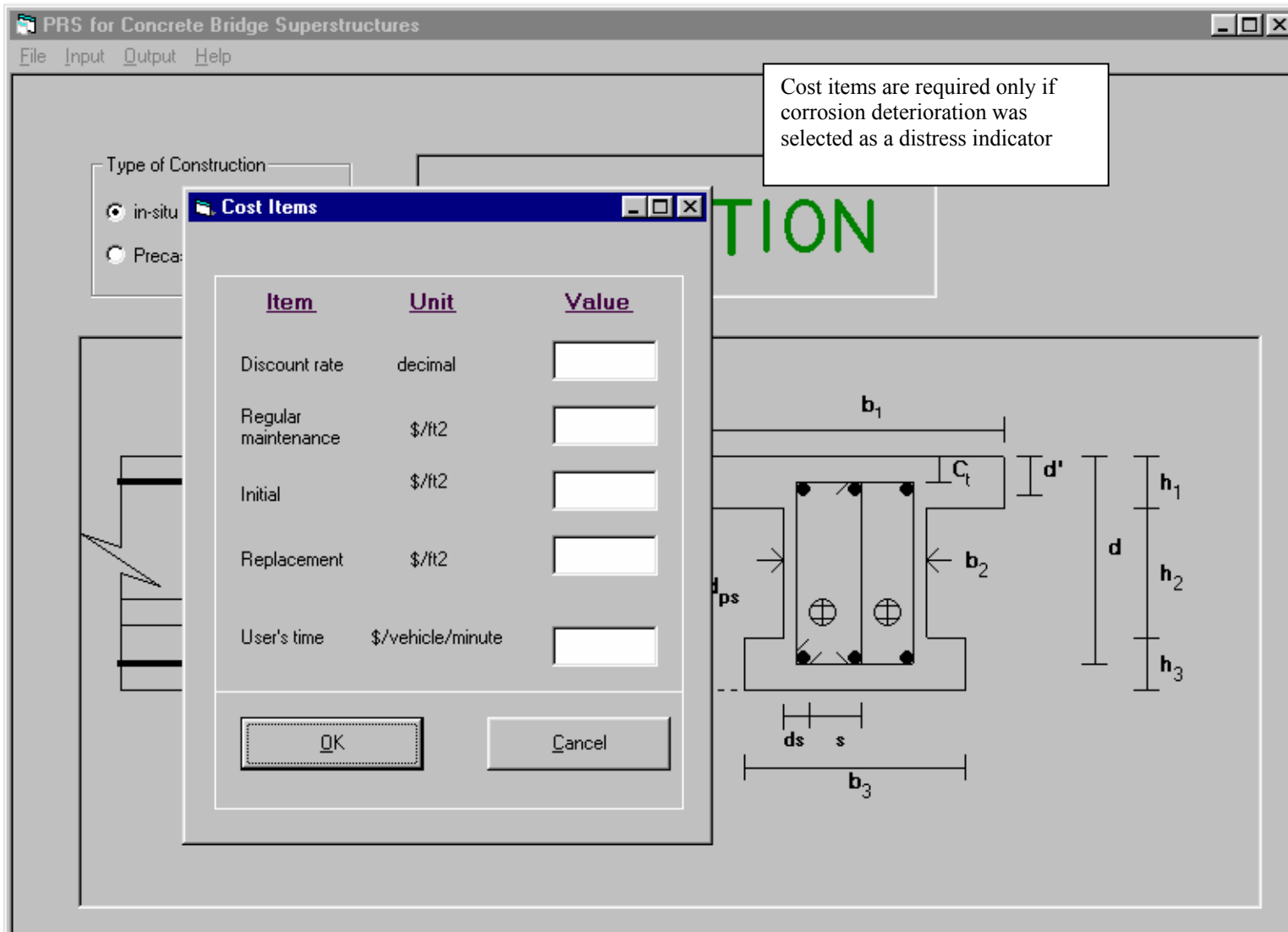


Figure E.8: Cost Items (Input Menu of Computer Program)

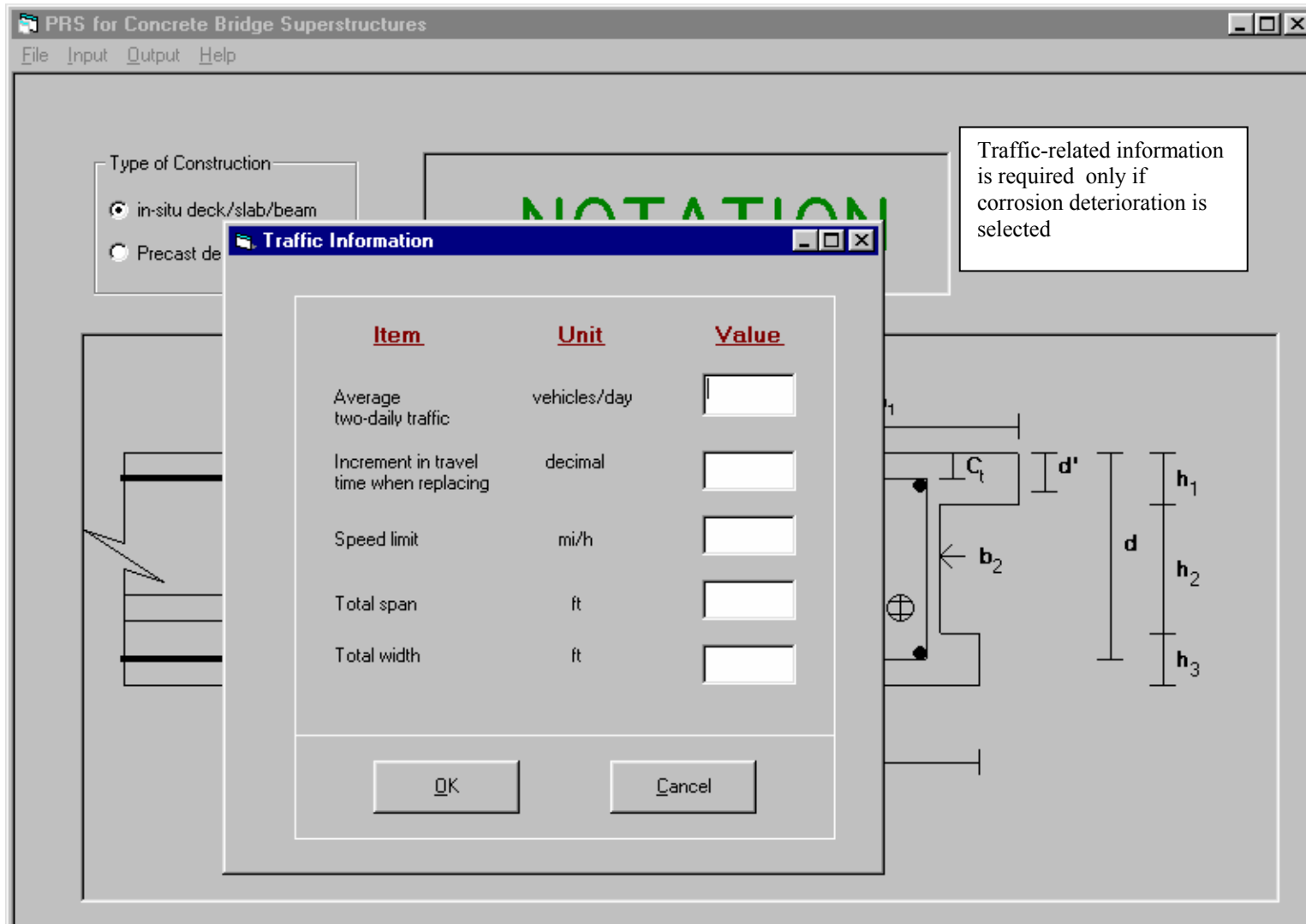


Figure E.9: Traffic-Related Information (Input Menu of Computer Program)

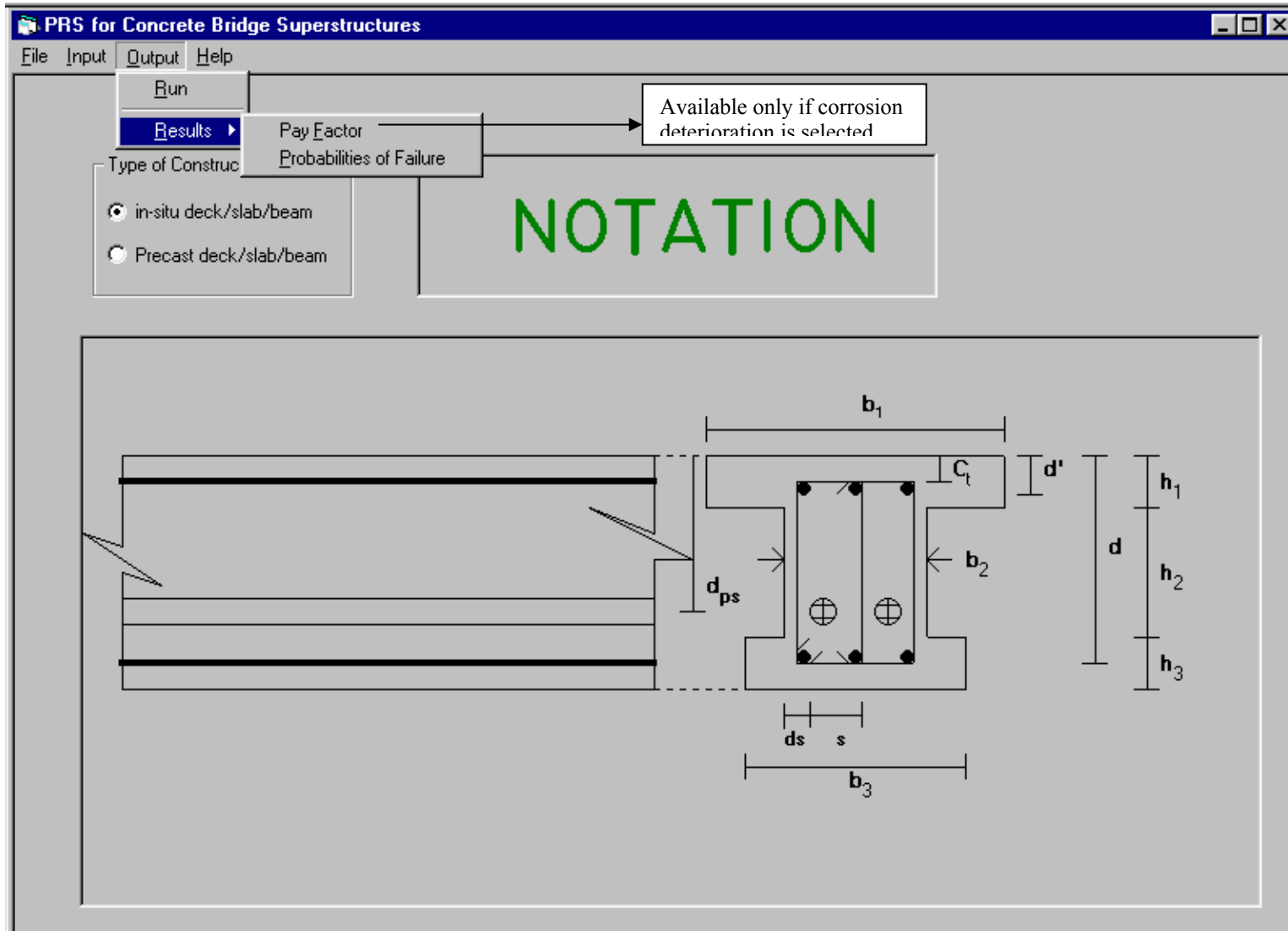


Figure E.10: Output of Computer Program

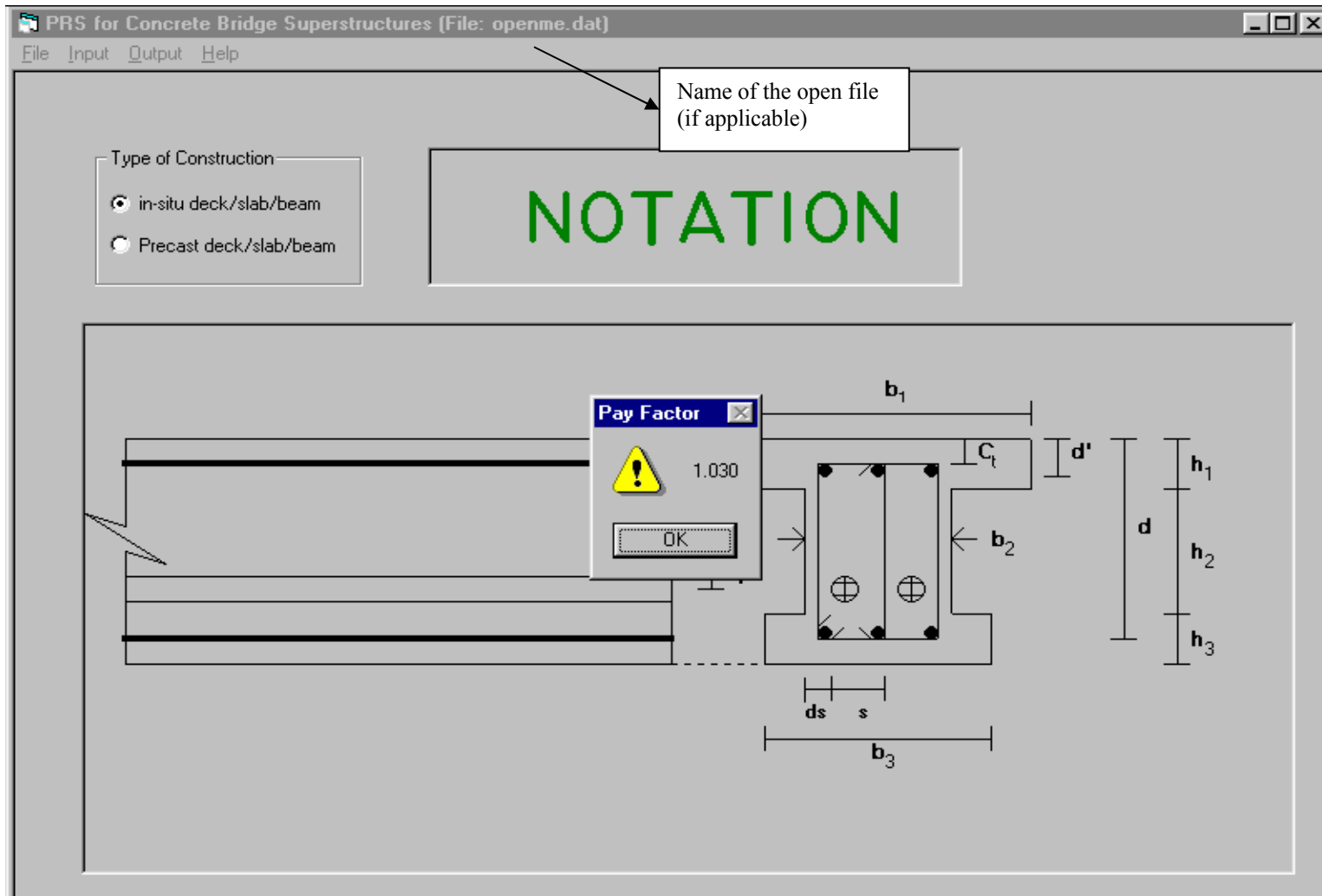


Figure E.11: Pay Factor (Output Menu of Computer Program)

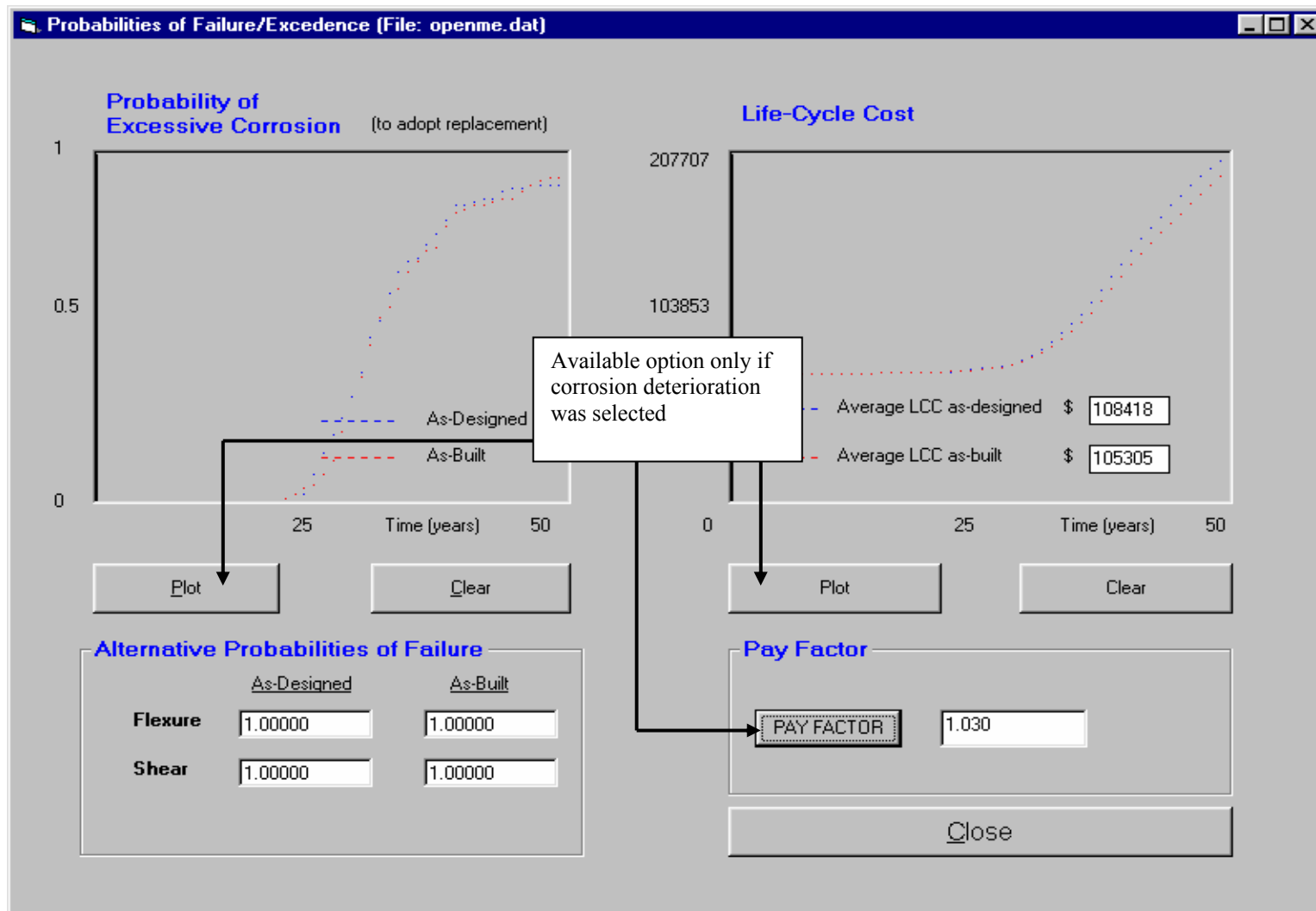


Figure E.12: Probabilities of Failure (Output Menu of Computer Program)